(12)

ARL-TR-85-32

Copy No. 12

NONLINEAR EFFECTS IN LONG RANGE UNDERWATER ACOUSTIC PROPAGATION

Frederick D. Cotaras

APPLIED RESEARCH LABORATORIES
THE UNIVERSITY OF TEXAS AT AUSTIN
POST OFFICE BOX 8029, AUSTIN, TEXAS 78713-8029

1 November 1985

Technical Report

Approved for public release;
distribution unlimited.

Prepared for:

OFFICE OF NAVAL RESEARCH
DEPARTMENT OF THE NAVY
ARLINGTON, VA 22217

12

REPORT DOCUMENTATION PAGE	READ INSTRUCTIONS BEFORE COMPLETING FORM
1. REPORT NUMBER	2. GOVT ACCESSION NO. AD-A166492	3. RECIPIENT'S CATALOG NUMBER
4. TITLE (and Subtitle) NONLINEAR EFFECTS IN LONG RANGE UNDERWATER ACOUSTIC PROPAGATION	5. TYPE OF REPORT & PERIOD COVERED technical report
	6. PERFORMING ORG. REPORT NUMBER ARL-TR-85-32
7. AUTHOR(s) Frederick D. Cotaras	8. CONTRACT OR GRANT NUMBER(s) N00014-75-C-0867 N00014-84-K-0574
9. PERFORMING ORGANIZATION NAME AND ADDRESS Applied Research Laboratories The University of Texas at Austin Austin, Texas 78713-8029	10. PROGRAM ELEMENT, PROJECT, TASK AREA & WORK UNIT NUMBERS 61153N RR011-08-01 NR 384-317
11. CONTROLLING OFFICE NAME AND ADDRESS Office of Naval Research Department of the Navy Arlington, Virginia 22217	12. REPORT DATE 1 November 1985
	13. NUMBER OF PAGES 217
14. MONITORING AGENCY NAME & ADDRESS(if different from Controlling Office)	15. SECURITY CLASS. (of this report) UNCLASSIFIED
	15a. DECLASSIFICATION/DOWNGRADING SCHEDULE

16. DISTRIBUTION STATEMENT (of this Report)

Approved for public release; distribution unlimited.

17. DISTRIBUTION STATEMENT (of the abstract entered in Block 20, if different from Report)

18. SUPPLEMENTARY NOTES

19. KEY WORDS (Continue on reverse side if necessary and identify by block number)

underwater explosions
ray theory
long range underwater propagation
eikonal equation
numerical model
finite amplitude effects

20. ABSTRACT (Continue on reverse side if necessary and identify by block number)

In this report the propagation of finite amplitude acoustic signals through an inhomogeneous ocean ~~is investigated~~ both analytically and numerically. The effects of reflections and focusing are not considered. From simplified versions of the lossless hydrodynamics equations the theories of linear and nonlinear geometrical acoustics are developed. Losses are accounted for directly in the numerical routine. The eikonal equation, from which an equation for the ray paths is derived, is assumed to be the same for both small-signal

20. (cont'd)

and finite amplitude waves. The transport equation is found to be different, however. The transport equation leads to a standard first-order progressive wave equation, linear for small-signals waves, but nonlinear for finite amplitude waves. All the analysis is carried out in the time domain and is for a fully inhomogeneous ocean.

In the numerical study the ocean is assumed to be stratified. The effects of inhomogeneity, ordinary attenuation and dispersion, and nonlinear propagation are investigated using a numerical implementation of nonlinear geometrical acoustics. Two explosion waveforms are considered: a weak shock with an exponentially decaying tail and a more realistic waveform that includes the first bubble pulse. Numerical propagation of the simpler wave along a 58.1 km path starting at a depth of 300 m leads to the following conclusions: (1) The effect of inhomogeneity on nonlinear distortion is small. (2) Dispersion plays an important role in determining the arrival time of the pulse. (3) Neither nonlinearity nor ordinary attenuation (and dispersion) are paramount; both need to be included. For the more realistic wave, the propagation is along a 23 km ray path starting from a depth of 4300 m. Two charge weights, 0.818 kg and 22.7 kg TNT, are assumed. In each case the energy spectrum of the signal obtained by considering finite amplitude effects for the entire 23 km path is compared with spectra obtained by neglecting finite amplitude effects (1) entirely, (2) after the first 150 m, and (3) after the first 1100 m. Finite amplitude effects are found to be of small consequence in the case of the 0.818 kg TNT explosion for frequencies below 6 kHz at distances beyond 1100 m. For the 22.7 kg explosion the corresponding quantities are 4 kHz and 1100 m.

TABLE OF CONTENTS

LIST OF FIGURES

LIST OF IMPORTANT SYMBOLS

A_0	Ray tube area
A_{0s}	A_0 at source position
c	Sound speed
c_0	Small-signal sound speed
c_{0s}	c_0 at source position
$D/Dt \equiv (\partial/\partial t + \mathbf{u}\cdot\nabla)$	Material derivative
e	Internal energy
$\mathbf{g}$	Gravity
G	A parameter indicating the influence of the inhomogeneous medium upon finite amplitude distortion
h	Gradient of the sound speed profile
$\mathbf{i},\mathbf{j},\mathbf{k}$	Cartesian system basis vectors
K	Curvature
M	Acoustic mach number
$\mathbf{n}$	Unit normal to the eikonal wavefront
$\mathbf{N}$	Principal normal
P	Total pressure

P_0	Static pressure
$P' \equiv P - P_0$	Acoustic pressure
r	Radial range
r_0	Reference range
$\mathbf{r}$	Ray position vector
R	Radius of curvature
R_*	Characteristic distance
s	Ray path length
S_0	Reference path length
t	Time
$t' \equiv t - \Psi(r)$	Retarded time variable
t_c	Characteristic time
T	Temperature
$\mathbf{T}$	Tangent to ray path
u	Fluid particle velocity
W	Transformed pressure
x	Distance in x direction
z	Depth
Z	Distortion range variable
$\alpha \equiv \beta(\rho_0 c_0^5)^{-1/2}$	Convenient thermodynamic variable
β	Coefficient of nonlinearity
β_s	β at source position

δ_j^i	Kronecker delta
θ	Acute angle between ray path and horizontal
κ	Thermal conductivity
λ	Dilatational viscosity coefficient
μ	Shear viscosity coefficient
ξ	Salinity
ρ	Total density
ρ_0	Static density
$\rho' \equiv \rho - \rho_0$	Acoustic density
σ	Nondimensional distance
Σ	Viscous stress tensor
ϕ, ψ	Ray launch angles
χ	Entropy
$\Psi(r)$	Eikonal

FOREWORD

This report is adapted from the master's thesis of the same title by Frederick D. Cotaras. Beginning in September 1983 Mr. Cotaras was enrolled in the Department of Electrical and Computer Engineering. He received his degree in August 1985. During this two-year period he was on educational leave from Defence Research Establishment Atlantic (DREA), Halifax, N. S., Canada, and was supported jointly by DREA and a Canadian Natural Science and Engineering Research Council Postgraduate Scholarship.

The research was carried out at Applied Research Laboratories and was supported in part by the Office of Naval Research (ONR) under Contracts N00014-75-C-0867 and N00014-84-K-0574. The Scientific Officer for ONR was L. E. Hargrove.

David T. Blackstock
Supervisor

CHAPTER I

INTRODUCTION

The subject of this report is the propagation of intense acoustic signals through an inhomogeneous ocean. The analysis is conducted both analytically and numerically. Our approach is to use nonlinear geometrical acoustics. The self-refraction of acoustic waves is neglected, and the acoustic field is assumed to consist of outgoing waves only. The effects of reflections from the ocean bottom and surface and the effects of the focusing of acoustic rays near caustics are not considered. In our numerical algorithm we assume a stratified ocean even though the analytic development is for a fully inhomogeneous ocean in which temperature, salinity, density, and sound speed vary with position. No losses are considered in the analytic work. In the numerical algorithm, however, the losses due to viscosity and relaxation are accounted for in an ad hoc fashion. Our algorithm is designed to propagate signals, which may contain weak discontinuities, along a ray path using a stepwise time domain technique and to apply absorption in the frequency domain.

When considering how to approach a problem involving an intense sound wave, one usually examines the corresponding small-signal problem.

Popular techniques for dealing with the propagation of small-signal sounds include the following: normal modes, parabolic approximation to the wave equation, and geometrical acoustics. Since we are interested in handling discontinuities, an approach which lends itself to a time domain implementation is preferred. Thus geometrical acoustics and the parabolic approximation are both good avenues for dealing wih intense sounds. As noted above, we have chosen to use geometrical acoustics. The alternative approach, the parabolic approximation, is being explored by McDonald and Kuperman (1984).

Our implementation of nonlinear geometrical acoustics is somewhat restricted. Since self-refraction is neglected, the ray paths are assumed to be determined solely by the inhomogeneous medium and not affected by the amplitude of the signal (Whitham 1956). It turns out that this assumption places a limit of 282 dB//1 μPa on the peak amplitude of the signal. Reflections and focusing are neglected because neither are fully understood for the case of intense sound waves. Reflections and focusing are avoided in the numerical work by a careful selection of the acoustic ray paths. Because the acoustic rays are not permitted to either interact with ocean surface and bottom or to pass through caustics, the propagation range is limited to a maximum of about 70 km in the deep ocean.

The primary objective of this work is to investigate the importance of nonlinear effects at long ranges from an intense acoustic source such as an explosive. Because the amplitude of most underwater sounds is small, the most commonly used theory in underwater acoustics is small-signal theory. When dealing with underwater explosions,

investigators commonly assume that, after propagating a certain distance, the intense sound is sufficiently diminished that small-signal theory applies. One of the goals of this thesis is to attempt to quantify this assumption.

A. Review of Finite Amplitude Effects

An intense, or *finite amplitude*, acoustic signal is distinguished from the better known small, or *infinitesimal*, signal by the amplitude of the field variables such as the pressure or particle velocity. To aid in the distinction, we introduce the acoustic Mach number M, a nondimensional number equal to the ratio of the maximum fluid particle velocity to the small-signal sound speed. In the case of small-signals, M is approximately zero, *infinitesimally* small. However, for the finite amplitude signals considered in this report, M may be as large as 0.06, a small, but *finite* value.

It is well known that the propagation of a finite amplitude wave cannot be accurately modeled by a small-signal acoustical theory. The reason small-signal theory fails is that it does not correctly predict the propagation speed of the wave. The physical mechanisms that cause the propagation speed to vary from the small-signal value are (1) the nonlinearity of the pressure-density relationship of the medium and (2) convection. Convection occurs when the fluid particles themselves are set into motion by the passing acoustic wave and contribute their velocity to the total wave speed. The two phenomena, the nonlinearity of the pressure-density relationship and convection, are embodied in the

coefficient of nonlinearity β. These phenomena are present even in the cases of small signals; they are just not perceivable. As the amplitude of the signal increases, so does the significance of their effects. To incorporate these effects into acoustical theory, one must consider the nonlinear terms in the hydrodynamics equations. Therefore the theory that governs a finite amplitude wave must be a nonlinear theory. Hence the words finite amplitude and nonlinear are used interchangeably in this report. Similarly the words small-signal and linear are used interchangeably since small-signal theories are derived neglecting all terms except linear terms.

The problem of propagation of plane finite amplitude waves through a homogeneous medium has a solution that is well established; see, for example, Blackstock (1972). The nonlinear acoustical theory described by Blackstock is referred to as weak-shock theory. A shock is a discontinuity in the field variable. If the shock is small enough to be dealt with by a nonlinear theory that is quadratic in the field variable, the shock is referred to as weak (see, for example, Whitham 1974, p. 37). The highest amplitude dealt with in this report corresponds to $M = 0.06$ or, equivalently, a peak pressure level of 282.6 dB // 1 μPa. According to Pestorius and Williams (1974), this level is within the amplitude limits of weak-shock theory. Pestorius (1973) developed a computer based version of the weak-shock solution to plane finite amplitude acoustic propagation. He used the computer program to solve problems involving both finite amplitude noise and periodic waves. As previously noted, a modified form of Pestorius's algorithm is used in this report.

The extension of finite amplitude plane wave theory to nonplanar waves is of notable importance to this work (see, for example, Blackstock 1964). Blackstock extended the plane wave solution to the problem of spherical and cylindrical finite amplitude acoustic waves. His approach was to use two transformations to reduce the spherical (cylindrical) wave equation to the form of the finite amplitude plane wave equation. The two transformations, one for the field variable and the other for the range, permit the use of the solution of the plane wave problem. The transformations required to deal with plane waves propagating vertically in a stratified medium were developed by Carlton and Blackstock (1974). The idea of reducing a complex problem to a simpler one with a known solution is used in this thesis.

B. Review of Linear Geometrical Acoustics

Two separate geometrical acoustic theories, one for infinitesimal signals and one for finite amplitude signals, exist. The extension of linear geometrical acoustics to incorporate finite amplitude signals is a comparatively recent development. The two theories predict different wave shapes, but the same ray paths. The older of the two, linear geometrical acoustics, is described in the literature survey that follows.

Several methods for developing linear geometrical acoustics exist. One approach originates in geometrical, or short-wave, optics as developed by Hamilton (1832; see Conway and Synge 1931). The central equation in the geometrical technique for both acoustics and optics is the so called eikonal equation. The eikonal equation defines the ray paths (see,

for example, Born and Wolf 1980, p. 112). The word eikonal comes fom the Greek word *eikon*, for image, and was introduced into physics by Bruns (1895) (see, for example, Sommerfeld 1949, p. 207). Bruns developed a function similar to the one developed by Hamilton and called it the eikonal. The eikonal is a function of the spatial coordinate system and defines "a system of surfaces the orthogonal trajectories of which are rays" (Sommerfeld 1949, p. 337). Sommerfeld and Runge (1911) were the first to derive the eikonal equation from the scalar wave equation. Their derivation clearly shows that ray theory is exact only in the case of infinite frequency. Ray theory is, however, a valid approximation to surprisingly low frequencies. It turns out that the approximation depends on the degree of inhomogeneity in the medium.

Sommerfeld (1949, p. 210) provides some interesting comments about the eikonal and linear geometrical techniques in general. He states that the eikonal equation is a specialization of Hamilton's equation of dynamics. He notes that Hamilton worked on optical problems, then went on to apply his knowledge to dynamics. Hamilton's work in dynamics is embodied in the Hamilton-Jacobi equation, and analogies between the eikonal and the action of the material particle are often made. Goldstein (1950, p. 312) states that the Hamilton-Jacobi equation "tells us that classical mechanics corresponds to the geometrical optics limit of a wave motion." Consequently geometrical acoustics is sometimes derived via the Hamilton-Jacobi equation (see, for example, Landau and Lifshitz 1959, p. 257). Sommerfeld observes that the WKB (Wentzel- Kramers- Brillouin)

approximation of the wave equation corresponds to a transition from wave optics (wave acoustics) to geometrical optics (geometrical acoustics).

Another way to develop linear ray theory is to use Huygens' principle and Snell's law. The first application (within acoustics) of this approach was to analyze the problem of propagation in a moving, inhomogeneous atmosphere (see, for example, Stuff 1979). The following is a brief summary of some derivations and applications of linear geometrical acoustics developed in this fashion.

Rayleigh (1896,§ 289) examined the problem of acoustic propagation in a windy atmosphere. However he did not acknowledge the difference between the direction of the acoustic ray path and that of the normal to the wave (eikonal) surface. This flaw has been commented on by several authors (Barton 1901; Kornhauser 1953; Lighthill 1965; Thompson 1972; Ugincious 1972). Several other researchers made use of linear ray theory to study propagation of airborne sound. An early application is given by Fujiwhara (1912; 1916). He derived three-dimensional acoustic ray theory and applied it to the problem of sounds produced by the volcano Asama in central Japan. Another interesting early work is that of Milne (1921). His work is an outgrowth of research done during the First World War on the acoustic detection of aircraft. Rothwell (1947) applied acoustic ray theory to the problem of meteorological investigations by acoustical techniques. It is interesting to note that Rothwell's data is from experiments performed in 1930 and 1931 in which 16 lb practice shells were fired from an anti-aircraft gun. The data were originally applied to the problem of acoustical detection of aircraft.

Because of the need to detect submarines, research on linear geometrical acoustics underwent a resurgence during the Second World War. In the years immediately following the war, much of this research was published. In a major work Blokhintzev (1946a; 1946b) derived the eikonal equation for a moving, inhomogeneous medium. Earlier researchers had assumed that the acoustic energy is constant along the ray path. Blokhinstzev found that a certain combination of the acoustic pressure, ray tube area, sound speed, particle velocity, and density (not necessarily the energy) stays constant along the ray path. From his work the term *Blokhintzev invariant* arose. Frank, Bergmann, and Yaspen (1969) discussed the derivation of ray theory and gave a good account of the frequency limits of the theory. Bergmann (1946) discussed the importance of the density variation and the gravity terms in the derivation of ray theory.

Over the years since the end of the Second World War, several other derivations of linear ray theory have been given. Using tensor calculus and a general curvilinear coordinate system, Haselgrove (1954) derived ray theory via reciprocal surfaces. He applied his theory to radio wave propagation, specifically to the calculation of ionospheric ray paths, a requirement for determining the maximum usable frequencies for short-wave radio transmission. Haselgrove appears to have been the first to use an electronic computer (EDSAC, Cambridge University Mathematical Library) to calculate ray paths.

More recent derivations of ray theory include those of Eby and Mal'tsev. Eby (1967) derived three-dimensional ray tracing using a Frenet formulation. In another paper (Eby 1970) he examined the ray paths as

temporal geodesics. Mal'tsev (1983) derived equations in barycentric coordinates, a technique that simplifies the calculation of the ray paths.

C. Geometrical Acoustics for Finite Amplitude Signals

Until now the discussion has centered on the problem of deriving ray theory for small-signal waves. We now address the problem of geometrical acoustics for finite amplitude signals. Heller (1953) derived the equation for the ray path of an acoustic discontinuity propagating in a moving, inhomogeneous medium. He referred to this equation as a "generalized eikonal equation" and showed that weak shocks move along the same ray paths as small-signal acoustic waves. Kornhauser (1953) showed that Heller's generalized eikonal equation could be obtained by a simple extension of the small-signal eikonal equation. Keller (1954) was the first to discuss the variation of the shock strength along the ray path. Keller solved the problem by examining the jump of the field variables across the surface of discontinuity (see, for example, Jeffrey and Taniuti 1964). This approach is not common in acoustics today. Whitham (1956), in a major work on the propagation of weak shocks, described extensions of linear geometrical acoustics to encompass weak shocks. His development is very closely related to the nonlinear geometrical acoustical theory developed in this report. Whitham assumed, as we do, that the self-refraction of the acoustic ray paths is insignificant. Thus he used the ray paths from linear ray theory and went on to develop a set of improved relations to predict the shock strength. In a discussion on the inadequacies of linear geometrical acoustics, Whitham said, "It should be stressed that this inaccuracy is a

failure of the linear theory of sound and is not introduced by the approximations of geometrical acoustics."

Also using a geometrical technique, Gubkin (1958) addressed the problem of propagation of acoustic discontinuities in an inhomogeneous medium. The solution was presented in a way more familiar to researchers in acoustics, that is, by starting with the hydrodynamical equations and making simplifying assumptions based on the degree of smallness of the terms in the equations. Using similar notation, Ostrovsky (1963) examined linear geometrical acoustics in nonstationary media. He then extended the theory to include finite amplitude waves and applied the theory to the problem of a sinusoidal finite amplitude wave in a steadily moving gas. Ostrovsky introduced a parameter "g" which indicates the influence of medium inhomogeneity upon the shock formation distance.

In the late 1960's, there was a large interest in the propagation of finite amplitude acoustic waves in an inhomogeneous moving atmosphere. The stimulation was the problem of sonic booms from supersonic transports (SST). Hayes, Haefeli, and Kulsrud (1969) developed a computer program that uses small-signal acoustic ray theory, and then modifies the result to account for finite amplitude effects. Seebass (1969) presented the derivation of the equation for the acoustic pressure behind a propagating weak shock. The equation was obtained by correcting small-signal ray theory results for nonlinear effects. Seebass's result shows how the acoustic pressure depends on the acoustic ray tube area in the case of finite amplitude waves.

In the mid-1970's, interest in finite amplitude propagation in stationary inhomogeneous media reappeared. Carlton and Blackstock (1974) analyzed the problem of vertical propagation of finite amplitude plane waves in a horizontally stratified ocean. The transform technique that Carlton and Blackstock used is similar to that used by Blackstock (1964) for nonplanar waves in a homogeneous medium. In a comment in the abstract, Carlton and Blackstock (1974) state that their results were intended to be incorporated in a ray theory for finite amplitude acoustic waves in the inhomogeneous ocean.

Before Carlton and Blackstock had an opportunity to perform this extension, however, the results of a parallel development were disclosed. Ostrovsky, Pelinovsky, and Fridman (1975; 1976) described the solution of the problem of propagation of finite amplitude waves in a stationary, inhomogeneous medium. Their work is central to the discussion of nonlinear geometrical acoustics (NGA) in this report.

Nonlinear geometrical techiques have been used in many investigations. Ostrovsky (1976) discussed applications of nonlinear geometrical techniques to problems such as acoustic propagation in nonstationary media and the heating of the sun chromosphere. Pelinovsky, Petukhov, and Fridman (1979) extended NGA to include the effects of ocean salinity. NGA was also expanded to encompass the effects of small dissipation and dispersion (Pelinovsky and Fridman 1983). Warshaw (1980) extended the results of Blokhintzev (1946a, 1946b) to account for the cumulative effects of the dissipative and second-order convective terms. More recently the work of Pelinovsky, Petukhov, and Fridman (1979) was

examined by Morfey (1984a). Morfey introduced a parameter "G" to describe the effect of the inhomogeneity on the shock formation distance. He calculated the parameter for a variety of oceanic environments and concluded that the effect of inhomogeneity upon finite amplitude propagation is small. Morfey's work is used in this report.

D. Scope of the Investigation

This report is divided as follows: In Chapter 2 we establish the criteria for simplifying the equations of hydrodynamics. The equations are then simplified for the cases of small signals in homogeneous fluids, small signals in inhomogeneous fluids, and finite amplitude signals in inhomogeneous fluids. In Chapter 3 we discuss linear geometrical acoustics and derive the eikonal and transport equations. At the same time we introduce some of the techiques required for the case in which the signals are of finite amplitude. Nonlinear geometrical acoustics is presented in Chapter 4. The notation used varies slightly from that of Pelinovsky et al. (1979) and adheres more closely to that of Blackstock (1964). In Chapter 5 we discuss the numerical implementation of the findings of Chapter 4. The method of handling shocks in the waveform and the transformation to the frequency domain to correct for absorption is due to Pestorius (1973). The computer based ray model used is due to Foreman (1983) Some of the results of the testing of the numerical algorithm are presented. In Chapter 6 the numerical algorithm is used to study the effects of viscosity, relaxation, and dispersion on the propagation of waves through the ocean. It is also used to provide examples of the

effects of ocean inhomogeneity on finite amplitude propagation. The waveforms considered are a weak shock with an exponentially decaying tail and Morfey's (1985) modified form of the Wakeley explosion waveform (Wakeley 1977).

CHAPTER 2

RANKING OF TERMS

A. Introduction

In this chapter a method for simplifying the equations of hydrodynamics is discussed. An equation of state for seawater and the hydrodynamics equations, including loss terms, are presented. As mentioned in Chapter 1, it is our intention to neglect all losses during the analytic development, and then account for viscosity and relaxation by a special procedure in the numerical propagation routine. The viscosity and heat conduction terms have, however, been included in the hydrodynamics equations so that the ranking system can be fully demonstrated. Basic assumptions about (1) the amplitude of the signal, (2) the magnitude of the loss coefficients, and (3) the type and degree of inhomogeneity of the medium are made. The terms in the equations are then ranked according to their relative importance. Use of the ranking system enables simplified forms of the hydrodynamics equations to be readily obtained (Lighthill 1956; Carlton and Blackstock 1974).

For an inhomogeneous, thermally conducting, viscous fluid, an equation of state and the hydrodynamics equations are as follows (see, for

example, Panton 1984; the momentum equation is from Hunt 1955):

$$\text{State} \qquad P = P(\xi, \chi, \rho) \quad , \tag{A.1}$$

$$\text{Continuity} \qquad \partial\rho/\partial t + \nabla\cdot\rho\mathbf{u} = 0 \quad , \tag{A.2}$$

$$\begin{aligned}\text{Momentum} \qquad \rho\partial\mathbf{u}/\partial t + \rho(\mathbf{u}\cdot\nabla)\mathbf{u} = {} & -\nabla P + \rho\mathbf{g} + (\lambda+2\mu)\nabla(\nabla\cdot\mathbf{u}) \\ & - \mu\nabla\times(\nabla\times\mathbf{u}) + (\nabla\cdot\mathbf{u})\nabla\lambda \\ & + 2(\nabla\mu\cdot\nabla)\mathbf{u} + \nabla\mu\times(\nabla\times\mathbf{u}) \quad ,\end{aligned} \tag{A.3}$$

$$\text{Energy} \qquad \rho\partial e/\partial t + \rho(\mathbf{u}\cdot\nabla)e = -P(\nabla\cdot\mathbf{u}) + \underline{\tau}:\underline{\nabla\mathbf{u}} + \nabla\cdot(K\nabla T) \quad , \tag{A.4}$$

where P is the pressure, ξ is the salinity, χ is the entropy, ρ is the density, t is the time, $\mathbf{u}$ is the particle velocity, $\mathbf{g}$ is gravity, λ and μ are, respectively, the dilatational and shear viscosity coefficients, e is the internal energy, $\underline{\tau}$ is the viscous stress tensor, K is the coefficient of thermal conductivity, and T is the temperature. Since the emphasis of this work is on acoustic propagation in the ocean, the salinity of the ocean is included in the equation of state. Note also that our coordinate system has gravity acting in the positive z direction; that is, z is positive downward.

We expand the continuity and momentum equations. First we express the density as the sum of a static value ρ_0 and a small fluctuation ρ', and the pressure as the sum of a static value P_0 and a small fluctuation p',

$$\rho \equiv \rho_0 + \rho' \quad , \tag{A.5}$$

$$P \equiv P_0 + p' \quad . \tag{A.6}$$

In a static fluid the pressure and density fluctuations are zero. In this case, the continuity equation, Eq. (A.2), is identically satisfied while the momentum equation, Eq. (A.3), reduces to

$$\nabla P_0 = \rho_0 \mathbf{g} \quad . \tag{A.7}$$

If Eqs. (A.5) and (A.6) are substituted into the continuity and momentum equations, and Eq. (A.7) is used to reduce terms in the latter, the following equations are obtained:

$$\text{Continuity} \qquad \partial\rho'/\partial t + \rho_0 \nabla\cdot\mathbf{u} = -\mathbf{u}\cdot\nabla\rho_0 - \mathbf{u}\cdot\nabla\rho' - \rho'\nabla\cdot\mathbf{u} \quad , \tag{A.8}$$

$$\begin{aligned}\text{Momentum} \qquad \rho_0 \partial\mathbf{u}/\partial t + \nabla P' = {} & (\rho'/\rho_0)\nabla P_0 - \rho'\partial\mathbf{u}/\partial t - \rho_0(\mathbf{u}\cdot\nabla)\mathbf{u} - \rho'(\mathbf{u}\cdot\nabla)\mathbf{u} \\ & + (\lambda+2\mu)\nabla(\nabla\cdot\mathbf{u}) - \mu\nabla\times(\nabla\times\mathbf{u}) \\ & + (\nabla\cdot\mathbf{u})\nabla\lambda + 2(\nabla\mu\cdot\nabla)\mathbf{u} + \nabla\mu\times(\nabla\times\mathbf{u}) \\ & + (\nabla\cdot\mathbf{u})\nabla(\lambda + 2\mu) \quad .\end{aligned} \tag{A.9}$$

To simplify Eqs. (A.8) and (A.9), we must have some knowledge of the relative importance of each of the terms.

We now state our basic assumptions: The magnitude of the particle velocity, $|\mathbf{u}|$, is assumed to be small with respect to the sound speed c_0, but not necessarily infinitesimal. It turns out that this assumption implies that the pressure fluctuation P' is small with respect to $\rho_0 c_0^2$ and that the fluctuation ρ' is small with respect to ρ_0. The above assumption is expressed mathematically as follows:

$$|u| \ll c_0 \ , \tag{A.10}$$

$$|\rho'| \ll \rho_0 \ , \tag{A.11}$$

$$|P'| \ll \rho_0 c_0^2 \ . \tag{A.12}$$

As for the inhomogeneity of the medium, it is assumed that environmental properties of the seawater such as the density, temperature, salinity, and sound speed vary with position. As can be seen from Eq. (A.7), the static pressure is assumed to vary only with depth. We assume that the ocean is only mildly inhomogeneous; that is, the environmental properties vary slowly on a wavelength scale. Consequently the derivative of an environmental property, for example $\nabla\rho_0$, is small; that is,

$$\lambda|\nabla\rho_0| \ll \rho_0 \ , \tag{A.13}$$

where λ is the wavelength. Losses due to heat conduction and the diffusion of dissolved salts are assumed to be zero; however, losses due to viscosity and relaxation are assumed to be small, but not zero.

Before stating the ranking system, we define some nomenclature. A linear term with a coefficient containing a first derivative of an environmental parameter is referred to as an inhomogeneity term; examples are $\mathbf{u}\cdot\nabla\rho_0$ or $\nabla P_0(\rho'/\rho_0)$. Linear terms with coefficients containing a constant loss coefficient, such as $(\lambda + 2\mu)(\nabla\cdot\mathbf{u})$, are referred to as dissipation terms. Similarly terms containing a quadratic nonlinear term with a coefficient that contains neither a derivative of an environmental property of the fluid nor a loss coefficient are referred to

as nonlinearity terms; examples are $\rho_0(\mathbf{u}\cdot\nabla)\mathbf{u}$ and $\rho'(\nabla\cdot\mathbf{u})$. Nonlinearity terms are associated with finite-amplitude behavior.

Use of the assumptions stated above enables the various terms in the hydrodynamics equations to be ranked by degree of smallness as first-order terms, second-order terms, and higher-order terms. A first-order term is defined as a linear term with a coefficient that involves neither derivatives of environmental properties of the fluid nor a loss coefficient. Examples of first-order terms are $\rho_0(\nabla\cdot\mathbf{u})$ and $\rho_0\partial\mathbf{u}/\partial t$. Second-order terms represent only the most important effects of nonlinearity, inhomogeneity, and losses. Accordingly inhomogeneity terms, nonlinearity terms, and dissipation terms are classified as second-order terms. Since the effects of nonlinearity, inhomogeneity, and losses were assumed small, any term representing the interaction of any two effects would be expected to be negligible. Such terms are encompassed in the third major category, higher-order terms. Examples of higher-order terms are cubic terms such as $\rho'(\mathbf{u}\cdot\nabla)\mathbf{u}$ and nonlinear inhomogeneity terms such as $\nabla\rho_0(\mathbf{u}\cdot\nabla)\mathbf{u}$. Linear terms with coefficients that contain higher-order derivatives of environmental properties, or that are nonlinear in the first derivative of an environmental property are also higher-order terms; examples are $(\nabla\rho_0\cdot\nabla P_0)\rho'$ and $\rho'\nabla^2 P_0$.

Use of the ranking system makes it relatively easy to deal with special cases such as small-signal waves in a lossless inhomogeneous fluid and finite amplitude (but not strong) waves in dissipative homogeneous fluid. The hydrodynamics equations can be simplified and, in most cases, combined to form the wave equation corresponding to the situation at hand.

B. Simplifying the Lossless Hydrodynamics Equations

The analysis from this point on deals solely with lossless fluids. The effects of the dissipation terms are considered in the numerical propagation routine discussed in Chapter 5. In this section the hydrodynamics equations are simplified to find (1) linear equations for a homogeneous fluid, (2) linear equations for an inhomogeneous fluid, and (3) nonlinear equations for an inhomogeneous fluid. Since all three sets of equations are for lossless fluids, the loss terms can be dropped from the expanded momentum equation, Eq. (A.9), and from the energy equation, Eq. (A.4). The state and hydrodynamics equations are then as summarized below:

State $\quad P = P(\xi, \chi, \rho) \quad ,$ (A.1)

Continuity $\quad \partial\rho'/\partial t + \rho_0(\nabla\cdot\mathbf{u}) = -\mathbf{u}\cdot\nabla\rho_0 - \mathbf{u}\cdot\nabla\rho' - \rho'(\nabla\cdot\mathbf{u}) \quad ,$ (A.8)

Momentum $\quad \rho_0\partial\mathbf{u}/\partial t + \nabla P' = (\rho'/\rho_0)\nabla P_0 - \rho'\partial\mathbf{u}/\partial t - \rho_0(\mathbf{u}\cdot\nabla)\mathbf{u} \quad ,$ (B.1)

Energy $\quad D\chi/Dt = 0 \quad ,$ (B.2)

where $D(\cdot)/Dt$ is the material derivative and is defined as follows:

$$D(\cdot)/Dt = \partial(\cdot)/\partial t + (\mathbf{u}\cdot\nabla)(\cdot) \quad . \tag{B.3}$$

A physical interpretation of the energy equation for an inhomogeneous fluid, Eq. (B.2), is that the entropy of any given fluid particle remains constant (see, for example, Pierce 1981, p.12). In the case of a

homogeneous fluid, the energy equation would be a little simpler. It would be interpreted as meaning that the entropy is the same for all fluid particles.

Since there are five variables and only four equations, we need another equation. We can get it from our earlier assumption that the losses due to the diffusion of dissolved salts are zero. This assumption is equivalent to saying that the change in salinity of any one fluid particle is zero (Landau and Lifshitz 1959, sec. 57),

$$D\xi/Dt = 0 \quad . \tag{B.4}$$

1. Linear Hydrodynamics Equations for Lossless Homogeneous Fluids

Retention of only first-order terms simplifies the hydrodynamics equations into a set of linear equations for homogeneous fluids. Since all the terms on the right-hand side of Eqs. (A.8) and (B.1) are second-order terms, they must be dropped. This leads to the following:

Linear Continuity $$\partial\rho'/\partial t + \rho_0 \nabla\cdot\mathbf{u} = 0 \quad , \tag{B.5}$$

Linear Momentum $$\rho_0 \partial\mathbf{u}/\partial t + \nabla P' = 0 \quad . \tag{B.6}$$

Turning our attention to the equation of state, Eq. (A.1), we see that by using a Taylor series expansion and retaining terms up to first order, the following equation can be obtained:

$$P = P_0 + (\rho - \rho_0)\left\{\frac{\partial P}{\partial \rho}\right\}_{\chi,\xi,\rho=\rho_0} \quad . \tag{B.7}$$

The small-signal sound speed is defined as follows:

$$c_0^2 \equiv \left\{\frac{\partial P}{\partial \rho}\right\}_{\chi,\xi,\rho=\rho_0} \quad . \tag{B.8}$$

Substituting Eq. (B.8) into the equation of state, Eq. (B.7), and using the expressions for the density and pressure given in Eqs. (A.5) and (A.6), we arrive at the following:

$$p' = c_0^2 \rho' \quad . \tag{B.9}$$

Equations (B.5), (B.6), and (B.9) are the linearized continuity, momentum, and state equations for a lossless homogeneous ocean.

2. Linear Hydrodynamics Equations for Lossless Inhomogeneous Fluids

Retention of first-order terms and inhomogeneity terms simplifies the hydrodynamics equations into a set of linear equations for inhomogeneous fluids. The continuity equation is obtained from Eq. (A.8) by dropping the nonlinear terms, the last two terms on the right-hand side. Similarly, the momentum equation is obtained from Eq. (B.1):

Continuity $$\partial\rho'/\partial t + \rho_0 \nabla\cdot\mathbf{u} + \mathbf{u}\cdot\nabla\rho_0 = 0 \quad , \tag{B.10}$$

Momentum $$\rho_0 \partial\mathbf{u}/\partial t + \nabla P' - (\rho'/\rho_0)\nabla P_0 = 0 \quad . \tag{B.11}$$

The equation of state is obtained by taking the material derivative of Eq. (A.1),

$$\frac{DP}{Dt} = \frac{D\rho}{Dt}\left\{\frac{\partial P}{\partial \rho}\right\}_{\chi,\xi,\rho=\rho_0} + \frac{D\chi}{Dt}\left\{\frac{\partial P}{\partial \chi}\right\}_{\rho,\xi,\chi=\chi_0} + \frac{D\xi}{Dt}\left\{\frac{\partial P}{\partial \xi}\right\}_{\rho,\chi,\xi=\xi_0}, \quad (B.12)$$

If Eqs. (B.2) and (B.4) are substituted into Eq. (B.12), the second and third terms of Eq. (B.12) drop out. Expansion using the definition of the small-signal sound speed, Eq. (B.8), yields

State $$\partial P'/\partial t + \mathbf{u}\cdot\nabla P_0 = c_0^2\,(\partial \rho'/\partial t + \mathbf{u}\cdot\nabla \rho_0) \quad . \quad (B.13)$$

Thus the linear equations of continuity, momentum, and state for a lossless, inhomogeneous fluid are Eqs. (B.10), (B.11), and (B.13).

3. Nonlinear Hydrodynamics Equations for Lossless Inhomogeneous Fluids

Retention of first-order terms as well as inhomogeneity and nonlinearity terms simplifies the hydrodynamics equations into a set of nonlinear equations for inhomogeneous fluids. The nonlinear equations of continuity and momentum for a lossless inhomogeneous fluid are Eqs. (A.8) and (B.1); no terms need to be dropped. The equation of state is more complicated than it was in the previous two cases. Retaining terms up to second-order in the Taylor series expansion of Eq. (A.1), we obtain

$$P = P_0 + (\rho - \rho_0)\left\{\frac{\partial P}{\partial \rho}\right\}_{\chi,\xi,\rho=\rho_0} + \frac{1}{2}(\rho - \rho_0)^2\left\{\frac{\partial^2 P}{\partial \rho^2}\right\}_{\chi,\xi,\rho=\rho_0}$$

$$+ (\xi - \xi_0)\left\{\frac{\partial P}{\partial \xi}\right\}_{\rho,\chi,\xi=\xi_0} + (\chi - \chi_0)\left\{\frac{\partial P}{\partial \chi}\right\}_{\rho,\xi,\chi=\chi_0} , \quad (B.14)$$

where it has been assumed that variations in the salinity and entropy are of second-order in smallness. Using the definition of the small-signal sound speed, Eq. (B.8), and the expressions for the density and pressure given in Eqs. (A.5) and (A.6), we see that Eq. (B.14) becomes

$$P' = c_0^2\rho' + \frac{1}{2}\rho'^2\left\{\frac{\partial^2 P}{\partial \rho^2}\right\}_{\chi,\xi,\rho=\rho_0} + (\xi - \xi_0)\left\{\frac{\partial P}{\partial \xi}\right\}_{\rho,\chi,\xi=\xi_0}$$

$$+ (\chi - \chi_0)\left\{\frac{\partial P}{\partial \chi}\right\}_{\rho,\xi,\chi=\chi_0} . \quad (B.15)$$

The nonlinear continuity, momentum, and state equations for a lossless inhomogeneous fluid are Eqs. (A.8), (B.1), and (B.15).

C. Substitution into Second-Order Terms Using First-Order Relations

Once a simplified form of the hydrodynamics equations has been obtained, the same level of approximation must be maintained consistently throughout any subsequent analysis. In the course of such analysis, it is often necessary for the dependent variable in a term to be replaced with an equivalent expression. It is therefore useful to note that the dependent variables in second-order terms may be replaced using first-order

relations without decreasing the overall level of the approximation. For example, suppose we decided to recast the $\rho' \partial u/\partial t$ term in Eq. (B.1). By using Eq. (B.6) we could substitute $\nabla P'/\rho_0$ for $\partial u/\partial t$; thus an equivalent second-order expression, $(P'/\rho_0)\ \nabla P'$, is formed. If we had substituted using an expression from Eq. (B.11), however, a higher-order term, $\rho'^2 \nabla P_0/\rho_0$, would be introduced. This term would have to be dropped in order to maintain the same level of approximation. This extra step is avoided by using the following rule: When substituting for the dependent variable in a second-order term, use a first-order relation (see, for example, Lighthill 1956).

D. Epilogue

In this chapter a ranking system was defined, and then used to simplify the lossless hydrodynamics equations into specialized forms. These forms can be readily combined into (1) the small-signal wave equation for homogeneous fluids, (2) the small-signal wave equation for inhomogeneous fluids, and (3) the nonlinear wave equation for inhomogeneous fluids.

CHAPTER 3

LINEAR GEOMETRICAL ACOUSTICS

A. Introduction

In this chapter linear geometrical acoustics, commonly referred to as ray theory, is discussed, and the mathematical techniques required for nonlinear geometrical acoustics are introduced. The linear hydrodynamics equations for a lossless inhomogeneous medium are combined to form the corresponding wave equation. A Galilean transformation in which the speed of the moving coordinate system is the small-signal sound speed c_0 is introduced. At the same time we introduce what is called the geometrical acoustics assumption. Use of the Galilean transformation and geometrical acoustics assumption enables us to separate the wave equation into two equations: the transport equation and the eikonal equation. The development is performed solely in the time domain. The gradient of the eikonal is related to the variation of the sound speed in the medium. For the case of a stratified ocean, we reduce the eikonal equation to an expression for the radius of curvature of the ray path. The transport equation is then reduced, via two transformations, to the form of the first-order plane wave equation for a homogeneous fluid.

The analysis starts with the linear hydrodynamics equations which include inhomogeneity terms. By the end of the derivation, however, all the inhomogeneity terms have been neglected. The inhomogeneity of the medium thus enters the wave equation solely through the dependence of the sound speed on position. Hence the results of this chapter are, within the ranking scheme of Chapter 2, valid to a first-order approximation.

B. Linear Lossless Wave Equation for Inhomogeneous Fluids

In this section the linear lossless hydrodynamics equations for an inhomogeneous fluid are combined to form a wave equation. First the continuity and state equations, Eqs. (2-B.10) and (2-B.13), are combined to eliminate the $\partial\rho'/\partial t'$ and $\mathbf{u}\cdot\nabla\rho_0$ terms. The time derivative of the result is

$$\frac{\partial^2 p'}{\partial t^2} + \frac{\partial \mathbf{u}}{\partial t}\cdot\nabla p_0 + \rho_0 c_0^2 \nabla\cdot\frac{\partial \mathbf{u}}{\partial t} = 0 \quad . \tag{B.1}$$

Use of the momentum equation, Eq. (2-B.11), eliminates the factor $\partial\mathbf{u}/\partial t$ term in Eq. (B.1). The result may be arranged in a convenient form

$$\nabla^2 p' - \frac{1}{c_0^2}\frac{\partial^2 p'}{\partial t^2} - \frac{\nabla\rho_0\cdot\nabla p'}{\rho_0} + \frac{\nabla p_0\cdot(\nabla p' - c_0^2\nabla\rho')}{\rho_0 c_0^2}$$

$$= \frac{\rho'|\nabla p_0|^2}{\rho_0^2 c_0^2} + \frac{\rho'}{\rho_0}\nabla^2 p_0 - \frac{2\rho'}{\rho_0}\nabla\rho_0\cdot\nabla p_0 \quad . \tag{B.2}$$

Since the three terms on the right-hand side of Eq. (B.2) are higher-order terms, they must be discarded in order to maintain the same level of

approximation. The fourth term on the left-hand side of Eq. (B.2) appears to be of second-order of smallness, an inhomogeneity term. Recalling the rule mentioned in Chapter 2, we may employ a first-order relation to substitute for the dependent variable P'. The appropiate first-order relation is the linear state equation for a homogeneous fluid, Eq. (2-B.9). Its use shows that the fourth term is actually of higher order and must therefore be dropped. The effect of discarding the fourth term is tantamount to having derived the wave equation disregarding the gravity term in the momentum equation, Eq. (2-A.3) (Bergmann 1946). By a more physical discussion, Bergmann concluded that the gravity term may be neglected in all but a few extreme situations, such as the propagation of very low frequency signals.

If all of the terms mentioned above are removed, Eq. (B.2) may be written as follows:

$$\nabla^2 p' - \frac{1}{c_0^2}\frac{\partial^2 p'}{\partial t^2} - \frac{\nabla \rho_0 \cdot \nabla p'}{\rho_0} = 0 \quad . \tag{B.3}$$

The first and second terms of Eq. (B.3) constitute the classical wave equation.

The third term is present because of the inhomogeneity of the fluid; this term was also discussed by Bergmann (1946). He concluded that it may be neglected if the density gradient is sufficiently small, or if the frequency of the signal is sufficiently high. (This may be shown by considering an example situation similar to that used below in Section E.) In fact Brekhovskikh and Lysanov (1982) state that the density gradient

term may be neglected for frequencies as low as 1 Hz. If the density gradient term is neglected, Eq. (B.3) becomes

$$\nabla^2 p' - \frac{1}{c_0^2} \frac{\partial^2 p'}{\partial t^2} = 0 \quad , \tag{B.4}$$

which has the form of the classical wave equation. Thus to a first-order approximation, all the effects of the fluid inhomogeneity enter through the variation of the small-signal sound speed c_0.

C. Geometrical Acoustics Assumption

The assumption that we are about to make is referred to as the geometrical acoustics assumption (see, for example, Landau and Lifshitz 1959, p. 256). The assumptions made up until now can be seen clearly with the aid of the ranking scheme; only first-order terms and second-order inhomogeneity terms have been retained, and the latter have been found insignificant. For geometrical acoustics another assumption is needed. We assume that the surface defined by an arbitrary wavefront is made up of many small segments of area, each of which may be regarded as plane. This is a reasonable assumption, since we are concerned with long range propagation. At long ranges the curvature of a spreading wave is very small. The signal associated with each small segment of area follows a path that is perpendicular to that segment. The path is called a ray; see Fig. 3.1. Within the geometrical acoustic assumption the travel time associated with propagation along each ray is defined as the integral of the reciprocal of the local sound speed along the ray path. All of the small

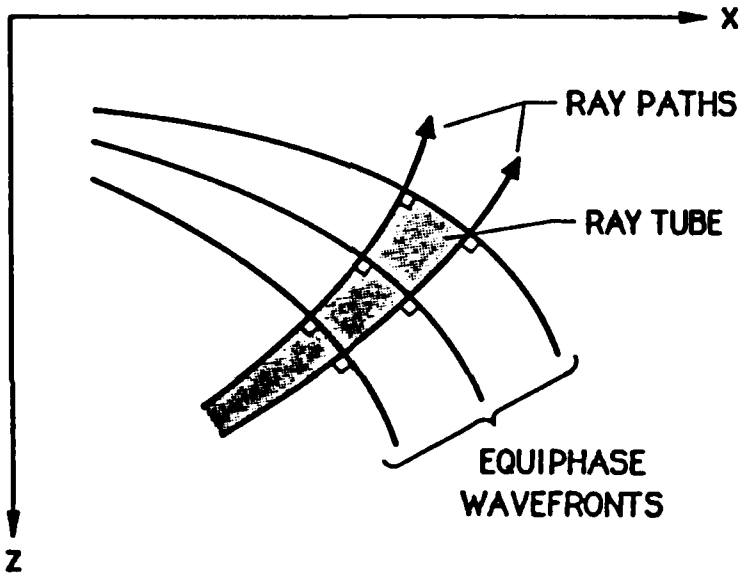

FIGURE 3.1
RAY PATHS AND EQUIPHASE WAVEFRONTS

plane surface elements that make up the wavefront are assumed to have the same phase (travel time), and hence the expression *equiphase wavefronts*. A small bundle of rays may be thought of as forming a tube. Since within the geometrical acoustics assumption no propagation takes place across rays, a propagating disturbance is bounded by the walls of its ray tube.

The geometrical acoustics assumption has, of course, a range of validity (see, for example, Frank, Bergmann, and Yaspan 1969, p. 63). When a ray turns appreciably over the distance of a wavelength, the equiphase wavefront assumption breaks down and diffraction has a strong effect on the propagation (signals do not remain confined to their ray tubes). It turns out that, for a ray to turn appreciably, the sound speed must vary rapidly over a wavelength. Hence, for geometrical acoustics to be a valid assumption, the sound speed must vary slowly on a wavelength scale.

Before imposing the geometrical acoustics assumption, we need to introduce the concept of retarded time. Consider a Galilean transformation in which the speed of the moving coordinate system is the small-signal sound speed c_0. In this system the new time t' is termed retarded time. For a plane wave, retarded time is defined as follows:

$$t' = t - x/c_0 \quad , \tag{C.1}$$

where x is the distance the wave is propagated. Note that x/c_0 is the travel time for all points on the wavefront; thus plane waves are equiphase wavefronts. For a spherical wave retarded time is

$$t' = t - (r-r_0)/c_0 \quad , \tag{C.2}$$

where r is the radial range and r_0 is the reference range. In this case the travel time is $(r-r_0)/c_0$. Note that geometrical acoustics is exact in the case of plane and spherical waves.

The use of retarded time as a new independent variable greatly simplifies wave equations. To illustrate this we use the retarded time variable in the first-order plane wave equation for a wave moving outwards through a homogeneous fluid. A first-order plane wave equation may be formed by separating the commutable derivatives in the classical wave equation as follows (see, for example, Pierce 1981, p. 20):

$$[\partial/\partial t - c_0^{-1}\,\partial/\partial x]\,[\partial/\partial t + c_0^{-1}\,\partial/\partial x]\,P' = 0 \quad . \tag{C.3}$$

The first term in square brackets may be thought of as an operator associated with incoming waves, and the second term, with outgoing waves. Integration with respect to one of the operators leads to a first-order wave equation. The integration constant must be zero to satisfy static conditions. The first-order wave equation for outgoing waves is as follows:

$$\partial P'/\partial t + c_0\,\partial P'/\partial x = 0 \quad . \tag{C.4}$$

Substitution of the outgoing wave function $P'(t - x/c_0)$ into Eq. (C.4) shows that Eq. (C.4) is the correct wave equation. If new independent variables x, t', where t' is given by Eq. (C.1), are introduced, Eq. (C.4) becomes

$$\partial P'/\partial x = 0 \quad . \tag{C.5}$$

This is a considerable simplification. The physical interpretation of Eq. (C.5) is simple: Since all points on the wave move with the same velocity as our new coordinate system, the wave appears motionless. Hence the derivative of the pressure with respect to x, holding t' constant, is zero.

The definition of retarded time in an inhomogeneous fluid is similar to its definition for plane and spherical waves. Because the small-signal sound speed may change along the ray path, the travel time is now a path integral:

$$t' = t - \int ds/c_0 \quad , \tag{C.6}$$

where ds is an incremental step along the ray path.

We now state a general definition of retarded time and introduce the eikonal $\Psi(\mathbf{r})$:

$$t' = t - \Psi(\mathbf{r}) \quad . \tag{C.7}$$

Note that the eikonal is a function of the ray path position vector $\mathbf{r}$; it is not a function of t'. The eikonal is defined to represent the travel time, or phase shift, associated with the distance between the origin of the wave and its current position. The integral in Eq. (C.6) plays the same role. It turns out that in the case of inhomogeneous media, this definition of the eikonal is equivalent to imposing the geometrical acoustics assumption. Note that if the eikonal $\Psi(\mathbf{r})$ is constant, an equiphase wavefront is defined. (For this reason, equiphase wavefronts are sometimes referred to as eikonal wavefronts.) Equiphase wavefronts are part of the geometrical

acoustics assumption. Thus use of the eikonal in our definition of retarded time means that the geometrical acoustics assumption is invoked.

The rate of change of the phase of the equiphase wavefront may be defined, by analogy with Eq. (C.6), as follows:

$$|\nabla\Psi| = 1/c_0 \quad . \tag{C.8}$$

This definition is important to our work in both this chapter and the next.

We now develop the relations necessary to apply the Galilean transformation based on Eq. (C.7) and thus to introduce the geometrical acoustics assumption. First the effect of the transformation on the spatial and temporal derivatives, ∇ and $\partial/\partial t$, is determined. Careful application of the chain rule leads to

$$\partial p'/\partial t \rightarrow \partial p'/\partial t' \quad , \tag{C.9}$$

$$\nabla p' \rightarrow \nabla p' - \nabla\Psi\partial p'/\partial t' \quad , \tag{C.10}$$

$$\nabla\cdot\mathbf{u} \rightarrow \nabla\cdot\mathbf{u} - \nabla\Psi\cdot\partial\mathbf{u}/\partial t' \quad , \tag{C.11}$$

$$\nabla^2 p' \rightarrow |\nabla\Psi|^2 \frac{\partial^2 p'}{\partial t'^2} - 2\frac{\partial}{\partial t'}(\nabla\Psi\cdot\nabla p') - \nabla^2\Psi\frac{\partial p'}{\partial t'} + \nabla^2 p' \quad . \tag{C.12}$$

As is shown below, the terms $\nabla\Psi\partial p'/\partial t'$ and $\nabla p'$ in Eq. (C.10) are, according to the ranking system of Chapter 2, associated with first-order effects and second-order effects, respectively. It is relatively simple to show that $\nabla\Psi\partial p'/\partial t'$ is associated with first-order effects. Recalling Eq. (C.5) we note that, after making the Galilean transformation, a linear

progressive plane wave appears motionless to the observer. The variation of the wave occurs solely with respect to the retarded time variable t'. Hence the derivative of a field variable, such as $\partial P'/\partial t'$, is a first-order term.

To show why the spatial variation $\nabla P'$ is associated with second-order effects, we again recall Eq. (C.5). In that equation we see that the spatial variation is zero in the case of a small-signal progressive plane wave. In the moving coordinate system the spatial variation term can have a non-zero value only if a wave changes its shape as it propagates. Three causes of change of shape are the decrease in amplitude due to geometric spreading, the effects of inhomogeneity, and finite amplitude effects. We are interested in propagation to long ranges, well into the farfield; hence the change due to geometrical spreading is small. In the ranking scheme of Chapter 2, the terms associated with small effects such as nonlinear distortion are ranked as second-order. Accordingly terms containing $\nabla P'$ are ranked as second-order. Note that we assume that the vector $\nabla P'$ is tangent to the ray path. This is in keeping with the geometrical acoustics assumption wherein the propagation of the signal down each ray tube is treated individually.

Because in the $\mathbf{r}$, t' system $\nabla P'$ is a second-order term, the first-order equivalent of Eq. (C.10) is

$$\nabla P' = -\nabla \Psi \partial P'/\partial t' \quad . \tag{C.13}$$

This relation is useful in reducing second-order terms. Recall the substitution rule that was mentioned in Chapter 2. For example, the

Galilean transformation of the second-order quantity $\nabla\rho_0\cdot\nabla P'$ in Eq. (B.3) has several parts, but on application of Eq. (C.13) reduces to $(\nabla\Psi\cdot\nabla\rho_0)\partial P'/\partial t'$.

Equation (C.13) is also useful for maintaining the same order of approximation in first-order relations. For example, consider the linearized momentum equation for a homogeneous medium, Eq. (2-B.6). The Galilean transformation of it with application of Eq. (C.13) in place of Eq. (C.10) is as follows:

$$\rho_0\partial u/\partial t' = \nabla\Psi\,\partial P'/\partial t' \quad . \tag{C.14}$$

Because Ψ is not a function of t', we may easily integrate Eq. (C.14) with respect to t'. Note that the integration constant must be zero in order to satisfy static conditions. The result is

$$\mathbf{u} = (P'/\rho_0)\nabla\Psi \quad . \tag{C.15}$$

This expression may be thought of as a generalization of the progressive plane wave impedance relation, $P' = \rho_0 c_0 u$. Equations (C.13) and (C.15) are used in the next chapter to simplify nonlinear terms.

We now apply the Galilean transformation to the small-signal wave equation for inhomogeneous media, Eq. (B.4). Using the transforms of the spatial and temporal derivatives, Eqs. (C.9) and (C.12), we obtain the following:

$$\left(\frac{1}{c_0^2} - |\nabla\Psi|^2\right)\frac{\partial^2 p'}{\partial t'^2} + \frac{\partial}{\partial t'}(2\nabla\Psi\cdot\nabla p' + \nabla^2\Psi p') = \nabla^2 p' . \qquad (C.16)$$

In order to assess the relative importance of the term on the right-hand side of Eq. (C.16), $\nabla^2 p'$, we need to understand its physical significance. The Laplacian of the acoustic pressure p' is defined to be the divergence of the gradient of p'; that is, $\nabla^2 p' \equiv \nabla\cdot\nabla p'$. It has already been argued that, in the moving coordinate system, $\nabla p'$ is related to second-order effects, the variation of the shape of propagating wave. Hence $\nabla\cdot\nabla p'$ is the rate of change of the variation. In the case at hand, small-signal propagation, the variation of the propagating wave is due solely to geometric spreading. In geometrical acoustics the ray paths are not permitted to turn appreciably over a wavelength; hence the spreading takes place gradually. The rate of change of the spreading is therefore assumed to be zero. In the case of finite amplitude waves, the situation is not so simple. As already noted the term $\nabla p'$ is assumed to be associated with the second-order effects of finite amplitude and inhomogeneity; it is also assumed to be tangent to the ray path. We now assume the distortion effects occur slowly and without sudden changes. With this assumption the term $\nabla^2 p'$ can be neglected since $|\nabla p'| \gg |\nabla^2 p'|$. Note that in other situations, such as those in which the rays turn rapidly, the term $\nabla^2 p'$ is important since it accounts for diffraction (Pelinovsky, Petukov, and Fridman 1979).

If the right-hand member is neglected, Eq. (C.16) may be expressed as follows:

$$\left(\frac{1}{c_0^2} - |\nabla\Psi|^2\right)\frac{\partial^2 p'}{\partial t'^2} + \frac{\partial}{\partial t'}\left[\frac{1}{p'}\nabla\cdot(\nabla\Psi p'^2)\right] = 0 \quad . \qquad (C.17)$$

We now split Eq. (C.17) into two parts. To do this we use Eq. (C.8) which was obtained from the geometrical acoustics assumption, and which shows that the first part of Eq. (C.17) vanishes,

$$1/c_0^2 - |\nabla\Psi|^2 = 0 \quad . \qquad (C.18)$$

Equation (C.18) is referred to as the eikonal equation. As is shown in the next section, the eikonal equation dictates the acoustic ray paths. The remainder of Eq. (C.17) may be integrated once with respect to the retarded time variable t'. Noting that the integration constant must be zero in order to satisfy static conditions, we arrive at the following:

$$\nabla\cdot(\nabla\Psi p'^2) = 0 \quad . \qquad (C.19)$$

Equation (C.19) is called the transport equation and is equivalent to Eq. (8-5.13) in the book by Pierce (1981). It turns out that this equation governs the variation of the acoustic pressure along the ray path.

D. Ray Paths from the Eikonal

In this section it is shown that the eikonal equation, Eq. (C.18), defines the acoustic ray paths. (A ray path and the coordinate system are shown in Fig. 3.2.) First the connnection between the eikonal and the ray path is found. Next the ray path is linked to the spatial variation of the

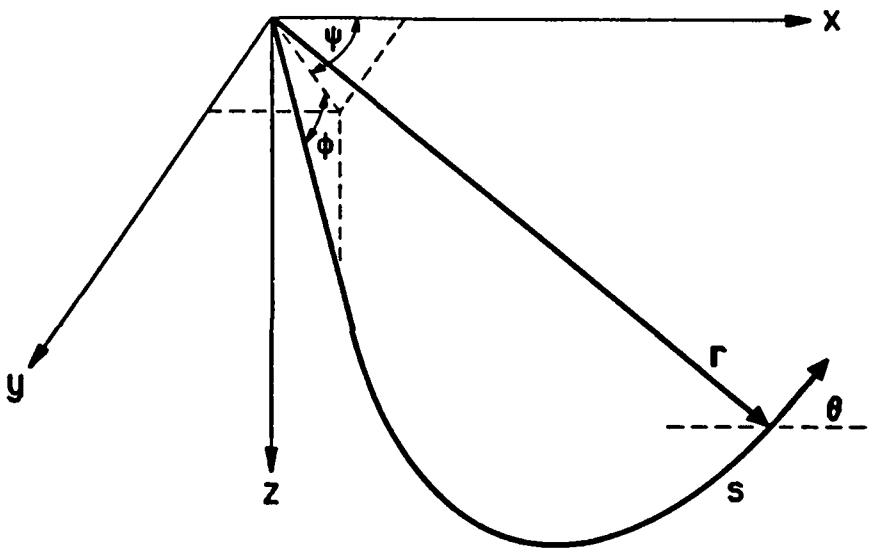

FIGURE 3.2
THE RAY COORDINATE SYSTEM

sound speed. We then combine the two ideas and find a general relation for the ray paths in terms of the gradient of the eikonal, the gradient of the sound speed, and the tangent to the ray path. The general relation is then simplified for the case of a stratified medium.

A connection between the eikonal and the ray path is sought. The eikonal defines an equiphase surface; thus $\nabla\Psi$ is by definition, normal to that surface (see, for example, Thomas 1968, Sec. 15.6). Since Eq. (C.18) gives the square of the magnitude of $\nabla\Psi$, it is easily seen that

$$c_0\nabla\Psi = \mathbf{n} \quad , \tag{D.1}$$

where $\mathbf{n}$ is the unit normal to the surface. It is known from vector calculus that the unit tangent to the ray path $\mathbf{T}$ is defined as the derivative of the ray path position vector $\mathbf{r}$ with respect to the ray path lengths,

$$\mathbf{T} \equiv \partial\mathbf{r}/\partial s \quad . \tag{D.2}$$

Since the ray path is normal to the wavefront, the unit tangent to the ray path and the unit normal to the wavefront are equal,

$$\mathbf{T} = \mathbf{n} \quad . \tag{D.3}$$

(Note that they are not necessarily equal in the case of a moving medium; see, for example, Pierce 1981, p. 371.) Combining Eqs. (D.1) and (D.2) yields the following relation:

$$c_0\nabla\Psi = \partial\mathbf{r}/\partial s \quad . \tag{D.4}$$

The gradient of the eikonal is thus closely related to the tangent to the ray path.

An equation that links the ray path with the variation of the sound speed in the medium is now sought. From the Frenet-Serret formulas (see, for example, Sokolnikoff and Redheffer 1958, Sec. 4.11), we know that a ray path may be thought of as a sequence of arcs of radius R, wherein R varies as a function of position along the ray path. The following equations are part of the Frenet-Serret formulas:

$$K\mathbf{N} \equiv \partial \mathbf{T}/\partial s \quad , \tag{D.5}$$

$$R \equiv 1/K \quad , \tag{D.6}$$

where K is the curvature and **N** is the principal normal. The principal normal is defined to be normal to **T** and point towards the center of curvature. From the above relations the radius of curvature R may be expressed as follows:

$$R = |\partial \mathbf{T}/\partial s|^{-1} \quad . \tag{D.7}$$

Because of its close relation to the ray path, let us find an expression for R or, equivalently, an expression for $\partial \mathbf{T}/\partial s$. Use of Eq. (D.2) yields

$$\partial \mathbf{T}/\partial s = \partial(\partial \mathbf{r}/\partial s)/\partial s \quad . \tag{D.8}$$

Noting Eq. (D.4) and the relation $\partial/\partial s = (\partial \mathbf{r}/\partial s \cdot \nabla)$, we see that Eq. (D.8) becomes

$$\partial T/\partial s = (\partial r/\partial s \cdot \nabla)(c_0 \nabla \Psi) \quad . \tag{D.9}$$

Reapplication of Eq. (D.4) gives

$$\partial T/\partial s = (c_0 \nabla \Psi \cdot \nabla)(c_0 \nabla \Psi) \quad . \tag{D.10}$$

Use of the chain rule and the following relation (see, for example, Gradshteyn and Ryzhik 1980, Eq. 10.31.3),

$$(\nabla \Psi \cdot \nabla) \nabla \Psi = 1/2 \nabla (\nabla \Psi \cdot \nabla \Psi) \quad ,$$

in Eq. (D.10) leads to

$$\partial T/\partial s = \nabla \Psi (c_0 \nabla \Psi \cdot \nabla c_0) + (c_0^2/2) \nabla (\nabla \Psi \cdot \nabla \Psi) \quad . \tag{D.11}$$

Use of the eikonal equation, Eq. (C.18), and the chain rule in Eq. (D.11) yields

$$\partial T/\partial s = c_0 \nabla \Psi (\nabla \Psi \cdot \nabla c_0) - (\nabla c_0)/c_0 \quad . \tag{D.12}$$

Recalling Eq. (D.7) we note that Eq. (D.12) connects the radius of curvature R to the variation in the sound speed ∇c_0. Since the ray paths are arcs of radius R, Eq. (D.12) may be thought of as connecting the ray paths with the variation of the sound speed. Equation (D.12) is equivalent to Eq. (66.6) in the book by Landau and Lifshitz (1959).

A physical understanding of Eq. (D.12) may be obtained by considering a simple example. Let the medium be azimuthally symmetric (thus restricting ourselves to the x,z plane) and stratified, that is, the sound speed profile does not vary in range. (Recall that **k** is in the direction

of increasing depth.) An expression for the radius of curvature R can be found by reexamining Eq. (D.12). Under conditions stated above, the terms in Eq. (D.12) may be defined as follows:

$$\nabla c_0 = \mathbf{k}\, h \quad , \tag{D.13}$$

$$\partial \mathbf{r}/\partial s = \mathbf{i} \cos\theta + \mathbf{k} \sin\theta \quad , \tag{D.14}$$

where h is the gradient of the sound speed profile $\partial c_0/\partial z$, θ is the acute angle between the ray path and the horizontal (see Fig. 3.2), and **i** and **k** are unit vectors in the Cartesian system. If Eq. (D.4) is used, Eq. (D.14) may be recast in the following form:

$$\nabla \Psi = \mathbf{i}\, c_0^{-1} \cos\theta + \mathbf{k}\, c_0^{-1} \sin\theta \quad . \tag{D.15}$$

Substituting Eq. (D.13) and (D.15) into (D.12) yields the following:

$$\partial \mathbf{T}/\partial s = h\, c_0^{-1} \cos\theta \; (\mathbf{i} \sin\theta - \mathbf{k} \cos\theta) \quad . \tag{D.16}$$

Let us interpret Eq. (D.16). From a geometrical consideration of the equation we see that, if the gradient h is positive, the center of curvature is above the current ray path position. The converse is true when h is negative. Thus the acoustic rays bend toward the region of the slower sound speed. From the reciprocal of the magnitude of Eq. (D.16), we obtain the radius of curvature:

$$R = c_0/(|h| \cos\theta) \quad . \tag{D.17}$$

The quantity $c_0/\cos\theta$ in Eq. (D.17) is, according to Snell's law, a constant. From Eq. (D.17) and Snell's law we see that, if h is constant, the radius of curvature R must be constant. Therefore rays in a constant gradient medium are circular arcs. Equation (D.17) appears in a variety of references (see, for example, Officer 1958, Eq. 2-82).

In summary it has been shown that, from the eikonal equation and the relations of vector calculus, a general expression for the ray paths may be found. Moreover, in the case of a constant gradient medium, the ray paths are circular arcs.

E. Acoustic Pressure from the Transport Equation

In this section it is shown that the transport equation, Eq. (C.19), may be placed in the form of the first-order plane wave equation in the moving coordinate system, Eq. (C.5). It turns out that the transport equation governs the acoustic pressure at any point along the ray path, and that the acoustic pressure is related to the area of the ray tube. To show this we introduce the concept of ray coordinates and use an expression that is required in our development of nonlinear geometrical acoustics. (The details of the transformation from Cartesian coordinates to ray coordinates are included in Appendix A.) The three ray coordinates are the ray path length s and the initial ray launch angles ϕ and ψ; see Fig. (3.2).

To reduce the transport equation we need an expression for $\nabla^2\Psi$. The following relationship is derived in Appendix A:

$$\nabla^2\Psi = \frac{1}{A_0}\frac{\partial}{\partial s}\left(\frac{A_0}{c_0}\right) \quad , \tag{E.1}$$

where A_0 is the ray tube area. It is shown below that the dependence of $\nabla^2\Psi$ on the variation in the sound speed may be neglected. We first rearrange Eq. (E.1) as follows:

$$\nabla^2\Psi = \frac{1}{c_0}\left[\frac{A_{0s}}{A_0}\frac{\partial}{\partial s}\left(\frac{A_0}{A_{0s}}\right) - \frac{c_{0s}}{c_0}\frac{\partial}{\partial s}\left(\frac{c_0}{c_{0s}}\right)\right] \quad , \tag{E.2}$$

where A_{0s} and c_{0s} are the ray tube area and the sound speed at the reference ray path length (1 meter in this example). Consider vertical propagation in a stratified ocean 5000 m deep. Let the sound speed increase linearly with depth from 1400 m/s to c_{0s} = 1600 m/s; i.e., $c_0 = 1400 + 0.04\,z$, where z is the depth. This is a larger variation than is usually expected in the ocean and may be regarded roughly as an upper bound. In the case of vertical propagation, $\partial/\partial s = \partial/\partial z$ and the ray tube areas may be approximated by using spherical spreading. The ratio of the ray tube areas A_0/A_{0s} is z^2; hence $\partial(A_0/A_{0s})/\partial z = 2z$. If the propagation path is the full ocean depth, 5000 m, the term $(A_{0s}/A_0)\partial(A_0/A_{0s})/\partial s$ is equal to 4×10^{-04}. Using the conditions given above, the term $(c_{0s}/c_0)\partial(c_0/c_{0s})/\partial s$ can be seen to be approximately 3×10^{-05}. Therefore, even when the variation of the sound speed is unusually large, the term $(c_{0s}/c_0)\partial(c_0/c_{0s})/\partial s$ is small with respect to $(A_{0s}/A_0)\partial(A_0/A_{0s})/\partial s$. The variation in the sound speed is therefore neglected in Eq. (E.2), and Eq. (E.1) reduces to

$$\nabla^2\Psi = (c_0 A_0)^{-1}\, \partial A_0/\partial s \quad . \tag{E.3}$$

One other relation is required to reduce the transport equation. Starting with the expression $\partial/\partial s = (\partial r/\partial s \cdot \nabla)$, and recalling Eq. (D.4), we see that

$$\nabla\Psi \cdot \nabla(\cdot) = (1/c_0)\partial(\cdot)/\partial s \quad . \tag{E.4}$$

Simplification of the transport equation, Eq. (C.19), is obtained by forcing it toward the form of Eq. (C.5). Substitution of Eqs. (E.3) and (E.4) in the transport equation gives the following:

$$\frac{\partial P'}{\partial s} + \frac{P'}{2A_0}\frac{\partial A_0}{\partial s} = 0 \quad . \tag{E.5}$$

Equation (E.5) may be expressed as a perfect differential by multiplying both sides by $A_0^{1/2}$ and rearranging,

$$\partial(P' A_0^{1/2})/\partial s = 0 \quad . \tag{E.6}$$

A physical interpretation of Eq. (E.6) is that $P' A_0^{1/2}$ is constant along the ray tube, a result consistent with the assumption that the energy is constant along the tube. The fact that $P' A_0^{1/2}$ is constant suggests a new dependent variable, one for which the amplitude is not affected by geometric spreading. To make the new dependent variable have the same units as P', it is defined as follows:

$$W \equiv (A_0/A_{0s})^{1/2} P' \quad . \tag{E.7}$$

If this transformation is used, Eq. (E.6) becomes

$$\partial W/\partial s = 0 \quad , \tag{E.8}$$

which has the desired form of Eq. (C.5)

We now obtain the solution of the problem of propagation of small-signal waves through an inhomogeneous medium. The analogous solution for a plane wave in a homogeneous fluid is as follows. Given the boundary condition

$$P' = g(t) = g(t') \quad \text{at} \quad x = 0 \quad , \tag{E.9}$$

the solution is

$$P' = g(t') \quad , \tag{E.10}$$

where t' is given by Eq. (C.1). For the problem of waves propagating in an inhomogeneous medium, the boundary condition is

$$P' = g(t) = g(t') \quad \text{at} \quad s = s_0 \quad . \tag{E.11}$$

Although the boundary condition does not have quite the same form as Eq. (E.9), the form can be made exactly the same by defining a new independent variable. The new variable should not, however, alter the form of Eq. (E.8). The desired transform is

$$Z = s - s_0 \quad . \tag{E.12}$$

(Note that Z is not the same as z, the depth.) The boundary condition is now

$$P' = g(t) = g(t') \quad \text{at} \quad Z = 0 \ , \tag{E.13}$$

where

$$t' = t - Z/c_0 \ . \tag{E.14}$$

Equation (E.8) now becomes

$$\partial W/\partial Z = 0 \ . \tag{E.15}$$

Equation (E.15) is in the form of Eq. (C.5). Since Eq. (E.13) is equivalent to Eq. (E.9), the solution of the problem of propagation in an inhomogeneous medium is, by analogy,

$$W = g(t') \ , \tag{E.16}$$

where Z and W are defined in Eqs. (E.12) and (E.7).

Thus the linear transport equation for an inhomogeneous fluid, Eq. (C.19), has been transformed into an equation in the form of the first-order plane wave equation for a homogeneous medium by making two simple transformations: one on the dependent variable P', Eq. (E.7), and the other on the independent variable s, Eq. (E.12). The main reason for introducing the W and Z transformations is to prepare the reader for similar, but more complicated, transforms in Chapter 4.

CHAPTER 4

NONLINEAR GEOMETRICAL ACOUSTICS

This chapter progresses in a fashion only slightly different from that of the previous chapter. In Chapter 3 the linear lossless hydrodynamics equations for an inhomogeneous fluid were combined to form the corresponding wave equation. Next a Galilean transformation, based on the use of the retarded time t', and the geometrical acoustics assumption were introduced. The Galilean transformation was then applied to the wave equation. In this chapter we start with the nonlinear lossless hydrodynamics equations. They are not, however, combined to form a nonlinear wave equation, but instead only partially combined. The Galilean transformation and the geometrical acoustics assumption are then introduced. The hydrodynamics equations are transformed and then combined to form a wave equation in the moving coordinate system. From this point on, the development parallels that in Chapter 3. After the $\nabla^2 p'$ term is dropped, the transformed wave equation is separated into the eikonal equation and the transport equation. The equations are then discussed. After simplification the transport equation is reduced to a first-order (nonlinear) wave equation. This equation has the same form as the first-order equation for plane waves of finite amplitude in a

homogeneous medium. The reason we depart from the procedure followed in Chapter 3 is that it is simpler to do so. It is easier to transform and approximate the hydrodynamics equations and then combine them to obtain a wave equation than vice versa.

In this chapter the standard geometrical acoustics assumption must be broadened. In particular the acoustic ray paths are assumed to be unaffected by the signal; that is, self-refraction does not occur. This assumption means that acoustic ray path equations developed in the previous chapter may be used even for signals of finite amplitude. Specifically, the eikonal equation, Eq. (3-C.18), and the equation developed in Appendix A, Eq. (3-E.3), are still valid.

The level of approximation used in this chapter differs from that used in the previous chapter. There the only second-order terms that were considered were the inhomogeneity terms. In the end even these terms were found to be so small that they were neglected. Within the ranking system of Chapter 2, this means that the results of the previous chapter are valid to a first-order approximation only. In this chapter we are specifically interested in examining the effects of another type of second-order term, nonlinear terms. In order to be consistent in our level of approximation, terms due to both inhomogeneity and nonlinearity are included throughout the entire derivation. Thus within the ranking system of Chapter 2, the results obtained in this chapter are valid to a second-order approximation.

As was mentioned in Chapter 1, no new material is presented in this chapter. The following derivation closely follows that of Pelinovsky,

Petukhov, and Fridman (1979), whose work is in turn related to that of Ostrovsky, Pelinovsky, and Fridman (1976). Both of the cited papers are, however, terse. So much so in fact that it was decided that the full derivation of nonlinear geometrical acoustics should be presented here. That decision in turn led to the inclusion of much background material that appears in Chapters 2 and 3.

A. Combining the Hydrodynamics Equations

The lossless nonlinear hydrodynamics equations for an inhomogeneous fluid were developed in Chapter 2. To combine the nonlinear continuity and momentum equations, Eqs. (2-A.8) and (2-B.1), we take the time derivative of continuity equation, the divergence of the momentum equation, and substitute the former into the latter via the $\nabla\cdot\rho_0\partial\mathbf{u}/\partial t$ term. Placing all nonlinear terms on the right-hand side, we obtain the following equation:

$$\frac{\partial^2\rho'}{\partial t^2} - \nabla^2 p' + \frac{\nabla\rho'\cdot\nabla p_0}{\rho_0} = \nabla\cdot\left[\rho_0(\mathbf{u}\cdot\nabla)\mathbf{u} - \frac{\rho'}{\rho_0}\nabla p' - \frac{\partial(\rho'\mathbf{u})}{\partial t}\right] \quad . \qquad (A.1)$$

To arrive at Eq. (A.1), we neglected several third-order terms: terms involving the Laplacian of environmental parameters such as $\nabla^2 p_0$, and terms involving the products of gradients of environmental parameters such as $\nabla\rho_0\cdot\nabla p_0$. It was also necessary to use the linear momentum equation for a homogeneous fluid, Eq. (2-B.6), to simplify one of the second-order terms.

The next step is to eliminate ρ' and u from Eq. (A.1). To develop some of the relations required to do this, we turn our attention to the equation of state, Eq. (2-A.1). The second-order Taylor series expansion of the equation of state is given in Eq. (2-B.15). We now find the temporal derivative of Eq. (2-B.15) and the gradient of Eq. (2-A.1):

$$\frac{\partial p'}{\partial t} = c_0^2 \frac{\partial \rho'}{\partial t} + 2c_0\rho' \frac{\partial \rho'}{\partial t}\left\{\frac{\partial c_0}{\partial \rho}\right\}_{\xi,\chi,\rho=\rho_0}$$

$$- (\mathbf{u}\cdot\nabla)\xi\left\{\frac{\partial p}{\partial \xi}\right\}_{\rho,\chi,\xi=\xi_0} - (\mathbf{u}\cdot\nabla)\chi\left\{\frac{\partial p}{\partial \chi}\right\}_{\rho,\xi,\chi=\chi_0} . \qquad (A.2)$$

$$\nabla p = c_0^2 \nabla\rho + \nabla\xi\left\{\frac{\partial p}{\partial \xi}\right\}_{\rho,\chi,\xi=\xi_0} + \nabla\chi\left\{\frac{\partial p}{\partial \chi}\right\}_{\rho,\xi,\chi=\chi_0} . \qquad (A.3)$$

In arriving at Eq. (A.2), we have made use of the fact that the entropy and salinity of a material particle remain constant; see Eqs. (2-B.2) and (2-B.4). We have also used the definition of the small-signal sound speed, Eq. (2-B.8).

To reduce the effort required to combine Eqs. (A.1), (A.2), and (A.3), we make use of the Galilean transformation and geometrical acoustics assumption, which are discussed at length in the previous chapter.

B. Geometrical Acoustics Assumption

The Galilean transformation and the geometrical acoustics

assumption are used in the previous chapter to reduce the linear wave equation to the eikonal equation and a first-order wave equation that has the form of Eq. (3-C.5). In this chapter we transform the ingredients of the wave equation, that is, the nonlinear hydrodynamics equations for inhomogenenous fluids. The equations are then combined to form a wave equation in the moving coordinate system.

Before the Galilean transformation is applied to the nonlinear hydrodynamics equations, it is useful to review the transformation as applied to the equation for finite amplitude plane waves propagating through a homogeneous medium. The equation is as follows (see, for example, Blackstock 1972):

$$P'_t + c_0 P'_x - (\beta/\rho_0 c_0^2)\, P' P'_t = 0 \quad , \tag{B.1}$$

where the subscripts t and x indicate derivatives with respect to time and distance, respectively, and β is the coefficient of nonlinearity (see Appendix B). Equation (B.1) is the nonlinear extension of Eq. (3-C.4). Introduction of the retarded time variable for plane waves, Eq. (3-C.1), transforms Eq. (B.1) into the following:

$$P'_x - (\beta/\rho_0 c_0^3)\, P' P'_{t'} = 0 \quad . \tag{B.2}$$

Equation (B.2) is the equation for outgoing plane waves in the second approximation. It is the nonlinear extension of Eq. (3-C.5). Equation (B.2) has been analyzed extensively in the past and its solution, called the Earnshaw solution, is well known (see, for example, Blackstock 1972). Use

of the Galilean transformation and the geometrical acoustics assumption enables the nonlinear hydrodynamics equations to be put into the form of Eq. (B.2); then the problem of propagation in an inhomogeneous medium will have been solved.

The Galilean transformation is now applied to Eqs. (A.1), (A.2), and (A.3). The new time variable t' is defined by Eq. (3-C.7). Expressions for various spatial and temporal derivatives are given in Eqs. (3-C.9) through (3-C.12). Since the Galilean transformation is a mathematical coordinate transformation, it is unaffected by the inclusion of nonlinear terms. Equation (A.1) becomes

$$\frac{\partial^2 \rho'}{\partial t'^2} - |\nabla\Psi|^2 \frac{\partial^2 p'}{\partial t'^2} + 2\frac{\partial(\nabla\Psi\cdot\nabla p')}{\partial t'} + \nabla^2\Psi\frac{\partial p'}{\partial t'} - \nabla^2 p' - \frac{\nabla\Psi\cdot\nabla p_0}{\rho_0}\frac{\partial \rho'}{\partial t'}$$

$$= -\nabla\Psi\cdot\frac{\partial}{\partial t'}\left[\rho_0(\mathbf{u}\cdot\nabla\Psi)\frac{\partial \mathbf{u}}{\partial t'} + \frac{\rho'}{\rho_0}\nabla\Psi\frac{\partial p'}{\partial t'} - \frac{\partial(\rho'\mathbf{u})}{\partial t'}\right] . \qquad \text{(B.3)}$$

To arrive at Eq. (B.3), we have used the first-order expression for the gradient, Eq. (3-C.13), in nonlinear and inhomogeneity terms. The spatial and temporal derivatives of the equation of state, Eqs. (A.2) and (A.3) become, respectively,

$$\frac{\partial p'}{\partial t'} = c_0^2\frac{\partial \rho'}{\partial t'} + 2c_0\rho'\frac{\partial \rho'}{\partial t'}\left\{\frac{\partial c_0}{\partial \rho}\right\}_{\xi,\chi,\rho=\rho_0} + (\mathbf{u}\cdot\nabla\Psi)\frac{\partial \xi'}{\partial t'}\left\{\frac{\partial p}{\partial \xi}\right\}_{\rho,\chi,\xi=\xi_0}$$

$$+ (\mathbf{u}\cdot\nabla\Psi)\frac{\partial \chi'}{\partial t'}\left\{\frac{\partial p}{\partial \chi}\right\}_{\rho,\xi,\chi=\chi_0} , \qquad \text{(B.4)}$$

$$\nabla p_0 + \nabla p' - \nabla\Psi\frac{\partial p'}{\partial t'} = c_0^2\left(\nabla\rho_0 + \nabla\rho' - \nabla\Psi\frac{\partial\rho'}{\partial t'}\right)$$
$$+ \left(\nabla\xi_0 + \nabla\xi' - \nabla\Psi\frac{\partial\xi'}{\partial t'}\right)\left\{\frac{\partial p}{\partial\xi}\right\}_{\rho,\chi,\xi=\xi_0}$$
$$+ \left(\nabla\chi_0 + \nabla\chi' - \nabla\Psi\frac{\partial\chi'}{\partial t'}\right)\left\{\frac{\partial p}{\partial\chi}\right\}_{\rho,\xi,\chi=\chi_0} \qquad \text{(B.5)}$$

Equations (B.4) and (B.5) are now rearranged in anticipation of combining them with Eq. (B.3). First consider Eq. (B.4); take its time (t') derivative, remembering that $\nabla\Psi$ is independent of t'. Use of the linear momentum equation in the moving coordinate system, Eq. (3-C.15), the eikonal equation, Eq. (3-C.18), and the linear equation of state, Eq. (2-B.9), results in the following equation:

$$\frac{\partial^2\rho'}{\partial t'^2} = \frac{1}{c_0^2}\frac{\partial^2 p'}{\partial t'^2} - \frac{2}{c_0^5}\frac{\partial}{\partial t'}\left(p'\frac{\partial p'}{\partial t'}\right)\left\{\frac{\partial c_0}{\partial\rho}\right\}_{\xi,\chi,\rho=\rho_0}$$
$$- \frac{1}{\rho_0 c_0^4}\frac{\partial}{\partial t'}\left(p'\frac{\partial\chi'}{\partial t'}\right)\left\{\frac{\partial p}{\partial\chi}\right\}_{\rho,\xi,\chi=\chi_0}$$
$$- \frac{1}{\rho_0 c_0^4}\frac{\partial}{\partial t'}\left(p'\frac{\partial\xi'}{\partial t'}\right)\left\{\frac{\partial p}{\partial\xi}\right\}_{\rho,\chi,\xi=\xi_0} \qquad \text{(B.6)}$$

Multiplication of Eq. (B.5) by $\nabla\Psi(\rho'/\rho_0)$ places it in a more readily usable form. The same relations used in arriving at Eq. (B.6), namely, Eqs. (3-C.14), (3-C.18), and (2-B.9) are then used to simplify the result. Rearranging and

taking the derivative with respect to t' yields

$$\frac{\partial \rho'}{\partial t'}\frac{\nabla\Psi\cdot\nabla P_0}{\rho_0} = \frac{\nabla\rho_0\cdot\nabla\Psi}{\rho_0}\frac{\partial p'}{\partial t'} - \frac{1}{\rho_0 c_0^4}\frac{\partial}{\partial t'}\left(p'\frac{\partial \xi'}{\partial t'}\right)\left\{\frac{\partial P}{\partial \xi}\right\}_{\rho,\chi,\xi=\xi_0}$$

$$- \frac{1}{\rho_0 c_0^4}\frac{\partial}{\partial t'}\left(p'\frac{\partial \chi'}{\partial t'}\right)\left\{\frac{\partial P}{\partial \chi}\right\}_{\rho,\xi,\chi=\chi_0} \quad . \tag{B.7}$$

Equations (B.6) and (B.7) may be combined with Eq. (B.3). First simplify the right-hand side of Eq. (B.3) using the same techniques used to arrive at Eqs. (B.6) and (B.7). Substitution of Eqs. (B.6) and (B.7) into the left-hand side of Eq. (B.3) leads to

$$\left(\frac{1}{c_0^2} - |\nabla\Psi|^2\right)\frac{\partial^2 p'}{\partial t'^2} + \frac{\partial}{\partial t'}\left[2\nabla\Psi\cdot\nabla p' + \left(\nabla^2\Psi - \frac{\nabla\rho_0\cdot\nabla\Psi}{\rho_0}\right)p'\right]$$

$$- \nabla^2 p' = \frac{2\beta}{\rho_0 c_0^4}\frac{\partial}{\partial t'}\left(p'\frac{\partial p'}{\partial t'}\right) \quad , \tag{B.8}$$

where the coefficent of nonlinearity β is defined as follows:

$$\beta \equiv 1 + \frac{\rho_0}{c_0}\left\{\frac{\partial c_0}{\partial \rho}\right\}_{\xi,\chi,\rho=\rho_0} \quad . \tag{B.9}$$

Equation (B.8) is similar to the linear geometrical acoustics equation, Eq. (3-C.16). The main difference is that Eq. (B.8) has a nonlinear term on the right-hand side. Another difference is that the left-hand side contains an inhomogeneity term, namely, $(\nabla\rho_0\cdot\nabla\Psi/\rho_0)p'$. The ancestor of this term

is the third term in Eq. (3-B.3), there referred to as the density gradient term. Neglected in Chapter 3 as being unimportant except for exceedingly low frequencies, the density gradient term is retained here. In this chapter we are specifically interested in examining finite amplitude effects. In order to be consistent in our level of approximation, we maintain the second-order terms due to both inhomogeneity and finite amplitude effects throughout the entire derivation.

Finally, as in linear geometrical acoustics, we discard $\nabla^2 p'$. It was noted in the previous chapter that this term is associated with the rate of change of the distortion. Since the distortion is assumed to occur slowly, the rate of change of distortion must be very small and is therefore neglected. The final form of the nonlinear geometrical acoustics equation is as follows:

$$\left(\frac{1}{c_0^2} - |\nabla\Psi|^2\right)\frac{\partial^2 p'}{\partial t'^2} + \frac{\partial}{\partial t'}\left[2\nabla\Psi\cdot\nabla p' + \left(\nabla^2\Psi - \frac{\nabla\rho_0\cdot\nabla\Psi}{\rho_0}\right)p'\right]$$

$$= \frac{2\beta}{\rho_0 c_0^4}\frac{\partial}{\partial t'}\left(p'\frac{\partial p'}{\partial t'}\right) \quad . \tag{B.10}$$

C. Reduction of the Nonlinear Geometrical Acoustics Equation

The techniques used in this section to reduce the nonlinear geometrical acoustics equation are the same as those used in Chapter 3 to reduce the linear geometrical acoustics equation. Since we assume that the geometrical acoustics assumption is valid in the case of finite amplitude

waves, we may use the eikonal equation, Eq. (3-C.18), to eliminate the first two terms on the left-hand side of Eq. (B.10). The remaining terms constitute the transport equation which in this case is nonlinear. The procedure used in Chapter 3 to reduce the transport equation to a first-order wave equation is now repeated. In this case the first-order wave equation has the form of Eq. (B.2). Noting that $\nabla\Psi$ is independent of t', we integrate the remaining terms in Eq. (B.10) once with respect to t'. The integration constant must be zero in order to satisfy static conditions. The result is

$$2\nabla\Psi\cdot\nabla P' + \left(\nabla^2\Psi - \frac{\nabla\rho_0\cdot\nabla\Psi}{\rho_0}\right)P' = \frac{2\beta}{\rho_0 c_0^4}P'\frac{\partial P'}{\partial t'} \quad . \tag{C.1}$$

Use of the same equations used to reduce the linear transport equation, namely Eqs. (3-E.3) and (3-E.4) and the eikonal equation, Eq. (3-C.18), enables Eq. (C.1) to be rewritten as follows:

$$\frac{\partial P'}{\partial s} + P'\frac{c_0}{2A_0}\frac{\partial}{\partial s}\left(\frac{A_0}{c_0}\right) - \frac{1}{2\rho_0}\frac{\partial\rho_0}{\partial s} = \frac{\beta}{\rho_0 c_0^3}P'\frac{\partial P'}{\partial t'} \quad . \tag{C.2}$$

The transport equation, Eq. (C.2), would be very similar to the finite amplitude plane wave equation, Eq. (B.2), if the middle term could be forced to vanish. To force Eq. (C.2) towards the form of Eq. (B.2), we introduce a transformation of the dependent variable:

$$W \equiv kP' \quad , \tag{C.3}$$

where k is a function (not a constant) to be defined in such a way that the boundary condition at the source transforms conveniently, that is, W = P' at the source. Use of Eq. (C.3) in Eq. (C.2) yields

$$\frac{\partial W}{\partial s} + W\left[\frac{c_0}{2A_0}\frac{\partial}{\partial s}\left(\frac{A_0}{c_0}\right) - \frac{1}{2\rho_0}\frac{\partial \rho_0}{\partial s} - \frac{1}{k}\frac{\partial k}{\partial s}\right] = \frac{\beta W}{k\rho_0 c_0^3}\frac{\partial W}{\partial t'} \quad . \tag{C.4}$$

Setting the middle term to zero yields a differential equation in k, which may be cast in the form of a perfect differential

$$\partial[\ell n\,(A_0/\rho_0 c_0 k^2)]/\partial s = 0 \quad . \tag{C.5}$$

The solution of Eq. (C.5) is

$$k\,(\rho_0 c_0/A_0)^{1/2} = \text{constant} \quad . \tag{C.6}$$

We now choose the integration constant to suit the boundary conditions at the source. Accordingly the definition of k is as follows:

$$k \equiv (A_0\,\rho_{0s} c_{0s}/A_{0s}\rho_0 c_0)^{1/2} \quad , \tag{C.7}$$

where the density, the small-signal sound speed, and the ray tube area at the source position are denoted ρ_{0s}, c_{0s}, and A_{0s}, respectively. Thus Eq. (C.4) may be written

$$\frac{\partial W}{\partial s} - \frac{\beta W}{k\rho_0 c_0^3}\frac{\partial W}{\partial t'} = 0 \quad , \tag{C.8}$$

where

$$W \equiv (A_0 \rho_{0s} c_{0s} / A_{0s} \rho_0 c_0)^{1/2} p' \quad . \tag{C.9}$$

Equation (C.8) does not have quite the same form as Eq. (B.2). To get the desired form, we introduce another transformation, this time of the independent variable:

$$Z = Z(s) \quad . \tag{C.10}$$

By the chain rule, we find that Eq. (C.8) can be written as follows:

$$(\partial W/\partial Z)(\partial Z/\partial s) = [(\beta^2 A_{0s} \rho_{0s} c_{0s}^5)/(\beta_s^2 A_0 \rho_0 c_0^5)] (\beta_s/\rho_{0s} c_{0s}^3) W \partial W/\partial t' \quad . \tag{C.11}$$

Putting

$$\partial Z/\partial s = (\beta^2 A_{0s} \rho_{0s} c_{0s}^5)/(\beta_s^2 A_0 \rho_0 c_0^5) \tag{C.12}$$

gives Eq. (C.11) the form of Eq. (B.2):

$$\frac{\partial W}{\partial Z} - \frac{\beta_s W}{\rho_{0s} c_{0s}^3} \frac{\partial W}{\partial t'} = 0 \quad . \tag{C.13}$$

Equation (C.12) must now be solved subject to the condition that $Z = 0$ when $s = s_0$. The required solution is

$$Z = \int_{s_0}^{s} \left(\frac{\beta^2 A_{0s} \rho_{0s} c_{0s}^5}{\beta_s^2 A_0 \rho_0 c_0^5} \right)^{1/2} ds \quad ; \tag{C.14}$$

Z is called the distortion range variable. Equation (C.13) has the desired form.

In this section the simplification of the nonlinear geometrical acoustics equation, Eq. (B.10) is discussed. The approach taken to reduce the equation is similar to that used in the previous chapter to simplify the linear geometrical acoustics equation, Eq. (3-C.17). Since self-refraction is assumed to be negligible, the eikonal equation from linear geometrical acoustics, Eq. (3-C.18), is used to simplify the nonlinear geometrical acoustics equation. The transport equation is reduced via two transformations: one on the dependent variable, the pressure, and the other on the independent variable, the path length. The transformation of the pressure corrects for the geometrical spreading of the wavefront; the transformation of the path length corrects for the increase, or decrease, in distance required for the waveform to distort a prescribed amount. In the finite amplitude case, the transforms are Eqs. (C.9) and (C.14). The corresponding transforms in the linear case are Eqs. (3-E.7) and (3-E.11), respectively. Note that in the linear case the transform of the dependent variable does not depend on the static density or sound speed. This is because in the linear problem the level of approximation is only first order, whereas in this chapter the level of approximation is consistently maintained at second order.

D. The Solution

Now that the equation for propagation in an inhomogeneous medium has been cast in the same form as the equation for plane wave in a homogeneous medium, the solution may readily be obtained. The plane wave equation, Eq. (B.2), is satisfied by the Earnshaw solution (see, for example,

Blackstock 1972): Given the boundary condition

$$P' = g(t) = g(t') \quad \text{at} \quad x = 0 \quad , \tag{D.1}$$

the solution of Eq. (B.2) is

$$P' = g(\phi) \quad , \tag{D.2}$$

where

$$\phi = t' + \beta x g(\phi)/c_0^2 \quad . \tag{D.3}$$

For the case of an inhomogeneous medium the boundary condition is

$$P' = g(t) = g(t') \quad \text{at} \quad s = s_0 \quad . \tag{D.4}$$

This transforms to

$$W = g(t') \quad \text{at} \quad Z = 0 \quad . \tag{D.5}$$

The solution is therefore the following equation

$$W = g(\phi) \quad , \tag{D.6}$$

where

$$\phi = t' + \beta Z g(\phi)/c_0^2 \quad . \tag{D.7}$$

E. Simplification of the Distortion Range Variable Transformation

In this section the integral for the distortion range variable Z, Eq. (C.14), is placed in the more compact form suggested by Morfey (1984a). Since spreading waves in a mildly inhomogeneous medium are similar to spherical spreading waves, Morfey's approach is to define the distortion

range variable for an inhomogeneous medium in a form similar to that for a spherically spreading wave in a homogeneous medium ($Z = s_0 \ln (s/s_0)$; Blackstock 1966). Morfey's definition is as follows:

$$Z = s_0 \ln (sG/s_0) \quad , \tag{E.1}$$

where s is the path length, s_0 is the reference path length, and G is the dimensionless distance modification factor. As is shown below, G embodies the effects of both ray tube geometry and ocean inhomogeneity upon the finite amplitude distortion. If the quantity G is equal to 1, Eq. (E.1) reduces to the form for a spherically spreading wave in a homogeneous ocean. As Morfey (1984a) points out, if G is greater than 1, finite amplitude distortion is greater than it would be in a homogeneous medium. The converse is true if G is less than 1.

Starting with Eq. (C.12), we strive to force it into the form of Eq. (E.1). This is done by differentiating both equations with respect to the path length s, and then equating the differentials. First, in terms of a new thermodynamic variable α,

$$\alpha \equiv \beta(\rho_0 c_0^5)^{-1/2} \quad , \tag{E.2}$$

Eq. (C.12) may be expressed as follows:

$$Z = \int_{s_0} (\alpha/\alpha_s)(A_0/A_{0s})^{-1/2}\, ds \quad , \tag{E.3}$$

where α_s is α evaluated at the source position. If Eq. (E.3) is differentiated with respect to the the path length s, we are left with the integrand. We

define a new variable Y(s) equal to the integrand:

$$Y(s) \equiv (\alpha/\alpha_s)(A_0/A_{0s})^{-1/2} \quad . \tag{E.4}$$

In the next chapter, we use a computer ray model based on the assumption that the ocean is azimuthally symmetric. Using this assumption, we substitute for the ratio of the ray tube areas, A_0/A_{0s}, using a relation given by Foreman (1983),

$$A_0/A_{0s} = (r\zeta/s_0^2)(\cos\theta/\cos\theta_s) \quad , \tag{E.5}$$

where

$$\zeta \equiv (\partial z/\partial\theta_s)_r \quad , \tag{E.6}$$

r is the radial range, z is the depth, and θ_s is the launch angle. By defining a new variable B(s), we see that

$$Y(s) = s_0 B(s) \quad , \tag{E.7}$$

where

$$B(s) \equiv (r\zeta)^{-1/2}(\cos\theta/\cos\theta_s)^{-1/2}(\alpha/\alpha_s) \quad . \tag{E.8}$$

Equation (C.12) is now in the form of Eq. (E.7).

Now differentiate Eq. (E.1) with respect to the path length s and equate the result with Eq. (E.7). The differential of Eq. (E.1) is as follows:

$$dZ/ds = (s_0/G)(dG/ds) + s_0/s \quad . \tag{E.9}$$

If Eq. (E.7) is used, it may be shown that

$$1/G\,(dG/ds) = B(s) - 1/s \quad . \tag{E.10}$$

Solving Eq. (E.10) for G, and defining a new variable F(s), we see that

$$G = \exp F(s) \quad , \tag{E.11}$$

where

$$F(s) \equiv \int_0 f(s)\, ds \quad , \tag{E.12}$$

and

$$f(s) \equiv B(s) - 1/s \quad . \tag{E.13}$$

Thus the distortion range variable may be expressed in the form of Eq. (E.1), and the quantity G may be evaluated using Eq. (E.11) if both the ray path and the environment along the ray path are known. Thus G embodies both the effects of the ray tube geometry (via the area in Eq. E.8) and the environment (via α in Eq. E.8) on finite amplitude propagation.

As was mentioned in Chapter 2, the main difference between linear and nonlinear hydrodynamics equations can be explained using the mathematical term ranking system. To form the linear lossless hydrodynamics equations for inhomogeneous fluids, we retain first-order terms and one type of second-order terms, inhomogeneity terms. To form the nonlinear lossless hydrodynamics equations, we include one more set of second-order terms: quadratic nonlinear terms. These terms govern the finite amplitude behavior.

CHAPTER 5

NUMERICAL EVALUATION OF WAVEFORMS

A. Introduction

In this chapter we discuss a scheme for numerically implementing weak shock theory for a lossy inhomogeneous ocean. Recall that in Chapter 4 the transport equation for finite amplitude signals propagating through an inhomogeneous ocean was reduced, via two transforms, to the form of that for plane waves propagating through a homogeneous ocean. Pestorius (1973) developed an algorithm for numerically implementing weak shock theory in the case of plane waves propagating through a homogeneous medium in a pipe. We start this chapter by reviewing Pestorius's algorithm. We then describe the differences between his algorithm and the algorithm as it is used in this work; related details of the algorithm are examined. Next the testing of the algorithm is discussed, and the results of the testing are presented. In connection with the testing, typical results of the program are shown.

Pestorius's algorithm involves propagating an arbitrary finite amplitude waveform a small distance using a numerical implementation of weak shock theory. The waveform is then Fourier transformed, and the viscosity and tube wall effects incurred over that small distance are

accounted for in the frequency domain. The procedure is repeated until the desired propagation distance has been reached. Note that by using Pestorius's algorithm we may account for the loss terms neglected at the beginning of the analytic development.

Several differences exist between the algorithm as set forth by Pestorius and the modified algorithm used in this study. All the differences result from the fact that Pestorius's algorithm was designed to aid in the study of nonlinear propagation of plane waves through a homogeneous medium in a pipe, whereas we are concerned with spreading waves in an inhomogeneous ocean. Obviously the loss mechanisms themselves are different; we account for the viscosity and relaxation of seawater. From a computational point of view, two major differences are (1) that our absorption coefficients change with position, and (2) that we must calculate the distance over which the absorption acts. Other differences are related to the choice of step size and starting conditions. We recalculate the step size depending on the wave's current position, whereas Pestorious used a constant step size. Pestorius started his waveform at range zero; we must select a reference position.

A flowchart of the modified Pestorius algorithm is shown in Fig. 5.1. The modified Pestorius algorithm is implemented in the program PLPROP.

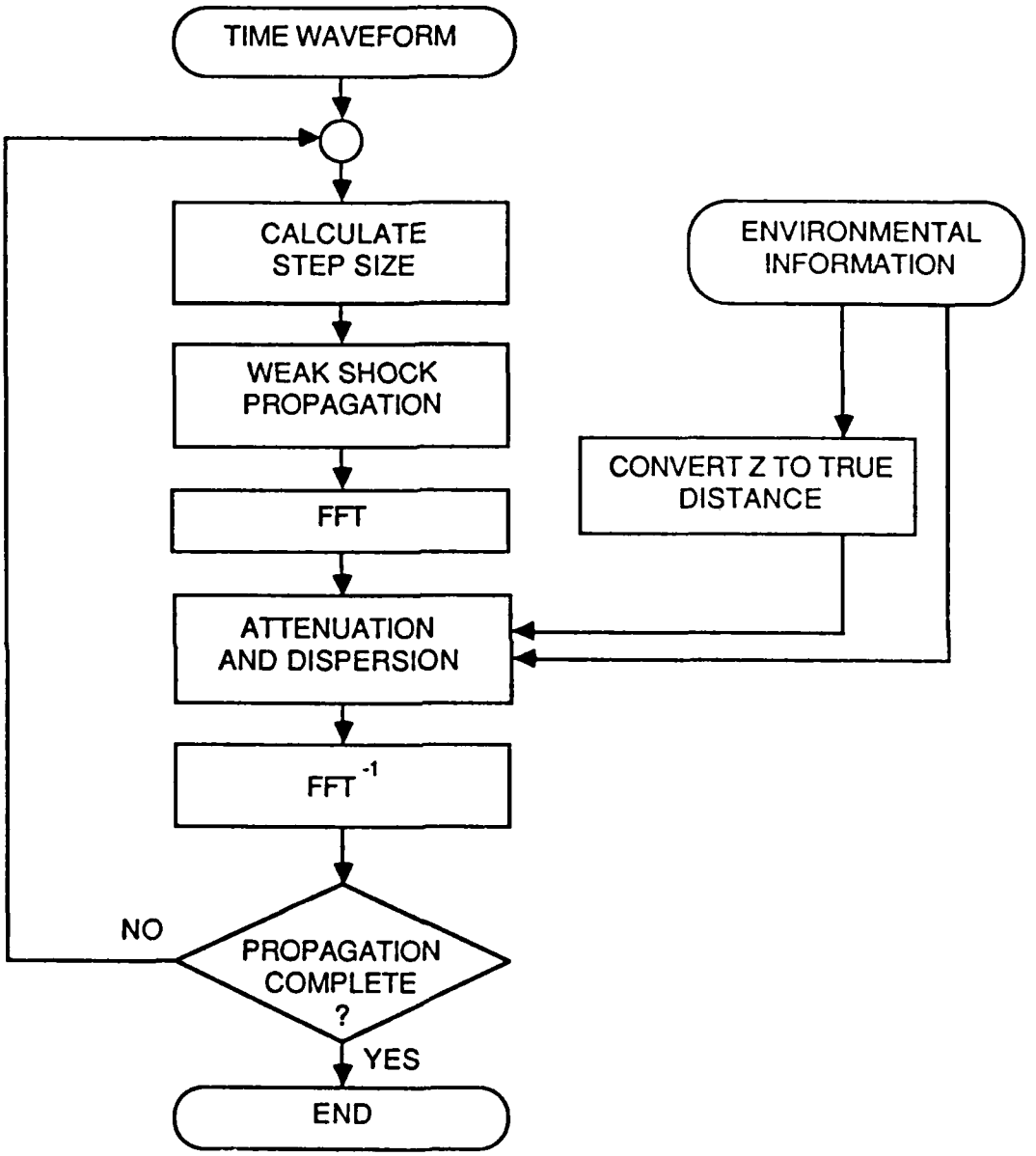

FIGURE 5.1
FLOWCHART OF THE MODIFIED PESTORIUS ALGORITHM

AS-85-1025

B. Application of Pestorius's Algorithm to Inhomogeneous Media

In this section we take a more detailed look at the modified Pestorius algorithm. We first examine the weak shock subroutine WAVPROP, and then focus our attention on the calculation of attenuation and dispersion. The section closes with a description of some considerations in the numerical evaluation such as choice of nondimensional variables, step size, and starting range.

1. The Weak Shock Subroutine

The program PLPROP is centered around the weak shock propagation subroutine WAVPROP. This subroutine uses the Earnshaw solution and the relative shock arrival time equation (see, for example, Blackstock 1972) in finite difference form (Pestorius 1973, Eqs. 4.2 and 4.3). From the Earnshaw solution which describes the distortion of the continuous portion of the waveform, one finds that the delay time associated with a given wavelet u is

$$t'[(k+1)h] = t'(kh) - \beta c_0^{-2} u\,[t'(kh)]h \quad , \qquad (B.1)$$

where $t'[(k+1)h]$ gives the position of the wavelet after $k+1$ incremental steps of size h, and $t'(kh)$ gives the position after k steps. The delay time for each wavelet is calculated individually because each wavelet propagates with a different velocity. The finite difference form of the relative shock arrival time equation gives the value of t' associated with a particular shock, denoted t_s', as follows:

$$t_s'[(k+1)h] = t_s'(kh) - \beta h c_0^{-2}\{u_2[kh, t_s'(kh)] + u_1[kh, t_s'(kh)]\}/2 \, , \qquad (B.2)$$

where $t_s'[(k+1)h]$ is the value of t_s' after k+1 steps of size h, and $u_{1,2}[kh,t_s'(kh)]$ is the value of particle velocity after k increments of size h. These two equations, Eqs. (B.1) and (B.2), are all that is required to describe the propagation of weak discontinuities within finite amplitude waves.

Several disadvantages are associated with having to transform back and forth between the time and frequency domains. These problems are discussed in detail by Pestorius (1973, p. 91). We now address the most significant of these problems. Equal time intervals between waveform points are required by the fast Fourier transform (FFT) which is used to transform the waveform into the frequency domain. After one step in the the WAVPROP subroutine, however, the waveform points are no longer spread at equal time intervals. To ensure that the points were equally spread through time, Pestorius wrote the subroutine RESAMP. The subroutine RESAMP unshocks the waveform by spreading the shock over at least one time interval. Therein lies the problem; this does not correspond with the physics of the situation. The effects of the problem are reduced by having many data points closely spaced in time. As can be seen in the later section on testing, the effects of this problem are small.

Another problem is aliasing (see, for example, Oppenheim and Schafer 1975). The waveform's spectrum shows some degree of aliasing because the resampled time waveform contains very high frequency information. The spectra of the waveforms studied in this report have a -6 dB/octave slope, and the effect of aliasing is therefore small. Also the

amount of attenuation increases with frequency and acts as a natural anti-aliasing filter.

2. The Application of Attenuation

In the introduction we mentioned that differences exist between Pestorius's algorithm and the modified algorithm implemented in PLPROP. It was also noted that the major differences center on the two components required to calculate the attenuation: the absorption coefficients and the distance over which they act. Since Pestorius's algorithm was intended for plane waves, our modified version operates in units of equivalent plane wave distance. Consequently the true distance must be calculated before the attenuation can be applied. To obtain the true propagation distance we use Eq. (4-E.1). The more compact form of the distortion range variable requires the calculation of the quantity G.

The numerical evaluation of G requires knowledge of both the acoustic ray path and the environment along the ray path. Knowledge of the environment is usually obtained by measurements made during the course of an experiment. For our purposes we consulted tabulated data and chose plots of temperature and salinity versus depth (hereafter referred to as temperature and salinity profiles) typical of the North Atlantic Ocean. The profiles are shown in Figs. 5.2 and 5.3. Once the temperature and salinity profiles are known, the sound speed profile may be readily calculated (Lovett 1978).

As was pointed out in Chapter 3, the acoustic ray paths depend solely on the sound speed. In Chapter 4 it was noted that finite amplitude waves follow the same ray paths as their small-signal counterparts. We

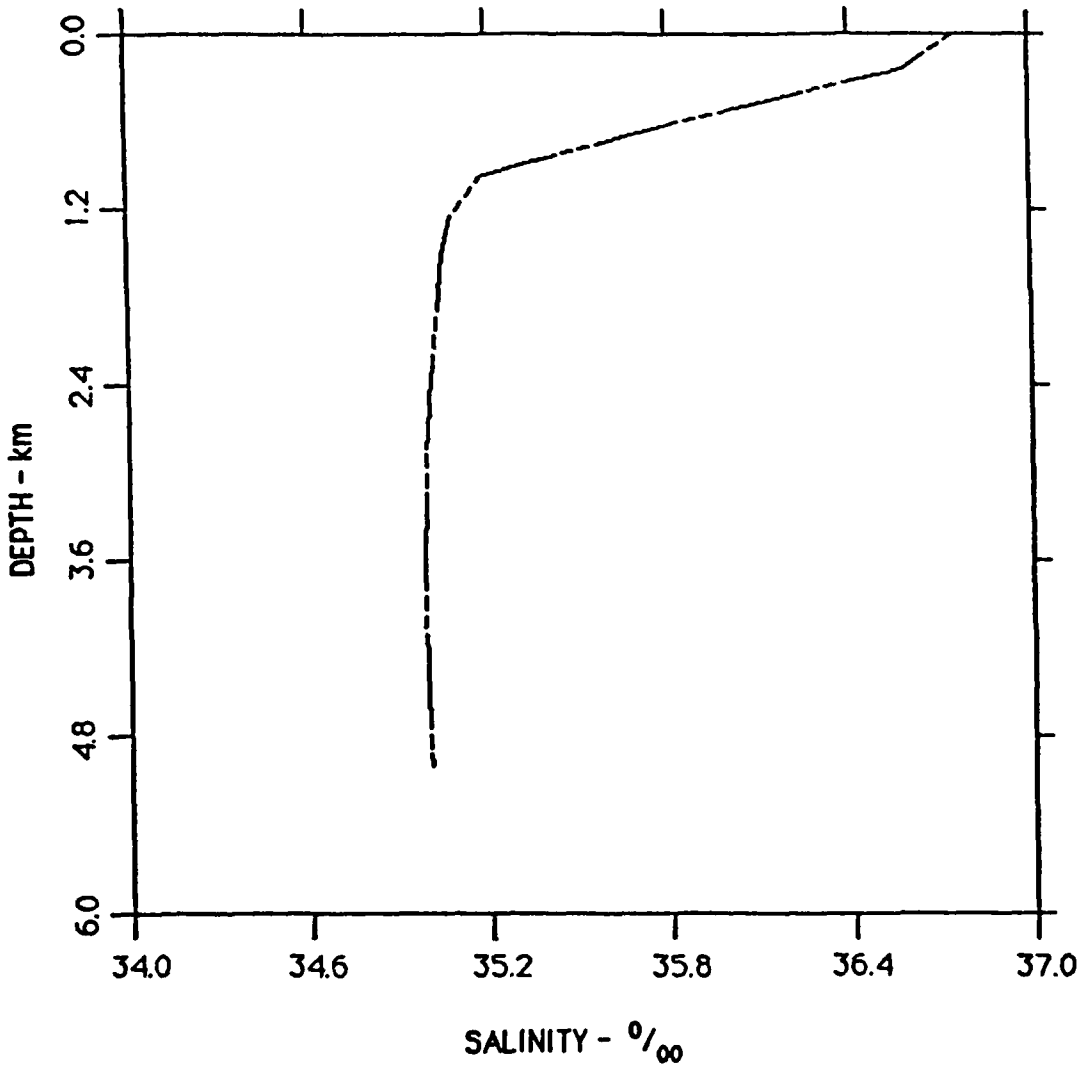

FIGURE 5.2
SALINITY PROFILE TYPICAL OF NORTH ATLANTIC OCEAN

AS-85-1026

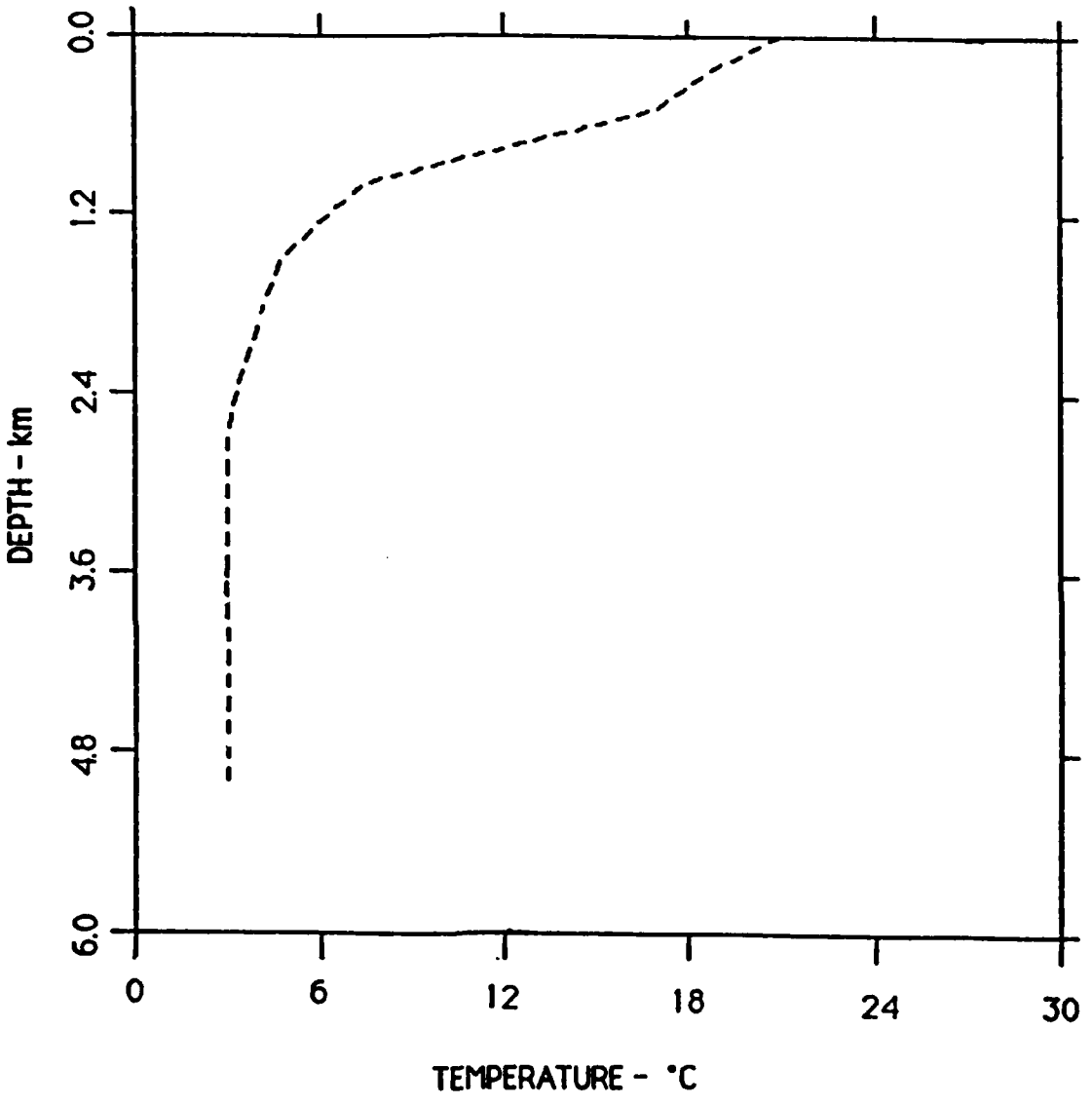

FIGURE 5.3
TEMPERATURE PROFILE TYPICAL OF NORTH ATLANTIC OCEAN

AS-85-1027

may therefore use a linear acoustic ray model to calculate the ray paths for the finite amplitude case; the ray model used in this study is MEDUSA (Foreman 1983). MEDUSA assumes an azimuthally symmetric environment and is capable of calculating the ray paths even if the sound speed varies with both depth and range. However, in order to keep our analysis simple, we do not make use of this capability. We are therefore assuming that an ocean may be modeled by a single sound speed profile, a stratified ocean.

The RAYFAN subroutine in MEDUSA was modified to output information about the ray path. The information includes path length, range, depth, cos θ, and ζ. The angle θ is defined in Fig. 3.2, and ζ is defined in Eq. (4-E.6). The cos θ and ζ values are required to calculate the ray tube area ratio defined in Eq. (4-E.5). This ray path information is calculated and stored by RAYFAN for each MEDUSA step. MEDUSA varies its step size in order to maintain a constant degree of accuracy. It is therefore assumed that this step size is sufficiently small to accurately perform the numerical integration outlined below.

Since both the environmental information and the ray path information are available, the quantity G may be numerically evaluated. Applying a second-order numerical integration scheme to Eq. (4-E.11), Morfey (1984a) obtained the following equation:

$$\int_{s_{i-1}}^{s_i} f(s)\, ds \approx h(f_i + f_{i-1})/2 - h^2(f_i' - f_{i-1}')/12 \quad , \qquad (B.3)$$

where h is the step size $(s_i - s_{i-1})$ in arc length. The function f(s) is defined

in Eq. (4-E.12), and f'(s) is the derivative of f(s) with respect to s. To obtain the quantity G, we integrate along the ray path using Eq. (B.3) and then substitute the resulting value into Eq. (4-E.10). The program CALCG implements Eq. (B.3) and calculates the quantity G at each of the MEDUSA steps. Since CALCG requires ray trace data as an input, MEDUSA is run first, and a file of ray trace data is stored. CALCG appends the value of G for each step to the ray trace data file. The modified ray trace data file is used as input to PLPROP. In this way PLPROP has access not only to the environmental information along the ray path, but also to the quantity G. PLPROP can therefore convert the distortion range variable into the true distance which is required to evaluate the amount of attenuation associated with a propagation step.

The second major difference between Pestorius's algorithm and the modified algorithm implemented in PLPROP is that our absorption coefficients vary along the propagation path whereas Pestorius's were constant. The variation of the temperature and salinity causes a corresponding variation in the absorption coefficients.

Empirical relations derived by François and Garrision (1982) are used to calculate the absorption coefficients. François and Garrision considered three sources of attenuation: viscosity and the relaxation mechanisms associated with magnesium sulfate and boric acid. Each of the relaxation mechanisms has a small amount of dispersion associated with it. The dispersion is calculated using Blackstock's technique (1985). The dispersion due to each of the two relaxation mechanisms is added.

The environmental information used as inputs to François and

Garrision's empirical relations was obtained from the temperature and salinity profiles via a cubic T-spline (see, for example, Foreman 1983). For the splines to be used, the depth at the position of interest must be known. The depth is, however, only known at specific points along the ray path since MEDUSA steps through range. To evaluate the depth for points in the middle of a MEDUSA step, PLPROP uses a linear interpolation scheme.

Once the true propagation distance and the absorption coefficients have been calculated, the attenuation and dispersion may be applied to the waveform. However, PLPROP applies the attenuation due to viscosity only when the waveform contains no shocks. The reason for this is that weak shock theory implicitly accounts for most of the viscous attenuation when shocks are present. Thus if PLPROP were to apply viscous attenuation to a waveform containing shocks, the viscous attenuation would have been accounted for twice, once by the weak shock theory and once by PLPROP. To separate the two cases, PLPROP measures the distance the wave propagates both with and without shocks, and then applies absorption accordingly.

The reason why the losses associated with weak shock theory are assumed to be due to viscosity is as follows: In weak shock theory the losses are assumed to be concentrated at the shock. Since the shock contains mostly high frequency information, and the attenuation mechanism which is dominant at high frequencies is viscosity, viscosity alone must be responsible for the losses at the shock. Other attenuation mechanisms, such as relaxation, do not attenuate the shock at a rate sufficient to stop the shock from becoming multivalued.

3. Other Considerations

PLPROP works with nondimensionalized time and distance variables. The time is nondimensionalized by dividing it by a time t_c characteristic of the input waveform. For example, in the case of a weak shock with an exponentially decaying tail, a convenient characteristic time is the initial 1/e decay time. The characteristic distance used to nondimensionalize the distortion range variable is defined as follows:

$$R_* = c_0 t_c / \beta\epsilon \quad . \tag{B.4}$$

The definition for R_* presented in Eq. (B.4) is preferred over $c_0 t_c$ alone because Eq. (B.4) represents a distance over which the waveform would undergo a significant amount of distortion. In the case of a sinusoidal wave, R_* is the shock formation distance. PLPROP propagates the waveform in steps of nondimensional distance sigma σ, defined as follows:

$$\sigma = z / R_* \quad . \tag{B.5}$$

Several factors must be considered in choosing PLPROP's step size, denoted $\Delta\sigma$. Pestorius (1973) tried a variety of step sizes and settled on the value of 0.01. Pestorius also noted that several, typically 10, of the 0.01 $\Delta\sigma$ steps should be taken before the attenuation and dispersion are applied. This reduces the number of FFTs, and hence, the effect of the errors associated with the transformations between the time and frequency domain.

Step size considerations for the modified Pestorius algorithm

implemented in PLPROP are somewhat different than those used in the original algorithm. One of the consequences of Eq. (4-E.1) is that the true distance corresponding to 0.01 $\Delta\sigma$ increases with the distance the wave has propagated. Close to the source, where the signal is stronger and finite amplitude effects are important, ten 0.01 $\Delta\sigma$ steps may correspond to a very small distance. To calculate the number of 0.01 $\Delta\sigma$ steps to take, PLPROP examines the absorption coefficient, calculated in dB/m, from the center frequency cell of the FFT. The magnitude of the reciprocal of this coefficent gives, for that particular frequency, the propagation distance required for a 1 dB drop in the amplitude. The waveform is then propagated the number of 0.01 $\Delta\sigma$ steps corresponding to the 1 dB drop distance. This differs from the fixed value of ten 0.01 $\Delta\sigma$ steps used by Pestorius. Compared with Pestorius's original approach, the number of applications of absorption near the beginning of the ray path is reduced. This corresponds to the decreased role of absorption.

On the other hand, the number of 0.01 $\Delta\sigma$ steps is never permitted to go below 10. When the wave is far from the source, the 1 dB drop distance may correspond to less than one 0.01 $\Delta\sigma$ step. Thus to combat the errors associated with transforming between the time and frequency domains, the number of 0.01 $\Delta\sigma$ steps between applications of absorption is fixed at 10.

Another difference between the algorithm as developed by Pestorius and the algorithm used in PLPROP is the requirement for a starting, or reference, range. Because Pestorius dealt solely with plane waves, his starting range was always zero. The reference range used in

PLPROP was developed by Morfey (1984b), who chose the reference range to be equal to the characteristic distance R_*. Morfey formed the ratio of the nondimensional shock pressure, $\Delta P/\rho_0 c_0^2$, to the nondimensional time constant, $c_0 t_c/R$. He observed that the ratio is approximately equal to $1/\beta$ if the nondimensional shock pressure is 0.06 and the range is R_*. The value of 0.06 for the ratio $\Delta P/\rho_0 c_0^2$ corresponds to the upper limit on weak shock theory (Pestorius and Williams 1974). Consequentially, Morfey chose the model's starting conditions to correspond to a nondimensional pressure of 0.06 and a starting range of R_*.

Another feature of considerable importance is PLPROP's ability to selectively include the physical mechanisms that affect the propagation. The finite amplitude effects may be switched off altogether or remain in effect only until the wave reaches a certain range. Viscosity and relaxation may be switched on individually. The dispersion due to relaxation may be included or not. The absorption coefficients may be calculated from the local environment or may be based on some average value. The ability to switch the mechanisms on or off permits each of them to be examined individually.

C. Verification of the Algorithm

In this section we present some of the results of the tests performed to verify the accuracy of the modified Pestorius algorithm. The first program discussed is CALCG which calculates the quantity G. The second program discussed is PLPROP. In each case the numerical results of the programs are compared to results obtained from analytic solutions.

The percent error in the numerical results are calculated.

As mentioned earlier in this chapter, the quantity G is calculated using Eq. (B.3). The program CALCG evaluates G from ray path information provided by the ray tracing program MEDUSA. To verify the accuracy of CALCG, we compare its results to the known analytic expression for G for the case of a constant gradient sound speed profile (Morfey 1984a). Morfey has shown that, in this case, G is related to θ by the following equation:

$$G(\theta_0, \theta) = \left(\frac{\sin\theta - \sin\theta_0}{(\theta - \theta_0)\cos\theta}\right)\left(\frac{\tan(\pi/4 + \theta/2)}{\tan(\pi/4 + \theta_0/2)}\right)^{\sin\theta_0} , \qquad (D.1)$$

where θ is the angle between the ray path and the horizontal, and θ_0 is the angle θ at the reference path length. In our test the dependence of sound speed on depth was as follows:

$$c_0 = 1462 + 0.01762\, z , \qquad (D.2)$$

where z is the depth in meters, and c_0 is the sound speed in m/s. The sound speed was assumed to be constant with range. The source was assumed to be at a depth of 2500 m, and the launch angle was 22.5°. The results of Eq. (D.1), the numerical result of CALCG, and the percent error are presented in Table 5.1. As can be seen from the table, the error is consistently below 0.01 %.

In an effort to check the accuracy of PLPROP, we compared the program's results with results obtained from the analytical expressions

TABLE 5.1
COMPARISON OF CALCG RESULT WITH ANALYTIC RESULT FOR G

Range (m)	Theta	Numeric	Analytic	% Error
100.000	22.4326	0.999274	0.999270	0.4×10^{-5}
1071.18	21.7841	0.992336	0.992341	0.5×10^{-5}
1332.08	21.6104	0.990506	0.990514	0.8×10^{-5}
2517.80	20.8236	0.982362	0.982386	2.5×10^{-5}
3863.73	19.9354	0.973451	0.973496	4.6×10^{-5}
4463.73	19.5411	0.969588	0.969642	5.6×10^{-5}
5377.93	18.9422	0.963833	0.963897	6.6×10^{-5}
8987.12	16.5976	0.942506	0.942600	1.0×10^{-4}
13306.34	13.8285	0.919569	0.919720	1.6×10^{-4}
18555.3	10.5065	0.894860	0.895194	3.7×10^{-4}
24160.3	6.99792	0.871775	0.872388	7.0×10^{-4}
30081.8	3.31941	0.850601	0.851538	1.1×10^{-3}
34156.5	0.797062	0.837745	0.838892	1.4×10^{-3}

developed in Appendix C. The expressions in the appendix are for a weak shock with an exponentially decaying tail which is spreading spherically through a homogeneous medium. The expressions give the nondimensionalized peak pressure, the nondimensional 1/e decay time, and the nondimensional relative shock arrival time. The peak pressure is normalized to the initial peak pressure. The 1/e decay time is normalized to the initial 1/e decay time. The shock arrival time is measured relative to the travel time calculated assuming the small-signal sound speed c_0. To make the comparison, we simulate a homogeneous ocean by giving MEDUSA a constant sound speed profile; the resulting acoustic ray paths are straight lines. If one of these ray paths is used as input to PLPROP, and the attenuation in PLPROP is "turned off", PLPROP's results should be the same as those for a spherically spreading wave in a lossless homogeneous ocean. A comparison of the analytic and numerical results is presented in Table 5.2. It is seen that the error is generally in the range ±0.25 %.

PLPROP plots the time waveforms and their corresponding energy spectra. The time waveforms and energy spectra corresponding to the values of the "numerical" column in Table 5.2 are shown in Figs. 5.4 and 5.5, respectively. The horizontal axis in Fig. 5.4 is in units of nondimensional retarded time. The vertical axis is the nondimensional pressure. The pressure shown here and that listed in Table 5.2 is the equivalent plane wave pressure, that is, the purely geometrical effect of spherical spreading has been removed. The plots of the time waveforms from different positions along the ray path have been superimposed.

TABLE 5.2
COMPARISON OF PLPROP RESULT WITH ANALYTIC RESULT

Range (m)	Sigma	Normalized Peak Particle Velocity			Relative Shock Arrival Time			1/e Decay Time		
		Analytic	Numeric	Error (%)	Analytic	Numeric	Error (%)	Analytic	Numeric	Error (%)
0.4	0.0	1.0	1.0		0.0	-0.0078		1.0	1.0	
100	5.579	0.446	0.447	0.25	-1.678	-1.680	0.12	2.572	2.578	-0.23
600	7.371	0.403	0.404	-0.32	-2.058	-2.063	0.22	2.876	2.883	-0.24
3100	9.013	0.373	0.374	-0.35	-2.376	-2.383	0.28	3.125	3.133	-0.25
15600	10.63	0.350	0.351	-0.26	-2.667	-2.672	0.17	3.350	3.360	-0.30
70000	12.13	0.332	0.333	-0.29	-2.923	-2.930	0.24	3.545	3.555	-0.28

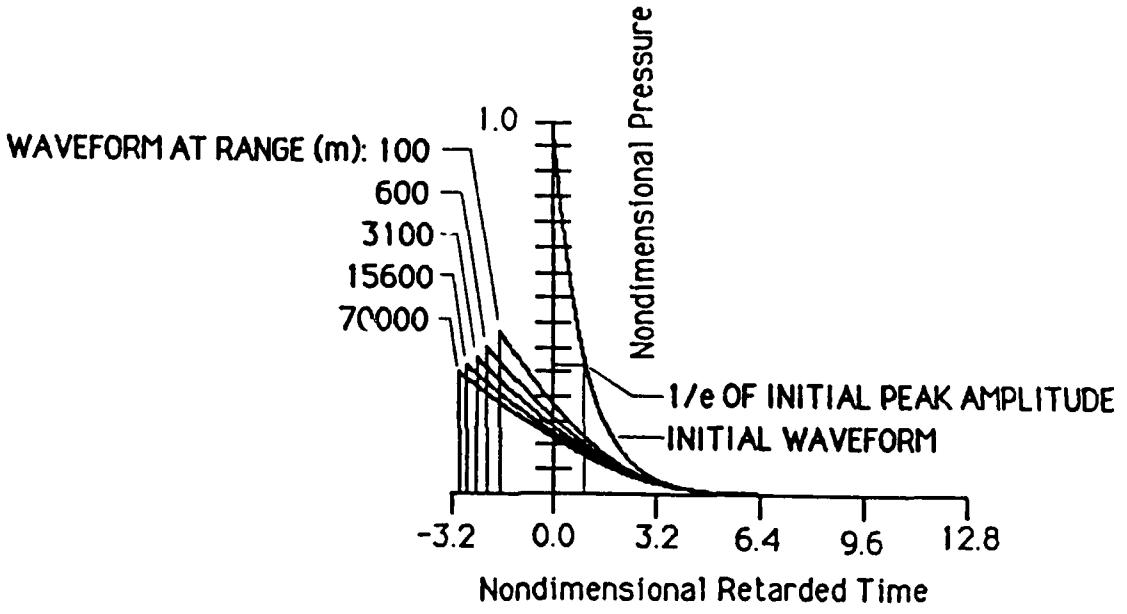

FIGURE 5.4
TIME WAVEFORMS FOR EXPONENTIALLY DECAYING PULSE PROPAGATING SPHERICALLY THROUGH A LOSSLESS OCEAN

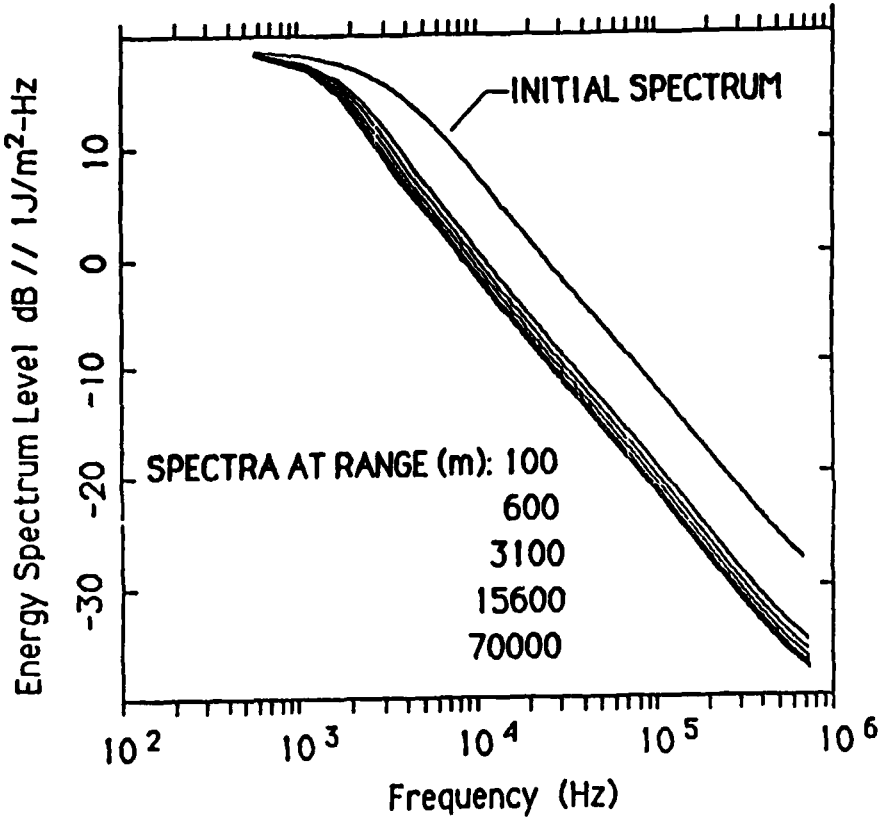

FIGURE 5.5
ENERGY SPECTRA FOR EXPONENTIALLY DECAYING PULSE PROPAGATING SPHERICALLY THROUGH A LOSSLESS HOMOGENEOUS OCEAN

AS-85-1029

The energy spectra in Fig. 5.5 are also superimposed. The horizontal and vertical axis in Fig. 5.5 are frequency in Hz and energy spectrum level in dB//1 J/m^2-Hz. The energy spectrum levels correspond to the energy in the equivalent plane wave; that is, the effects of spherical spreading are removed. The frequency scale is correct as shown. The different spectra correspond to the waveforms from different points along the ray path.

The above results indicate that the weak shock propagation in the modified Pestorius algorithm works to a high degree of accuracy, at least in the case when the inhomogeneous medium is made to appear homogeneous. The other main component in the algorithm is the application of absorption. It was tested by (1) checking as to whether the absorption coefficients are correct, and (2) propagating a sawtooth wave with finite amplitude effects switched off and the absorption switched on. The resulting waveform was compared with that obtained from a separate calculation based on the Fourier series solution of the sawtooth wave. Each of the Fourier coefficients was attenuated and phase shifted to simulate the application of attenuation and dispersion by PLPROP. The results of both calculations, the Fourier series summation and PLPROP, were in very close agreement.

No straightforward way of verifying the accuracy of the combination of finite amplitude effects and absorption exists. However, since the two major components of the program work well separately, it is reasonable to assume that they will work well together. The computer program PLPROP is presented in Appendix D.

CHAPTER 6

RESULTS

A. Introduction

In this chapter the effects of nonlinear distortion and ordinary attenuation and dispersion on the propagation of signals in an inhomogeneous ocean are investigated. The investigation is conducted using the numerical algorithm discussed in the previous chapter. Some of the results have been reported previously (Cotaras, Morfey, and Blackstock 1984). The signals examined are transients, specifically a weak shock with an exponentially decaying tail (hereafter referred to as an exponential pulse) and a more realistic explosion waveform containing one bubble pulse. First the ocean environment is discussed, and two specific ray paths are selected. Then the specific waveforms used are discussed and presented with their energy spectra. Next the effect of inhomogeneity on nonlinear distortion is examined. The effect is investigated by propagating an exponential pulse through a lossless stratified ocean and comparing the result with that obtained for a lossless homogeneous ocean. The combined and individual effects of nonlinear propagation and ordinary attenuation and

dispersion are then examined. These effects are investigated by propagating the same exponential pulse through a stratified ocean and comparing the results obtained considering ordinary attenuation and dispersion only, finite amplitude effects only, and the combination of the two. We also briefly examine, in terms of the arrival time of the peak pressure, the role of dispersion in long range propagation. Lastly we try to answer the question, "to what distance are finite amplitude effects important?" This is done by comparing and contrasting the energy spectrum obtained considering finite amplitude effects over the entire propagation path with those obtained by neglecting finite amplitude effects after certain distances, namely 150 m and 1100 m.

B. Design of the Numerical Experiment

1. Ray Paths

The ocean environment and the ray paths selected are shown in Fig. 6.1. The horizontal axis is the range in km, and the vertical axis is the depth in m. As mentioned in Chapter 5 the ocean is assumed to be stratified. The salinity and temperature profiles used to calculate the sound speed profile, shown in Fig. 6.1, are the same ones employed in Chapter 5; see Figs. 5.2 and 5.3. The sound speed profile is shown at both 0 km and 75 km, thereby indicating that the sound speed does not vary with range. The two ray paths shown start at different depths, 300 m and 4300 m, but have the same launch angle, 8° down from the horizontal. (The

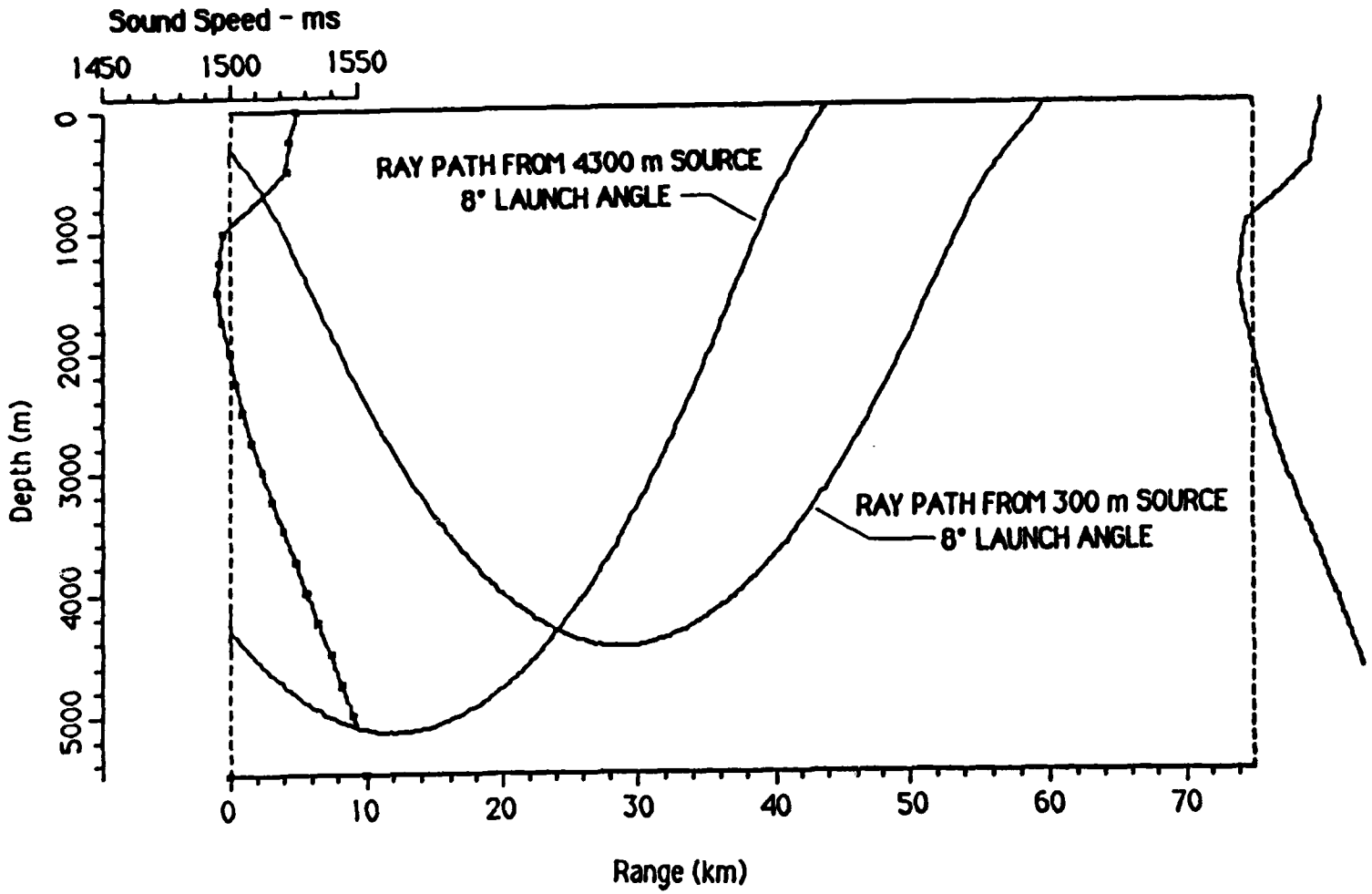

FIGURE 6.1
OCEAN ENVIRONMENT AND ACOUSTIC RAY PATHS

angle appears to be greater than 8° because the horizontal and vertical axes have different scales.)

The two particular source depths were selected for the following reasons. The shallow source depth was chosen because ocean acoustic measurements are commonly made at this depth. The deep source depth was chosen primarily to permit the study of an explosion waveform that includes the first bubble pulse. More details are given in the next section.

The criteria for selecting the ray path from each of the two depths are the same. Because reflections and caustics cannot be accommodated by our computer algorithm, they must be avoided. At the same time, a long ray path is needed in order to determine whether nonlinear distortion continues to accumulate after long propagation distances. The rays selected travel a moderate distance, 50 to 70 km, without interacting with the surface or the bottom and without passing through a caustic. Shown in Figs. 6.2 and 6.3 are the families of rays from which the rays shown in Fig. 6.1 were picked. In Fig. 6.2 (the shallow source) the ray launch angles vary in 0.5° increments from 0° to 15° measured down from the horizontal. The ray selected, noted in the figure, avoids the caustic region that starts at about 33 km on the upper edge of the family of rays. The deep source family (Fig. 6.3) has ray launch angles that vary in 0.5° increments from -5° to 10°. The ray paths all reflect from the surface before passing through a caustic at about 62 km. The ray selected from this family is noted. From now on the ray path starting at

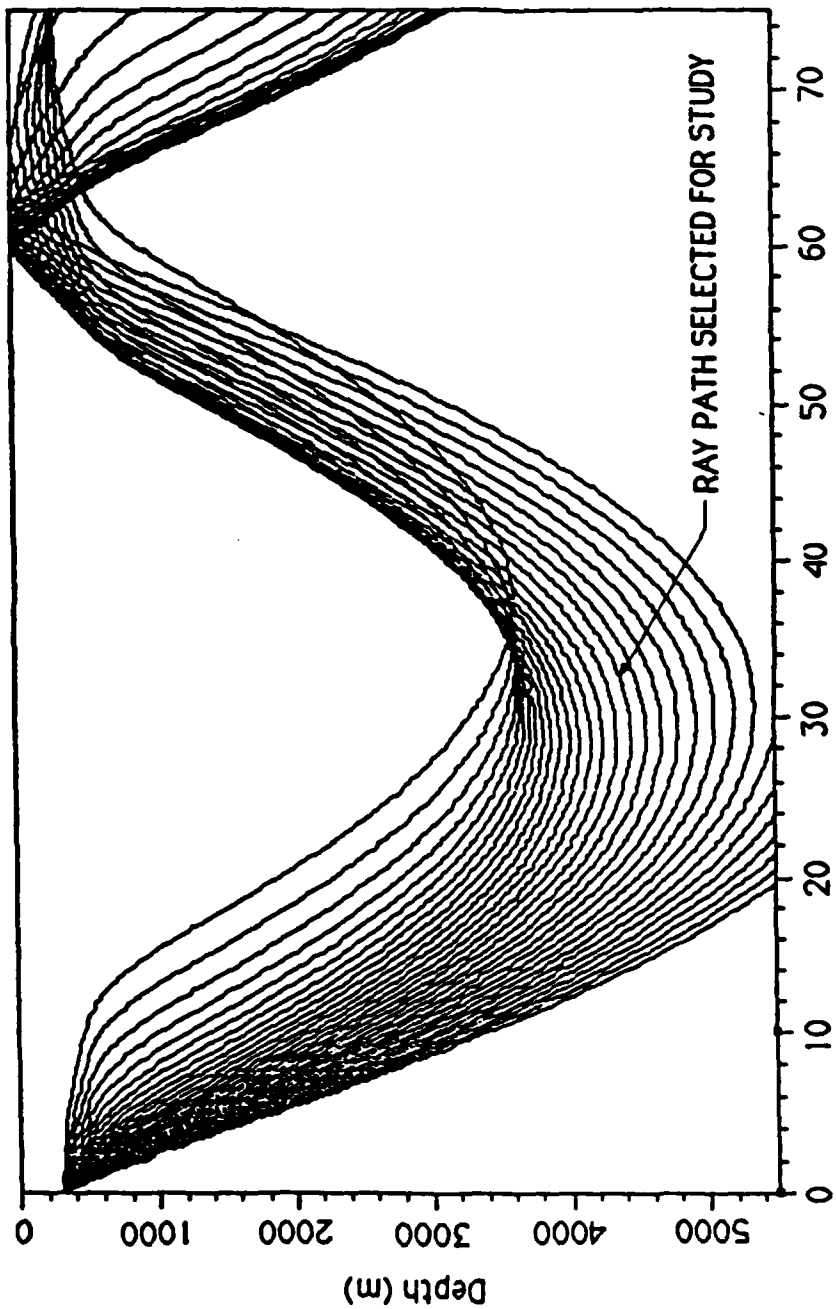

FIGURE 6.2
FAMILY OF RAYS FROM 0° TO 15° AT 0.5° INCREMENTS STARTING FROM 300 m

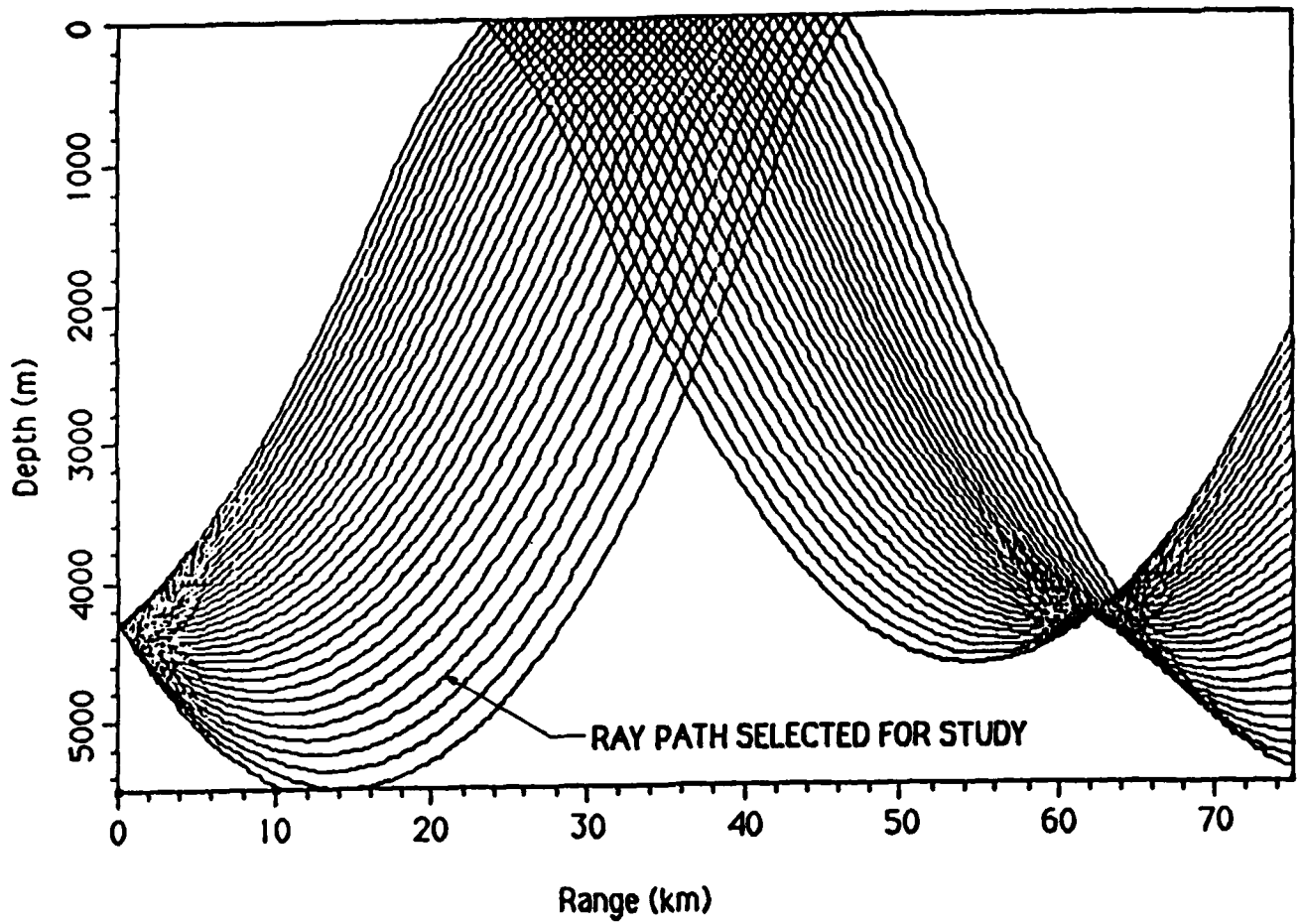

FIGURE 6.3
FAMILY OF RAYS FROM 5° TO 10° AT 0.5° INCREMENTS STARTING FROM 4300 m

AS-85-1032

the shallow source is referred to, for short, as the shallow path; similarly the other path is referred to as the deep path.

2. Signals

The basic criteria for selecting the waveforms to study are as follows: (1) They must be waveforms for which finite amplitude effects are important. (2) They must be as realistic as possible, and yet short enough to be properly sampled by our computer program. The signals examined are transient pulses similar to those caused by underwater explosions. The explosives commonly used in long range propagation studies generate the high sound pressure levels at which nonlinear effects play an important role in propagation. It is rare that a long range propagation experiment is conducted using an intense periodic source. For this reason we exclude the study of periodic signals.

With regard to realism of the waveforms used, it is noted that Wakeley (1977) developed an empirical relation for an underwater explosion waveform which includes the first four bubble pulses. The waveform has been shown to give a close fit to experimental data; it is, however, somewhat complicated. Morfey (1985) developed a simplified version of Wakeley's waveform which is shorter in time duration and is therefore more suitable for use in our computer program. (The simplified Wakeley waveform is shown on p. 111.) The approach taken by Morfey was to (1) truncate the Wakeley waveform at the zero crossing after the first bubble pulse and (2) remove the explicit dependence on the charge weight by selecting a nondimensional time base that is related to the charge weight.

As the characteristic time used for nondimensionalization, Morfey picked the initial 1/e decay time. He found that (Morfey 1984b) use of the empirical scaling law for the peak pressure (Arons 1954) and the starting conditions mentioned in Chapter 5 (nondimensional shock pressure of 0.06 at a range of R_*) leads to the following expression for the 1/e decay time:

$$\theta_m = 59\, W^{1/3} \quad , \tag{6.1}$$

where θ_m is the 1/e decay time in μs and W is the equivalent TNT charge weight in kg. Equation (6.1) connects the initial 1/e decay time of the pulse with the charge weight. By simplifying Wakeley's expression so that it includes only one bubble pulse and by using θ_m to calculate the nondimensional time T, Morfey (1985) obtained the following expression:

$$P = \exp(-T) + 0.16\exp[-(T - T_B)/T_1] - (\pi/2T_B)(1 + 0.16T_1)\left|\sin(\pi T/T_B)\right| \quad , \tag{6.2}$$

where T_B and T_1 are the nondimensional bubble pulse period and bubble pulse time constant, respectively. The bubble pulse period is the time between the initial pulse and the bubble pulse. The bubble pulse time constant is related to the rate of rise and decay of the bubble pulse. The bubble pulse period and time constant are defined in the following expressions:

$$T_B = 35600\,(z + 10.1)^{-5/6} \quad , \tag{6.4}$$

and

$$T_1 = 165\,(z + 10.1)^{-1/2} \quad , \tag{6.5}$$

where z is the depth in m.

It can be seen from Eq. (6.4) that, for large depths, the bubble pulse period of an explosion is approximately proportional to the inverse of the depth. Accordingly the explosion waveform from a source at 300 m has a long bubble pulse period, almost 300 times the initial 1/e decay time. In order to maintain the accuracy stated in Chapter 5, our computer program requires at least 32 points in the initial 1/e decay time. Thus 9600 points are required if the shallow source explosion waveform is to include the first bubble pulse. The total number of points in our time waveform is, however, restricted to 4096 by computer space limitations. Hence we cannot include the bubble pulse in the explosion waveform from the shallow source. A much deeper source, however, has the shorter bubble pulse period which fits within our limitations. We chose our second source depth to be 4300 m.

A simpler waveform is more appropriate for the shallow path since the details of the more complicated waveform cannot be included. Shown in Fig. 6.4 are the time waveforms and corresponding energy spectra of the modified Wakeley waveform for the 300 m source (Fig. 6.4a) and the exponential pulse (Fig. 6.4b). Both waveforms correspond to a 0.818 kg TNT explosion at the reference range of 0.4 m. The reference range is calculated using Eq. (5-B.4) which assumes a peak pressure level of 282.6 dB//1 μPa. The initial 1/e decay time is 55 μs. Since the time waveforms and frequency spectra of Figs. 6.4(a) and 6.4(b) are very similar, it was decided that the simpler signal, the exponential pulse Fig. 6.4(b), would be the signal used for the shallow path.

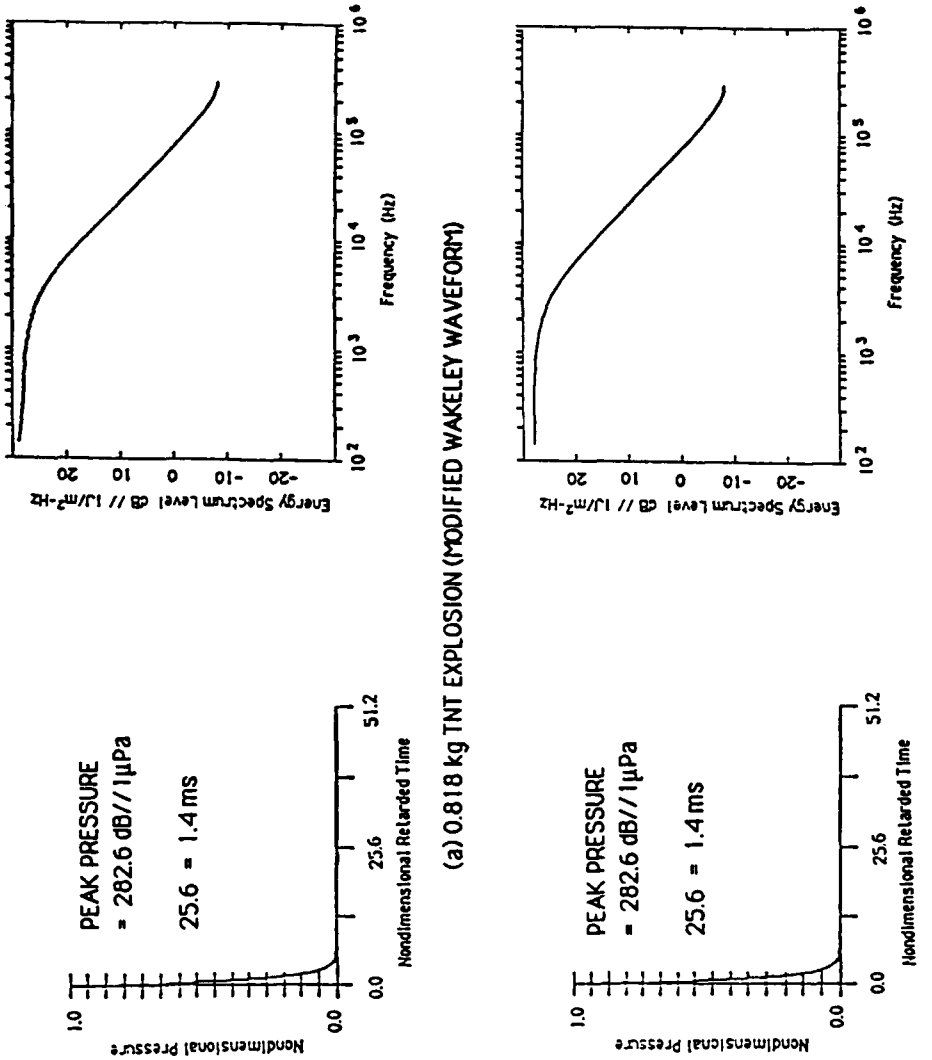

(a) 0.818 kg TNT EXPLOSION (MODIFIED WAKELEY WAVEFORM)

(b) WEAK SHOCK WITH AN EXPONENTIALLY DECAYING TAIL

FIGURE 6.4
TIME WAVEFORMS AND ENERGY SPECTRA FOR 300 m DETONATION

Shown in Figs. 6.5(a) and 6.5(b) are the modified Wakeley waveforms and corresponding energy spectra for the 0.818 kg and 22.7 kg TNT explosions at a depth of 4300 m. The waveforms are calculated at the reference ranges of 0.4 m and 1.1 m, respectively. Because the explicit dependence on charge weight has been removed from the expression for the explosion waveform, Eq. (6.2), the nondimensional time waveforms are identical. If the time waveforms had been plotted in terms of dimensional units, as are the frequency spectra, the waveforms would appear different. The larger explosion would have a longer bubble pulse period. This can be seen by noting that the 22.7 kg TNT explosion energy spectrum is shifted down in frequency in comparison to the other spectrum. The frequency shift is caused by the increase in charge weight. Since ordinary absorption and finite amplitude effects scale differently with frequency, it is expected that, after the signals propagate a moderate distance, their spectral shapes will be different. It is for this reason that two different charge weights are considered.

C. Effect of Medium Inhomogeneity on Nonlinearity

The effect of ocean inhomogeneity upon finite amplitude propagation is small. This conclusion was first quantitatively demonstrated by Morfey (1984a). To understand why the effect is small, recall the definition of the distortion range variable, Eq. (4-E.1). All the effects of ocean inhomogeneity are embodied in the nondimensional parameter G. The value of G for the shallow path is approximately 3.

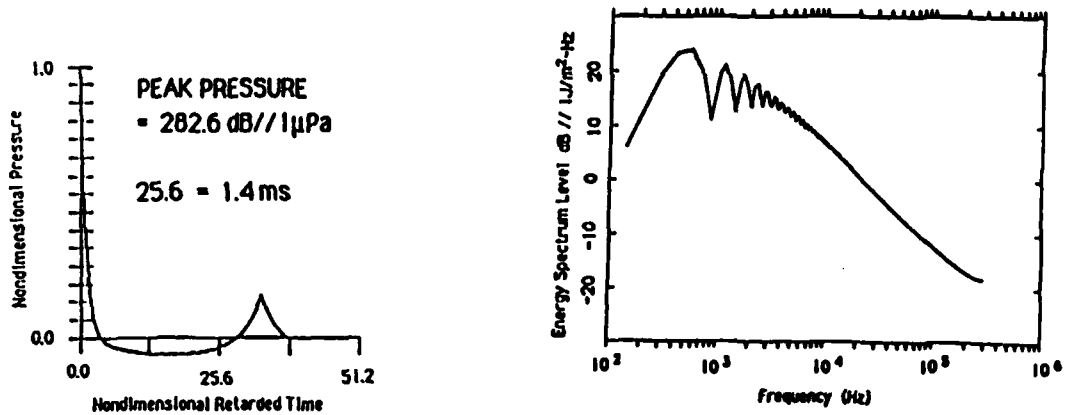

(a) 0.818 kg TNT EXPLOSION (MODIFIED WAKELEY WAVEFORM)

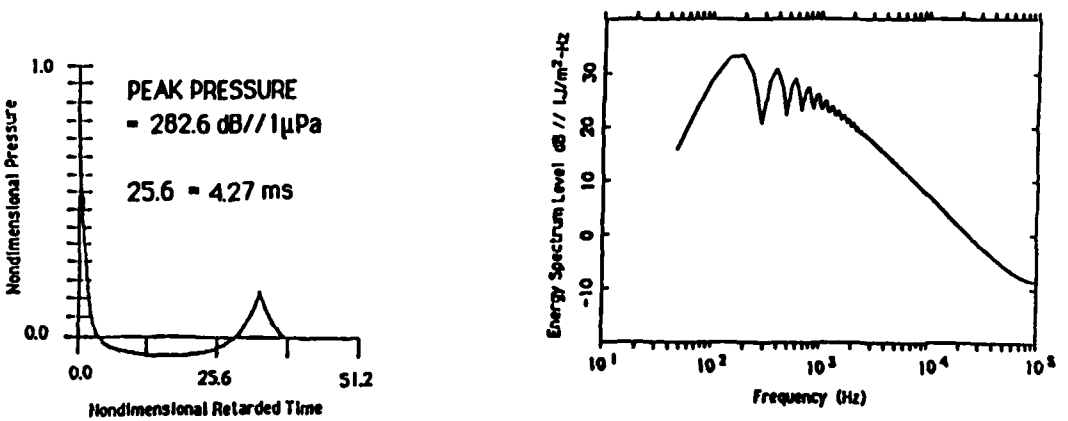

(b) 22.7 kg TNT EXPLOSION (MODIFIED WAKELEY WAVEFORM)

FIGURE 6.5
TIME WAVEFORMS AND ENERGY SPECTRA FOR 4300 m DETONATION

AS-85-1034

Physically this means that to undergo the same amount of distortion in a homogeneous ocean, the signal would have to propagate three times as far. This is not, however, a large enhancement because, as can be seen from Eq. (4-E.1), the distortion range variable--and hence the finite amplitude effects--are a function of the logarithm of the distance propagated.

As an example of how small an influence inhomogeneity has, consider a signal propagating along the shallow path. If the reference path length is 1 m, the path length is 20 km, and the value of G is 3, the distortion range variable is 11. If the ocean is homogeneous, the distortion range variable for a 20 km path and a 1 m reference range is 9.9. Since the amount of finite amplitude distortion is proportional to the distortion range variable, the inhomogeneity enhances the distortion by only 11% over the 20 km path length.

The enhancement of finite amplitude effects along the deep path is even smaller. There the maximum value of G is approximately 1. Hence in terms of nonlinear distortion there is effectively no difference between propagating through a homogeneous ocean and propagating along the deep path through an inhomogeneous ocean. It is therefore concluded that the effect of inhomogeneity upon nonlinear distortion is small.

We now quantitatively demonstrate the small effect of inhomogeneity on distortion by comparing the waveform for a homogeneous ocean with that for an inhomogeneous ocean; examine Fig. 6.6. The initial waveform is the exponential pulse shown in Fig. 6.4(b) but on an expanded time scale. The other waveforms result from (1) propagating the signal

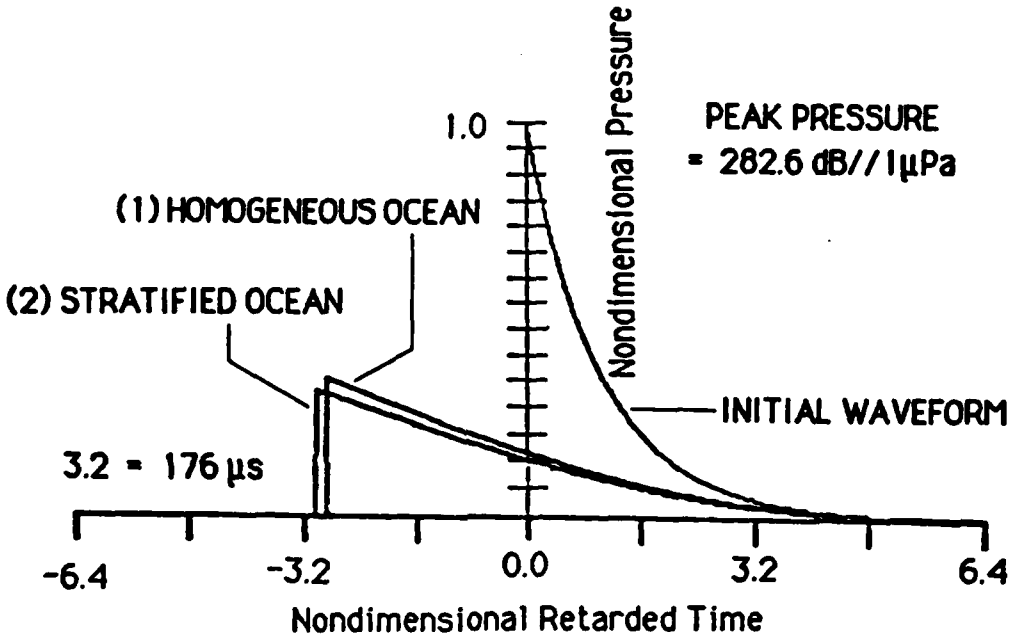

FIGURE 6.6
WEAK SHOCK WITH AN EXPONENTIALLY DECAYING TAIL AFTER PROPAGATING 58.1 km THROUGH (1) LOSSLESS HOMOGENEOUS OCEAN AND (2) LOSSLESS STRATIFIED OCEAN

58.1 km along the shallow path through a lossless ocean and (2) propagating the same signal to the same distance through a lossless homogeneous ocean. Note that the strong effect of geometrical spreading has been suppressed by plotting the transformed pressure given in Eq. (4-C.9) nondimensionalized by its initial value. The differences in amplitude and relative shock arrival time between the two resultant waveforms are clearly small (recall that $\ell n\ G$ is small compared to $\ell n\ (s/s_0)$).

On the other hand nonlinear effects are still important; reexamine Fig. 6.6. The shock arrival time is approximately 165 μs (three times the initial 1/e decay time) in advance of the linear theory prediction, and the peak pressure is approximately 1/3 of its original value. The nonlinear distortion may therefore be thought of as "stretching" the initial signal as well as attenuating it. Note that the "lossless ocean" is not really lossless because the nonlinear distortion takes account of losses at the shock. However, losses due to the medium which affect both continuous and discontinuous waves, such as relaxation, are not explicitly accounted for; hence the term lossless ocean.

D. The Combined Effects of Nonlinearity and Absorption

Throughout the propagation of a finite amplitude wave, the effects of both nonlinearity and ordinary attenuation and dispersion are at play. To more clearly examine the role of each in the propagation process, we first examine them separately, and then together. Figure 6.7 shows four waveforms, one of which is the initial waveform, the exponential pulse of

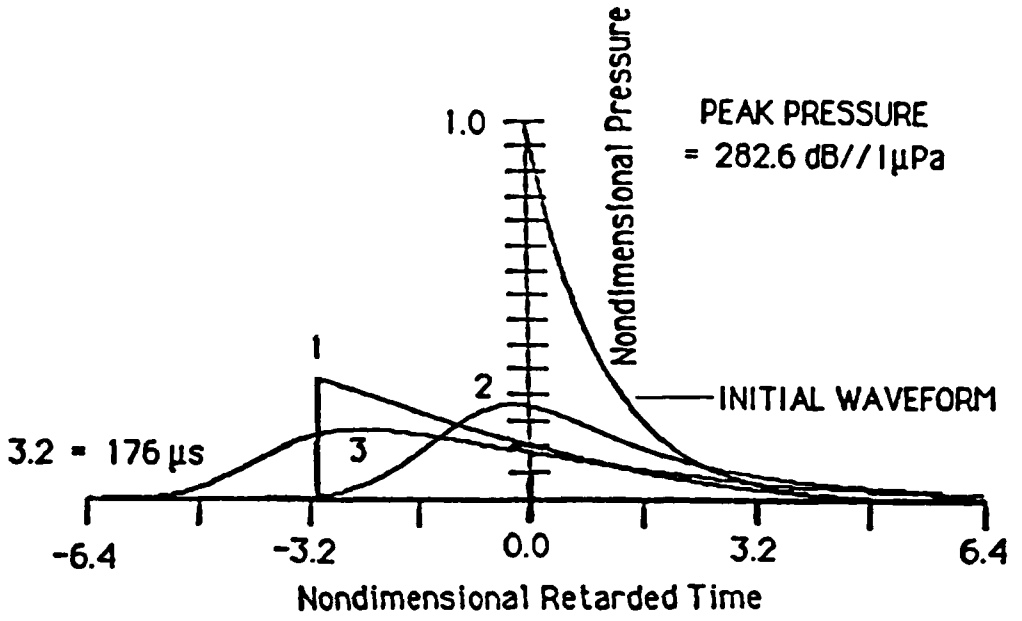

FIGURE 6.7
WEAK SHOCK WITH AN EXPONENTIALLY DECAYING TAIL AFTER PROPAGATING 58.1 km THROUGH A STRATIFIED OCEAN CONSIDERING (1) ORDINARY ATTENUATION AND DISPERSION ONLY (2) FINITE AMPLITUDE EFFECTS ONLY AND (3) FINITE AMPLITUDE EFFECTS AND ORDINARY ATTENUATION AND DISPERSION

Fig. 6.4(b) on an expanded time scale. The others are the resulting waveforms after propagating 58.1 km along the shallow path considering (1) ordinary attenuation and dispersion only, (2) finite amplitude effects only, and (3) both finite amplitude effects and ordinary attenuation and dispersion. It is clear from the figure that by itself neither finite amplitude effects nor ordinary absorption can correctly account for the shape of the resulting waveform; both are required. The finite amplitude effects attenuate the wave while causing it to try to form, or to maintain, a shock. Ordinary absorption attenuates the wave, thus causing the wave to become rounded.

It is interesting to examine the effect of dispersion on the position of the peak pressure. Consider the propagation, neglecting finite amplitude effects, of the exponential pulse along the shallow path. The waveforms in Figs. 6.8(a) and 6.8(b) are obtained at various positions along the shallow path, from the reference range 0.4 m out to 58.1 km. The calculations were made first without dispersion (Fig. 6.8a), and then with dispersion (Fig. 6.8b). At longer ranges the effect of dispersion is clear; it shifts the waveform forward. In Fig. 6.8(a) the peak pressure continuously moves backward; i.e., the effective propagation speed of the peak is less than c_0. The same is true of the waveforms in Fig. 6.8(b) for distances up to 8.6 km, but beyond that distance dispersion pulls the peak forward. By the time the wave has reached the maximum distance of 58.1 km, the shift of the peak pressure due to dispersion is approximately 0.8 of the initial 1/e

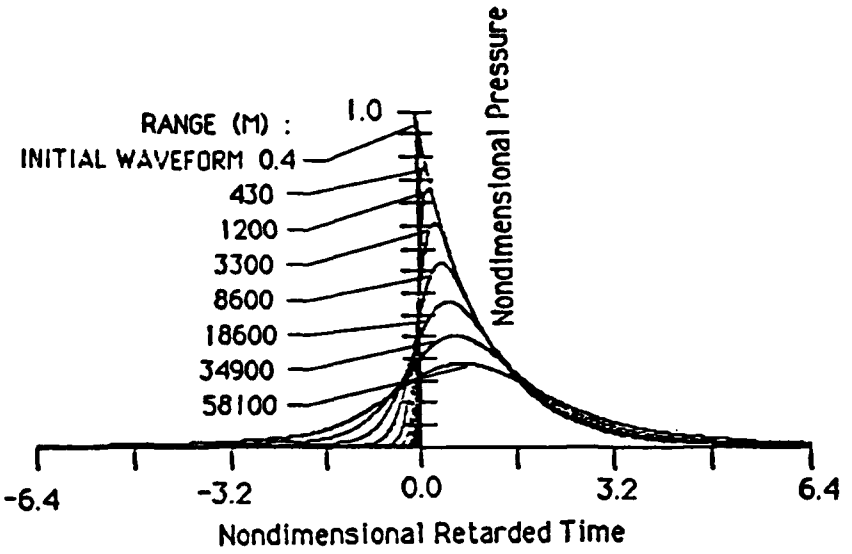

(a) WITHOUT DISPERSION

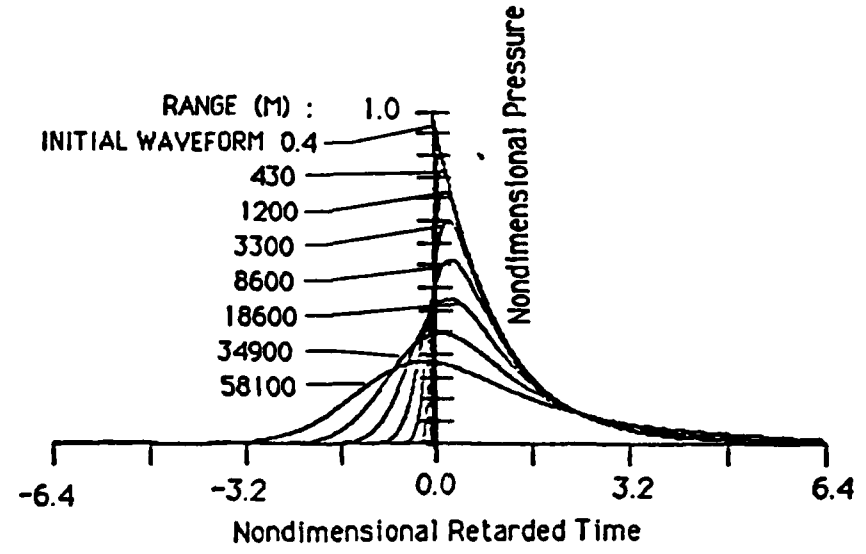

(b) WITH DISPERSION

FIGURE 6.8
PROPAGATION OF A WEAK SHOCK WITH AN EXPONENTIALLY DECAYING TAIL THROUGH A LOSSY STRATIFIED OCEAN NEGLECTING FINITE AMPLITUDE EFFECTS

AS-85-1037

decay time. This would be a significant amount of time if one were trying to add signals coherently.

In Fig. 6.9 we again examine the effect of dispersion, but this time finite amplitude effects are also included. In this case the waveforms at the lower ranges are resolved. Notice that in Fig. 6.9(a) the peak pressure moves forward until a range of 3300 m is reached and then moves backwards. In Fig. 6.9(b), however, the forward movement of the the peak pressure is monotonic. The forward movement is due first to finite amplitude effects and in the end due to dispersion.

Figure 6.9(a) enables us to examine the combined effects of nonlinearity and attenuation. As noted above, the peak pressure in Fig. 6.9(a) stops moving forward as the signal propagates beyond 3300 m. One might interpret this to indicate a change in the importance of finite amplitude effects relative to attenuation. From 3300 m on, ordinary attenuation is the dominant mechanism of diminution, whereas for ranges less than 3300 m finite amplitude effects are the principal mechanism. It is noted, however, that the amount of attenuation beyond 3300 m indicated in Fig. 6.8(a) is less than that over the corresponding distance in Fig. 6.9(a). It is therefore concluded that, even though finite amplitude effects are not dominant beyond 3300 m, they are still noticeable. Although the transition point, 3300 m, applies only to this particular example, one can expect a similar behavior for other signals of similar initial shape.

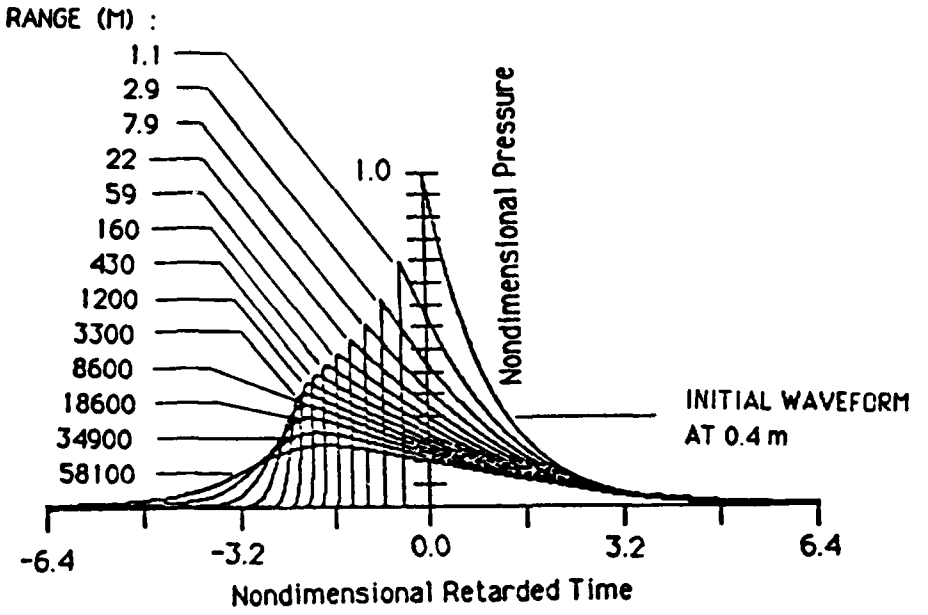

(a) WITHOUT DISPERSION

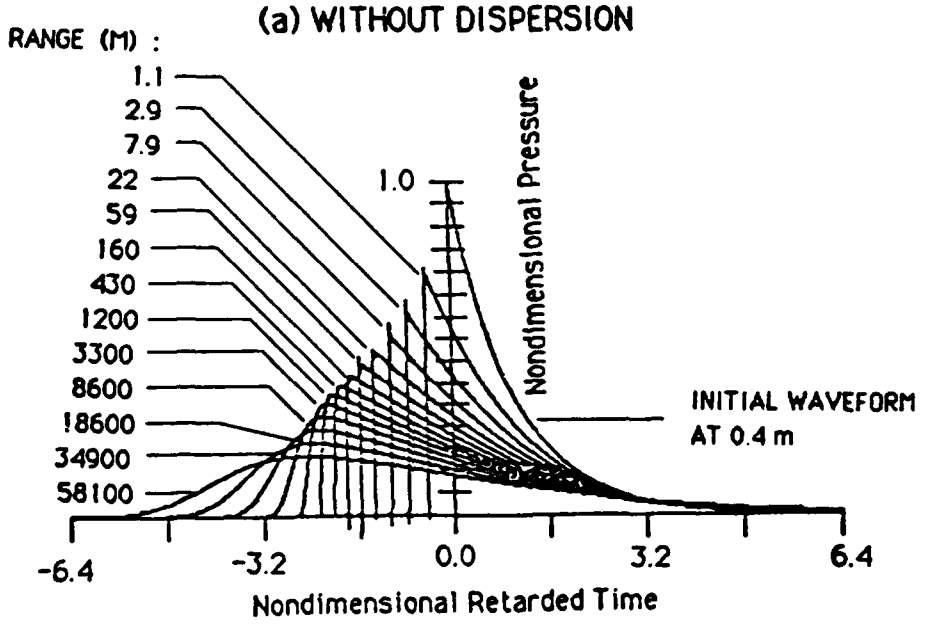

(b) WITH DISPERSION

FIGURE 6.9
PROPAGATION OF A WEAK SHOCK WITH AN EXPONENTIALLY DECAYING TAIL THROUGH A LOSSY STRATIFIED OCEAN CONSIDERING FINITE AMPLITUDE EFFECTS

AS-85-1038

E. To What Distance are Finite Amplitude Effects Important?

In this section we find that for a specific frequency range and source strength, finite amplitude effects may be neglected beyond a certain distance. Ordinary absorption appears to dominate the propagation beyond that distance. One explanation for the importance of ordinary absorption over finite amplitude effects is that the effects of ordinary absorption increase as $\exp(-\alpha s)$, whereas most finite amplitude effects depend on σ (Eq. 5-B.5) which is proportional to $\ell n\,(s/s_0)$.

To answer quantitatively the question posed in the heading of this section, we conducted a numerical experiment involving two different explosion pulses. The first is for a 0.818 kg TNT explosion at a depth of 4300 m, and the second, a 22.7 kg TNT explosion at the same depth. The source waveforms and their respective spectra are shown in Figs. 6.5(a) and 6.5(b). The procedure used is a simple one. The explosion waves are numerically propagated to a distance of 23 km along the deep path accounting for attenuation and dispersion over the entire 23 km and accounting for nonlinear effects as indicated below:

Case A: nonlinear effects neglected entirely,

Case B: nonlinear effects included only up to range 150 m,

Case C: nonlinear effects included only up to range 1100 m,

Case D: nonlinear effects included for the entire 23 km.

Case D is used as the basis of comparison.

Because the effective duration of the explosion pulses in Fig. 6.5 is much greater than that of the simple exponential pulses (compare the

waveforms of Fig. 6.5 with the initial waveform of Fig 6 6), time waveform resolution of the sort shown in Figs 6 6 through 6 9 is not possible Interesting results may, however, be found by comparing the spectra of the signals. The results are therefore presented in the form of energy spectrum plots. A few time waveforms are shown for clarity in interpreting changes in spectra.

1. The 0.818 kg TNT Explosion Results

The results of the numerical experiment involving the 0.818 kg TNT explosive are presented in Figs. 6.10 through 6.12. The dotted curve in Fig. 6.10 is the initial energy spectrum at the reference range, 0.4 m. The dashed curve is the energy spectrum calculated neglecting finite amplitude effects over the entire 23 km, Case A. The solid curve in the figures is the energy spectrum calculated accounting for finite amplitude effects over the entire path, Case D. Figure 6.11 shows a comparison of Cases B and D and Fig. 6.12, Cases C and D.

We start our discussion by examining the behavior of the solid curve (Case D) and the dashed curve (Case A) in Fig. 6.10. Note that, as for the time waveforms, the effect of geometric spreading has been removed. The differences between the two curves are itemized below.

(a) At the high frequency end (above 15 kHz) the solid curve is higher.

(b) In the middle range (approximately 1.5 - 15 kHz) the dashed curve is higher.

(c) At the low frequency end (below 1.5 kHz) the envelopes of the two curves are about the same.

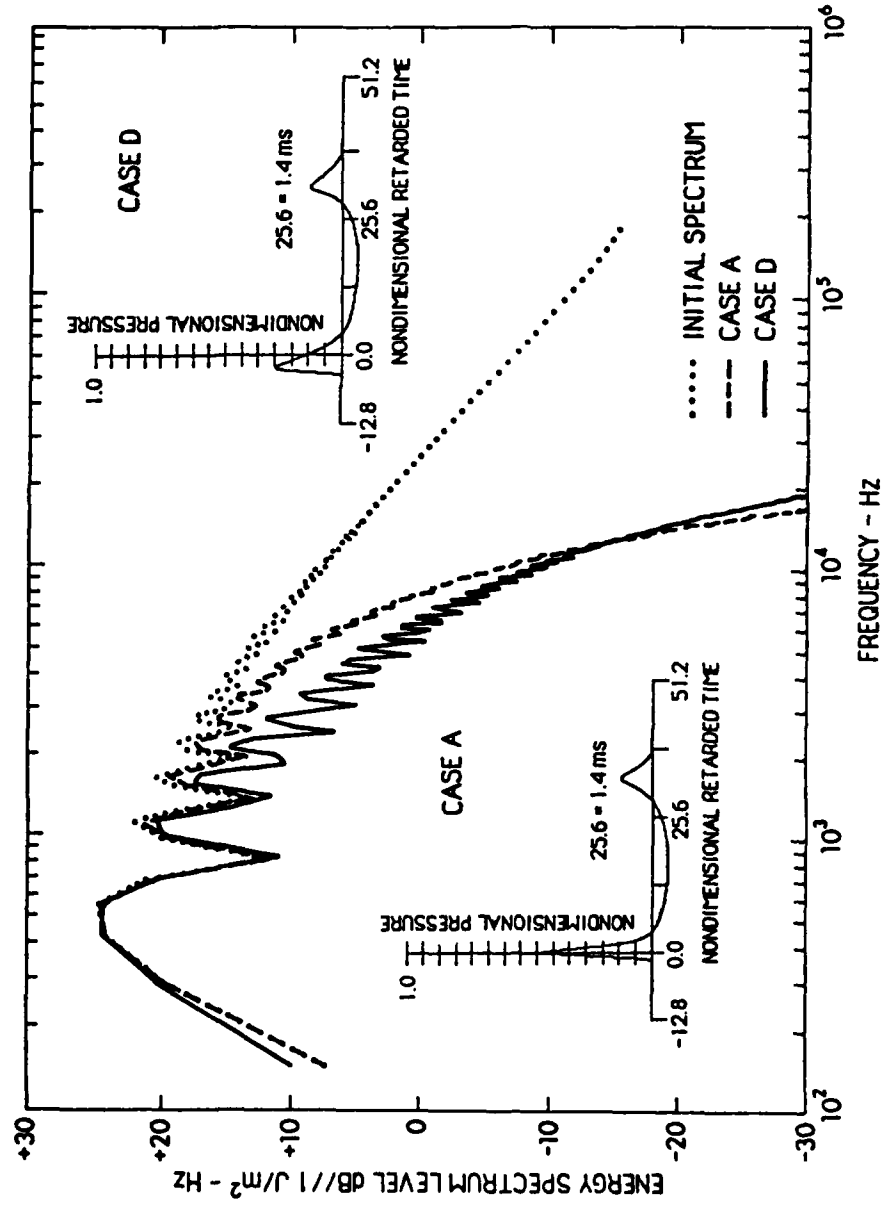

FIGURE 6.10
ENERGY SPECTRA OF 0.818 kg TNT EXPLOSION
(1) AT THE REFERENCE RANGE (0.4 m), (2) AFTER PROPAGATING 23 km NEGLECTING FINITE AMPLITUDE EFFECTS (CASE A), AND (3) AFTER PROPAGATING 23 km CONSIDERING FINITE AMPLITUDE EFFECTS (CASE D)

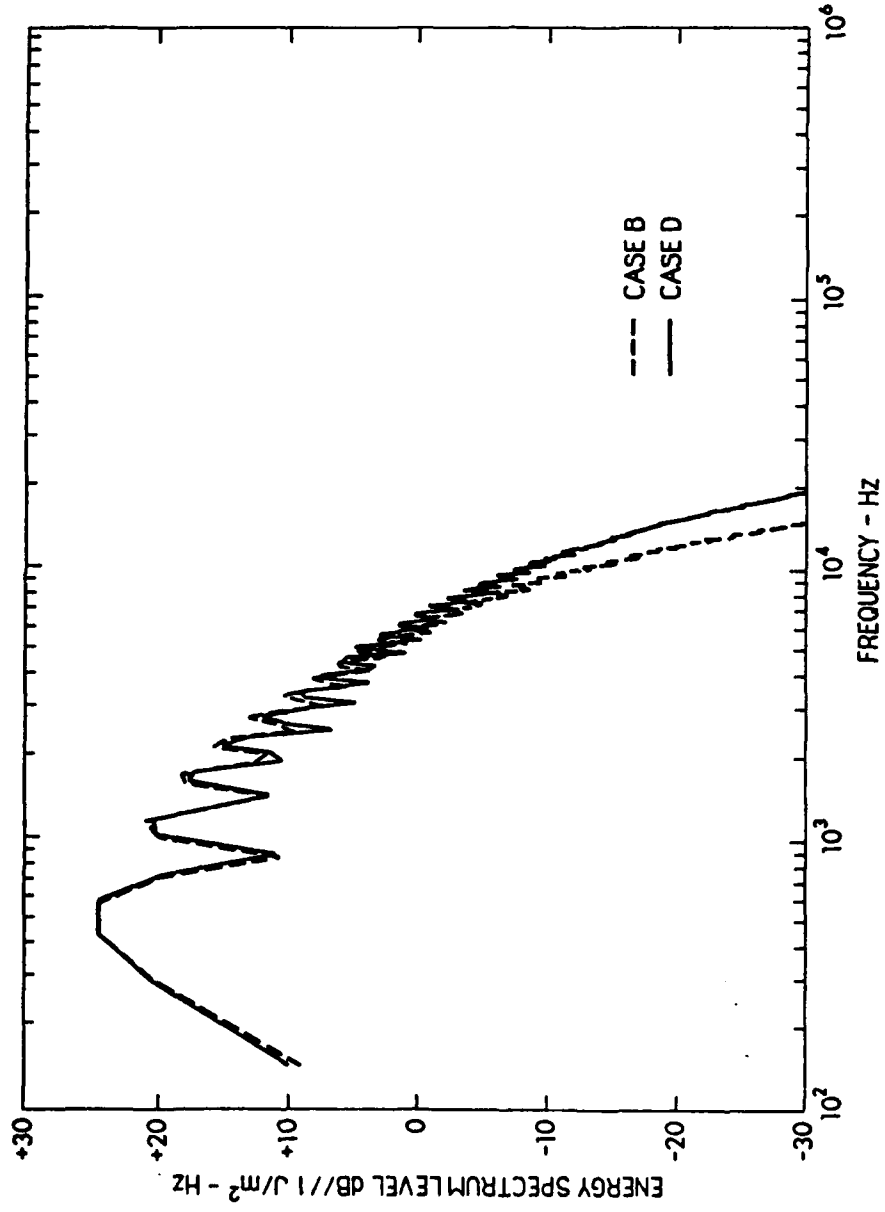

FIGURE 6.11
ENERGY SPECTRA OF 0.818 kg TNT EXPLOSION AFTER PROPAGATING 23 km
CONSIDERING FINITE AMPLITUDE EFFECTS (1) OVER THE FIRST 150 m (CASE B)
AND (2) OVER THE ENTIRE 23 km (CASE D)

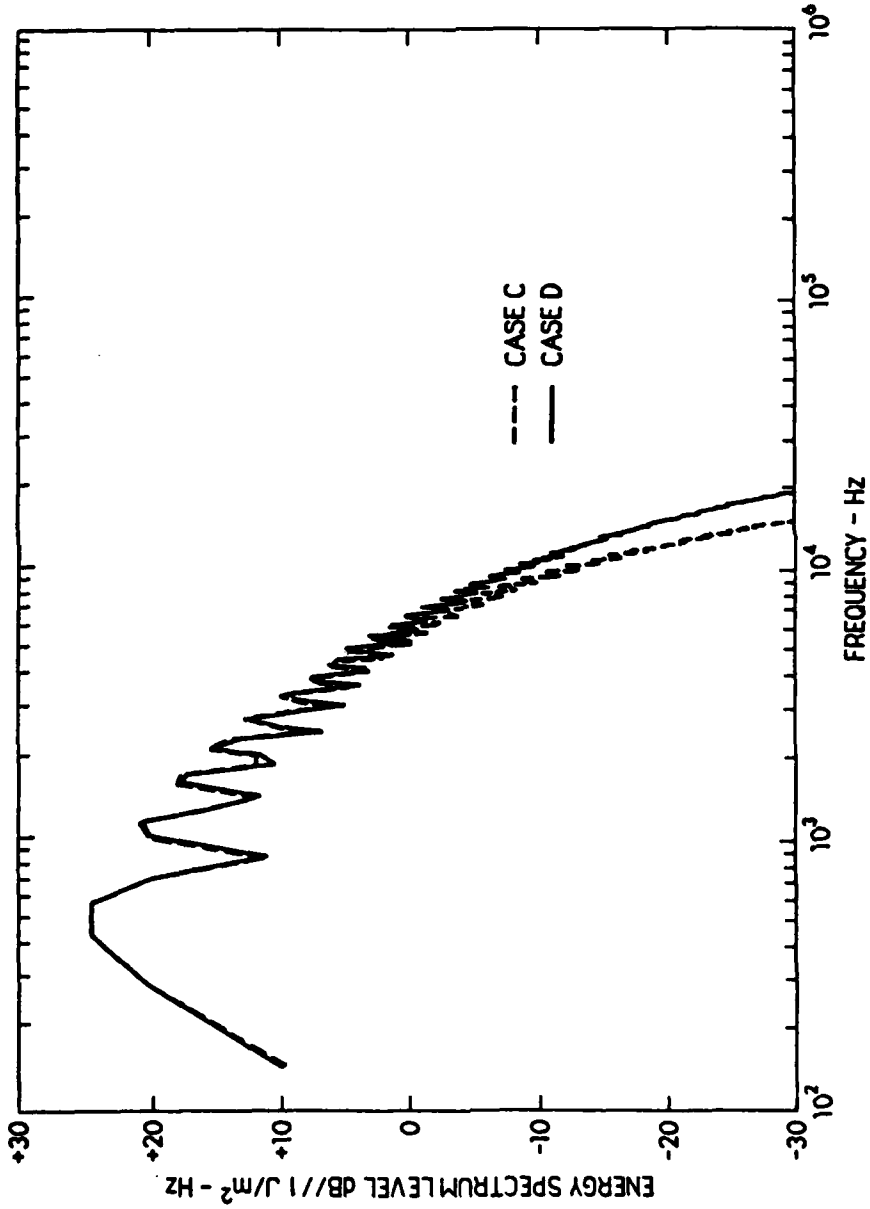

FIGURE 6.12
ENERGY SPECTRA OF 0.818 kg TNT EXPLOSION AFTER PROPAGATING 23 km
CONSIDERING FINITE AMPLITUDE EFFECTS OVER (1) THE FIRST 1100 m (CASE C)
AND (2) THE ENTIRE PROPAGATION PATH (CASE D)

(d) As the frequency decreases from about 400 Hz, the solid curve rises above the dashed curve.

(e) In the low frequency region the spectral peaks of the solid curve occur at slightly lower frequencies than the peaks of the dashed curve.

The differences cited above can be explained in terms of the nonlinear distortion of the wave. Compare the two time waveforms inserts. Difference (a) is probably caused by the steepening of the compression part of the bubble pulse. Difference (b) is probably due to the increase in the decay time of the first peak (as the shock pulls ahead of the first zero). Differences (d) and (e) are probably due to the stretching of the time interval between the initial peak and the bubble pulse peak.

We now examine the Case B and Case C spectra. In the following discussion of Figs. 6.11 and 6.12 we attempt to answer the question, "to what distance are finite amplitude effects important?" The inclusion of finite amplitude effects up to 150 m (Fig. 6.11) gives a 23 km spectrum that follows the Case D spectrum up to about 6 kHz. Less important effects are seen at the very low frequencies. Figure 6.12 shows that the Case C spectrum also follows the Case D spectrum up to about 6 kHz, although it does so more closely than the Case B spectrum. The tentative conclusion, namely that nonlinear effects may be ignored beyond a certain distance, depends on the frequency range in which one is interested.

2. The 22.7 kg TNT Explosion Results

We now turn our attention to the case of a 22.7 kg TNT explosion. As can be seen in Figs. 6.5(a) and 6.5(b), the energy spectra of the two explosions are very similar except that the larger explosion has an overall higher spectrum level and is shifted down in frequency. To avoid peak pressures too high to be handled correctly by weak shock theory, we increase our reference range to 1.1 m (for the 22.7 kg pulse only), thereby making the peak pressure at the reference range the same for both the 0.818 kg and the 22.7 kg TNT explosion (282.6 dB//1 μPa). Because of the frequency shift of the spectrum, the nonlinear distortion of the two pulses is much the same (finite amplitude effects scale with frequency). The only real difference is the effect of attenuation, which should be less for the pulse from the larger charge.

The results in the form of energy spectra are presented in Figs. 6.13 through 6.15. The initial spectrum is shown as the dotted curve in Fig. 6.13. In this figure the dashed curve is the energy spectrum calculated neglecting finite amplitude effects entirely, Case A. The solid curve in Figs. 6.13 through 6.15 is the 23 km energy spectrum calculated accounting for finite amplitude effects over the entire path, Case D. In Fig. 6.14 the dashed curve is the spectrum for Case B; in Fig. 6.15 the dashed curve is the spectrum for Case C.

The general observations made of the solid and dashed curves in Fig. 6.13 are the same as those made of Fig. 6.10, except that the

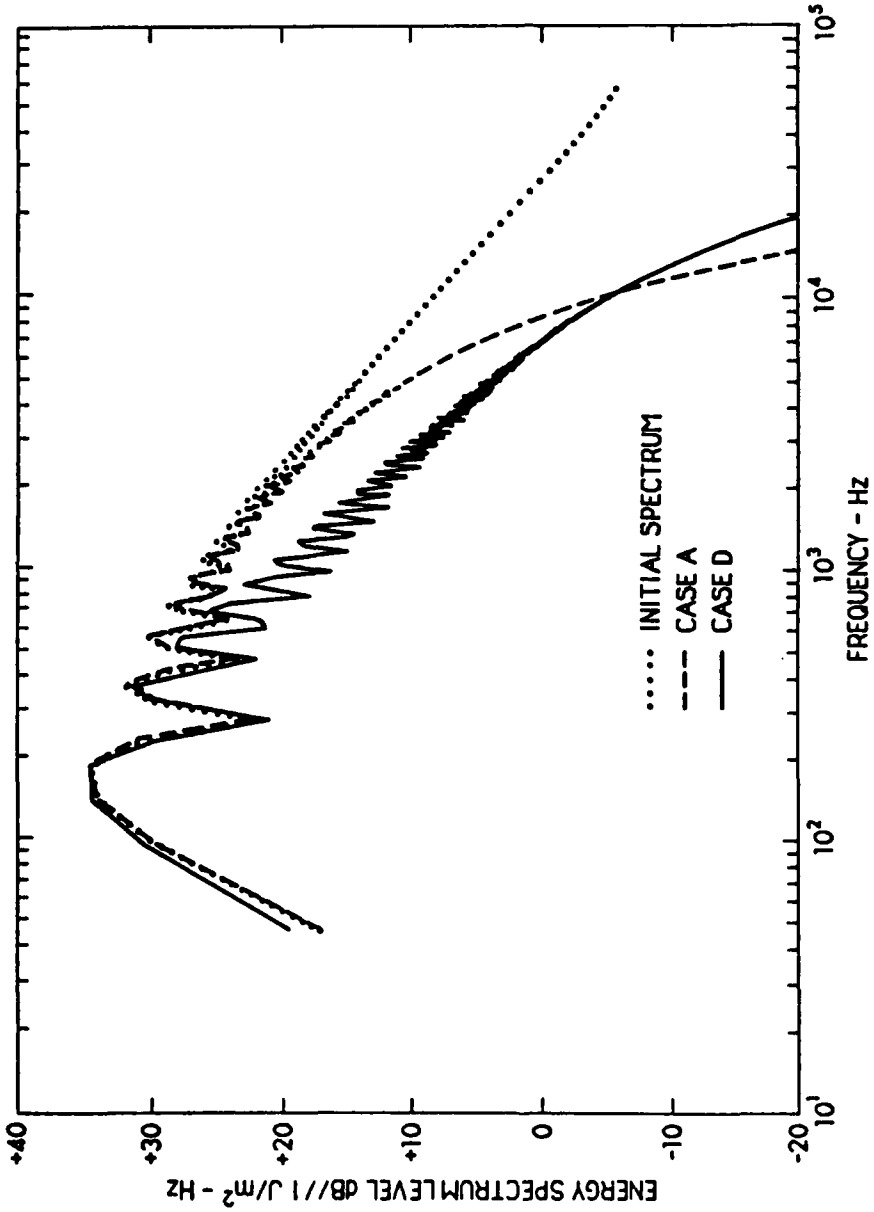

FIGURE 6.13
ENERGY SPECTRA OF 22.7 kg TNT EXPLOSION
(1) AT THE REFERENCE RANGE (1.1 m), (2) AFTER PROPAGATING 23 km NEGLECTING FINITE AMPLITUDE EFFECTS (CASE A), AND (3) AFTER PROPAGATING 23 km CONSIDERING FINITE AMPLITUDE EFFECTS (CASE D)

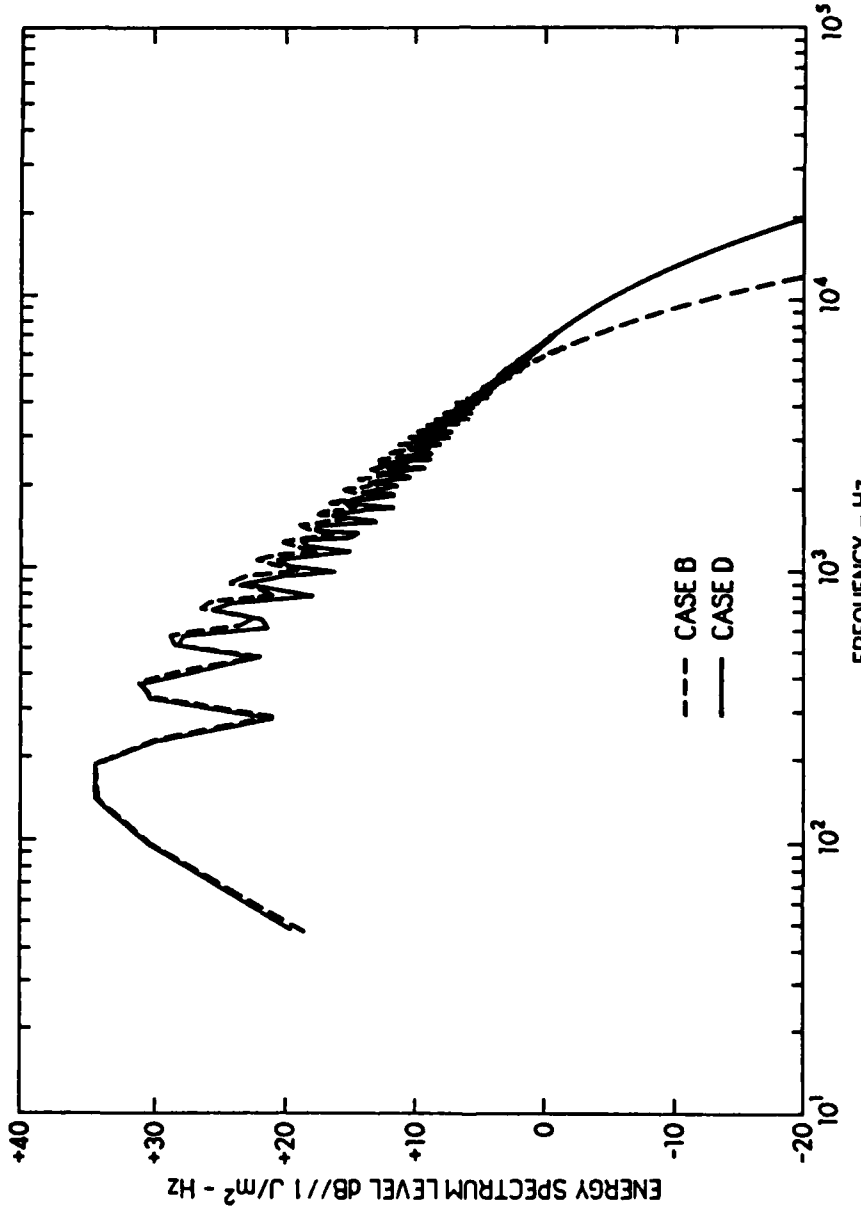

FIGURE 6.14
ENERGY SPECTRA OF 22.7 kg TNT EXPLOSION AFTER PROPAGATING 23 km
CONSIDERING FINITE AMPLITUDE EFFECTS (1) OVER THE FIRST 150 m (CASE B)
AND (2) OVER THE ENTIRE 23 km (CASE D)

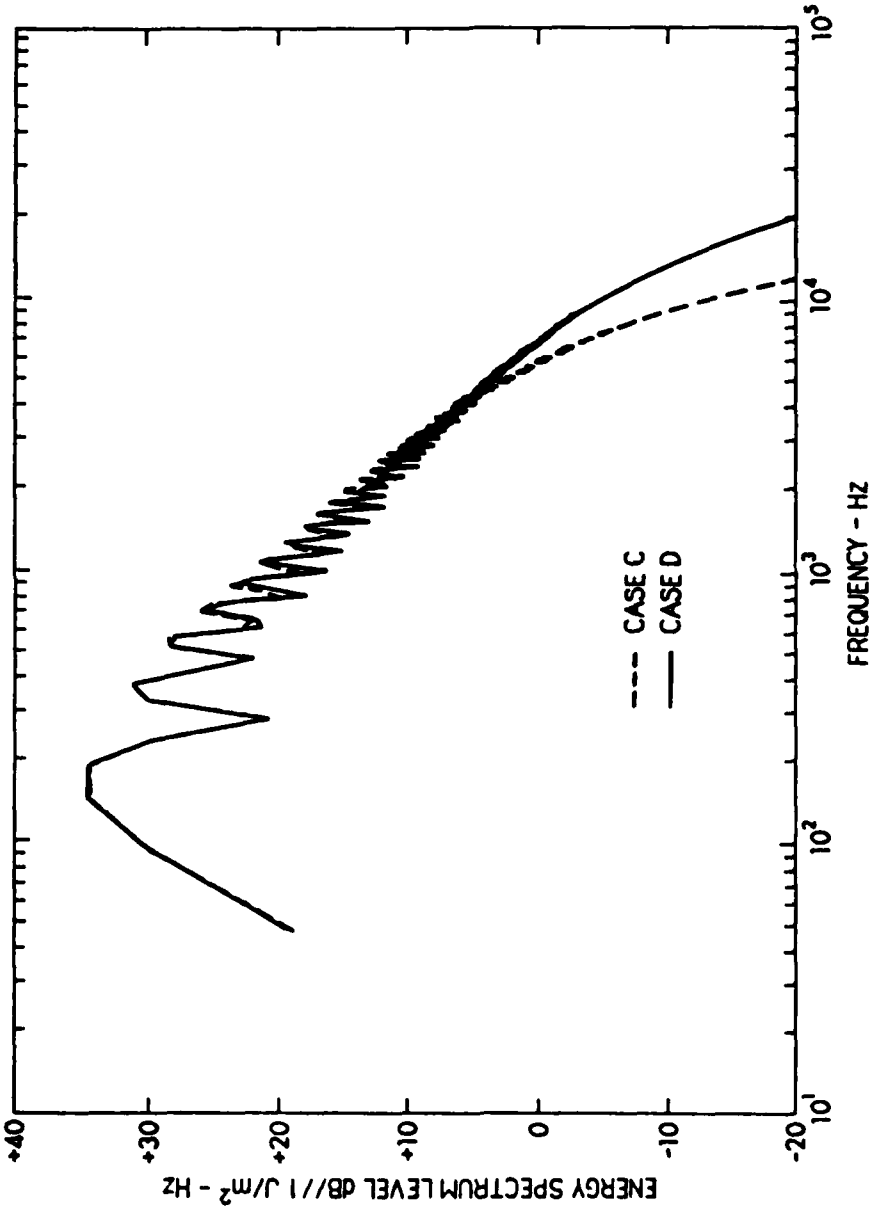

FIGURE 6.15
ENERGY SPECTRA OF 22.7 kg TNT EXPLOSION AFTER PROPAGATING 23 km CONSIDERING FINITE AMPLITUDE EFFECTS OVER (1) THE FIRST 1100 m (CASE C) AND (2) THE ENTIRE PROPAGATION PATH (CASE D)

AS-85-1044

frequencies cited previously are higher. The differences between the solid and dashed curves of Fig. 6.13 may be summarized as follows.

(a) Above approximately 10 kHz the solid curve is higher.

(b) From about 500 Hz to 10 kHz the dashed line is higher.

(c) The solid curve is slightly higher from 50 to 500 Hz.

(d) Over the same frequency range as (c) the spectral peaks of the solid curve exhibit a slight downward shift.

The physical explanations for these differences are the same as those for the differences witnessed in Fig. 6.10. The nonlinear steepening of the compressional part of the bubble pulse accounts for difference (a). Difference (b) is due to the increase in the decay time of the first peak. Differences (c) and (d) are due to the slight increase in the period between the initial pulse and the bubble pulse.

We now address the question, "to what distance are finite amplitude effects important?" As in the case of the 0.818 kg explosion, the answer may be obtained by comparing the Case B and Case C energy spectra with the Case D spectrum. The Case B and Case C spectra (Figs. 6.14 and 6.15, respectively) follow the Case D spectrum closely for frequencies below 4 kHz, although the Case C spectrum more closely duplicates that of the Case D. It is therefore concluded that the finite amplitude effects can be neglected after a certain distance, and that the distance depends on both frequency and source strength. Since the differences between the Case C and Case D spectra are approximately the same for both the 0.818 kg and

22.7 kg TNT explosions, it is also concluded that the differences between the two spectra due to absorption are small.

In summary it is noted that the prevailing sentiment that "nonlinear effects are important only close to the source" is confirmed quantitatively. Beyond a distance that depends on frequency and charge weight, nonlinear effects may be neglected. Notice, however, that the calculations are for rays that encounter neither reflections nor caustics.

CHAPTER 7

SUMMARY

In this report the propagation of finite amplitude signals through an inhomogeneous ocean is investigated both analytically and numerically. The theory used is that of nonlinear geometrical acoustics. The amplitude of the signal is assumed to be small enough that self-refraction may be neglected. Another assumption is that the acoustic field consists only of outgoing waves. The effects of reflections and focusing are not considered. Losses are accounted for directly in the numerical routine; the analytic work is performed neglecting all losses except those at the shock. In the numerical study the ocean is assumed to be stratified, whereas the analytic work is for a fully inhomogeneous ocean in which temperature, salinity, and density vary with position.

The analysis starts with the presentation of a scheme for ranking the terms in the hydrodynamics equations according to their degree of smallness. The ranking scheme is then used to simplify the hydrodynamics equations for lossless inhomogeneous fluids for (1) small-signal and

(2) finite amplitude waves. From these simplified equations the theories of linear and nonlinear geometrical acoustics are developed. The eikonal equation is obtained and found to be the same for both small-signal and finite amplitude waves. The transport equation is, however, different for the two cases. An equation for the ray paths is derived from the eikonal equation and the relations of vector calculus. In the case of a constant gradient sound speed profile, the ray paths are found to be circular arcs. The two transport equations are found to be equivalent to the first-order progressive wave equations for small-signal and finite amplitude waves, respectively. All the analysis is carried out in the time domain.

The numerical implementation of nonlinear geometrical acoustics is divided into three parts. First the ray paths are calculated using the ray tracing program MEDUSA. Next the program CALCG uses the environmental information to perform a numerical intregration along the ray path, thereby calculating the quantity G. The ray path information, the value G, and the environmental information are all inputs to the program PLPROP. PLPROP uses this information to calculate the distortion range variable, Z. PLPROP has at its center the subroutine WAVPROP, a finite difference implementation of weak-shock theory for plane waves (Pestorius 1973). Within PLPROP losses are accounted for in the frequency domain using the empirical relations of François and Garrison (1982). PLPROP has a variety of switches that allow the investigator to selectively include the effects of nonlinear distortion, ordinary attenuation, and dispersion. The finite amplitude effects may be "turned off" after a specific propagation distance

has been reached. The output of the program is in the form of plots of the time waveforms and energy spectra for preselected propagation distances. The accuracy of the program was verified by comparing its results with those of known analytic solutions for waves propagating through a lossless homogeneous media. The peak pressure, the relative shock arrival time, and the 1/e decay time of a weak shock with an exponentially decaying tail were all predicted by PLPROP to a high degree of accuracy.

In the numerical study the effects of inhomogeneity, ordinary attenuation and dispersion, and nonlinear distortion are investigated by considering the propagation of explosion waveforms The signals used in the investigation are a weak shock with an exponentially decaying tail (exponential pulse) and a more realistic explosion waveform which includes the first bubble pulse. The exponential pulse is propagated 58.1 km along a ray path starting at a depth of 300 m. The more realistic waveform is propagated 23 km along a ray path starting at a depth of 4300 m.

An exponential pulse corresponding to a 0.818 kg TNT explosion is used to investigate the separate and combined effects of inhomogeneity, ordinary attenuation, dispersion, and nonlinear distortion. The effect of inhomogeneity of the ocean on nonlinear distortion is found to be small. Dispersion is found to play an important role in the arrival time of the peak pressure. The propagation of a finite amplitude signal is found to depend on the combination of nonlinear distortion and ordinary attenuation and dispersion.

More realistic waveforms corresponding to two different explosions, 0.818 kg and 22.7 kg TNT, are used to quantify the answer to the question, "to what distance are finite amplitude effects important?" The spectra of the signals obtained by numerically propagating the signals to a distance of 23 km accounting for ordinary attenuation and dispersion over the entire 23 km and acounting for finite amplitude effects as indicated below:

Case A: finite amplitude effects neglected entirely,

Case B: finite amplitude effects included only up to distance 150 m,

Case C: finite amplitude effects included only up to distance 1100 m,

Case D: finite amplitude effects included for the entire 23 km path.

The Case D spectrum, relative to that of Case A, is lower in the middle frequency band and slightly higher in the low and high frequency bands. A small downward shift of the spectral peaks in the low frequency band is also noted. For the one ray path and waveform considered, finite amplitude effects are found, in the case of a 0.818 kg TNT explosion, to be of small consequence for frequencies below 6 kHz and distances beyond 1100 m. For a 22.7 kg TNT explosion the corresponding quantities are frequencies below 4 kHz and distances beyond 1100 m.

APPENDIX A

RAY COORDINATES AND THE EXPRESSION FOR $\nabla^2\Psi$

In this appendix ray coordinates are defined, and it is shown that $\nabla^2\Psi = A_0^{-1}\,\partial(A_0/c_0)/\partial s$, where A_0 is the area of the ray tube, c_0 is the small-signal sound speed, and s is the distance along the ray path. The expression for $\nabla^2\Psi$ is required to simplify the transport equation, Eq. (3-C.19). To derive the expression, we use tensor analysis and a nonorthogonal coordinate system called ray coordinates (see, for example, Pitre 1984, p. 54). General introductions to tensor analysis may be found in standard texts such as those by Sokolnikoff (1964) and Synge and Schild (1978).

The mathematical development proceeds as follows. The ray coordinate system and the Jacobian of the transformation from Cartesian coordinates to ray coordinates are found. It is then shown that the determinant of the Jacobian is related to the ray tube area. Next the covariant and contravariant forms of the metric tensor for the ray coordinate system are found. The contravariant form of the metric tensor and the determinant of the Jacobian are then substituted into the definition

of the Laplacian for a general coordinate system. The desired result for $\nabla^2\Psi$ follows directly.

We define some notation: Let us denote the determinant of a tensor by the same symbol, but without indices; for example, $|A^{ij}|$ is denoted A. Let x^i, where i = 1, 2, 3, stand for the rectangular Cartesian coordinate system, that is, $x^1 = x$, $x^2 = y$, $x^3 = z$. Let $\underline{x}^r$ stand for another set of coordinates, ray coordinates, namely $\underline{x}^1 = s$, $\underline{x}^2 = \phi$, and $\underline{x}^3 = \psi$, where s is the distance along the ray path, and ϕ and ψ are the ray launch angles with respect to the x and z axes. Both the ray coordinate system and the Cartesian system are shown in Fig. 3.2. Ray coordinates may be thought of as a coordinate system based on the path of a particle through space.

A physical understanding of the transformations between the two coordinate systems is sought. We define the coordinate transformations as follows:

$$x^i = x^i(\underline{x}) \quad , \tag{A.1}$$

and

$$\underline{x}^r = \underline{x}^r(x) \quad . \tag{A.2}$$

The Jacobian J^i_r of the transformation from Cartesian coordinates to ray coordinates is

$$J^i_r = \frac{\partial x^i}{\partial \underline{x}^r} = \begin{bmatrix} \partial x/\partial s & \partial y/\partial s & \partial z/\partial s \\ \partial x/\partial \phi & \partial y/\partial \phi & \partial z/\partial \phi \\ \partial x/\partial \psi & \partial y/\partial \psi & \partial z/\partial \psi \end{bmatrix} \quad . \tag{A.3}$$

Let **T** be the derivative of the ray path position vector **r** (see Fig. A.1):

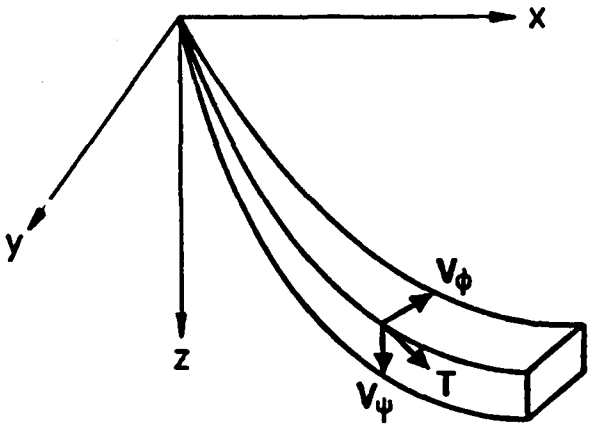

FIGURE A.1
THE DERIVATIVES OF THE RAY PATH POSITION VECTOR

$$\mathbf{T} = \left(\frac{\partial x}{\partial s}, \frac{\partial y}{\partial s}, \frac{\partial z}{\partial s}\right) \quad , \tag{A.4}$$

where the bracketed terms are the components in the x, y, and z directions. The derivatives with respect to the launch angles ϕ and ψ, denoted $\mathbf{V}_\phi$ and $\mathbf{V}_\psi$, are defined as follows:

$$\mathbf{V}_\phi = \left(\frac{\partial x}{\partial \phi}, \frac{\partial y}{\partial \phi}, \frac{\partial z}{\partial \phi}\right) \quad , \tag{A.5}$$

$$\mathbf{V}_\psi = \left(\frac{\partial x}{\partial \psi}, \frac{\partial y}{\partial \psi}, \frac{\partial z}{\partial \psi}\right) \quad . \tag{A.6}$$

Recall from vector calculus that the magnitude of the vector product, $\mathbf{B} \times \mathbf{C}$, equals the area of the parallelogram defined by $\mathbf{B}$ and $\mathbf{C}$. The vector product of $\mathbf{V}_\phi$ with $\mathbf{V}_\psi$ defines a cross-sectional area of the ray tube. The scalar triple product, $\mathbf{T}\cdot(\mathbf{V}_\phi \times \mathbf{V}_\psi)$, defines A_0, the cross-sectional area of the ray tube normal to the direction of propagation. As can be seen from Eq. (A.3), the scalar triple product is also equal to the determinant of the Jacobian:

$$\begin{aligned} J &\equiv |J_r'| \\ &= \mathbf{T}\cdot(\mathbf{V}_\phi \times \mathbf{V}_\psi) \\ &= A_0 \quad . \end{aligned} \tag{A.7}$$

The Laplacian of a function f in any general coordinate system is defined as follows (Sokolnikoff 1964, Eq. 92.11):

$$\nabla^2 f = \frac{1}{\sqrt{g}} \frac{\partial}{\partial \underline{x}^s} \left(\sqrt{g}\, \underline{g}^{rs} \frac{\partial f}{\partial \underline{x}^r} \right) \quad , \tag{A.8}$$

where f is a function in the original coordinate system. To use Eq. (A.8) we need $\underline{g}^{rs}$, the contravariant form of the metric tensor in the ray coordinate system. To find $\underline{g}^{rs}$ we first find the covariant form $\underline{g}_{rs}$. Since the contravariant and the covariant metric tensors are inverses of one another, the contravariant metric tensor can be found from the covariant.

In a Euclidian space of three dimensions, the covariant form of the metric tensor may be defined by considering an elemental distance ds. It is known (Sokolnikoff 1964, Art. 29) that in a Cartesian system, the square of the elemental distance ds may be defined as

$$ds^2 = \sum_i dx^i\, dx^i \quad , \tag{A.9}$$

or

$$ds^2 = dx^i\, dx^j\, \delta_{ij} \quad , \tag{A.10}$$

where δ_{ij} is the covariant form of the Kronecker delta δ_i^j for the Cartesian coordinate system. (In the Cartesian coordinate system, the contravariant and covariant forms of a tensor are the same; therefore $\delta_{ij} = \delta^{ij} = \delta_i^j$.)

We seek an expression for dx^i to use in Eq. (A.9). It follows from Eq. (A.1) that

$$dx^i = \left(\frac{\partial x^i}{\partial \underline{x}^r}\right) d\underline{x}^r \quad . \tag{A.11}$$

If Eq. (A.11) is substituted into Eq. (A.9), it can be seen that

$$ds^2 = \sum_i \left(\frac{\partial x^i}{\partial \underline{x}^r}\right)\left(\frac{\partial x^i}{\partial \underline{x}^s}\right) d\underline{x}^r d\underline{x}^s \quad . \tag{A.12}$$

Equation (A.12) may be written as follows (Synge and Schild 1978, Eq. 2.102):

$$ds^2 = \underline{g}_{rs}\, d\underline{x}^r\, d\underline{x}^s \quad , \tag{A.13}$$

where

$$\underline{g}_{rs} = \sum_i \left(\frac{\partial x^i}{\partial \underline{x}^r}\right)\left(\frac{\partial x^i}{\partial \underline{x}^s}\right) \quad . \tag{A.14}$$

Equation (A.14) is the covariant form of the metric tensor for the ray coordinate system.

The contravariant form of the metric tensor is now sought. The contravariant and covariant forms of the metric tensor are inverses; this may be expressed mathematically as follows:

$$\underline{g}_{rs}\underline{g}^{rt} = \delta_s^{\,t} \quad . \tag{A.15}$$

Use of Eqs. (A.15) and (A.14) leads to the following expression for the contravariant form of the metric tensor (Guy 1985):

$$\underline{g}^{rs} = \sum_j \left(\frac{\partial \underline{x}^r}{\partial x^j}\right)\left(\frac{\partial \underline{x}^s}{\partial x^j}\right) \qquad (A.16)$$

We need to know the determinant of the metric tensor. From Eqs. (A.3) and (A.14), it can be shown that

$$\begin{aligned} J^2 &= |J_j^i|^2 \\ &= |\underline{g}^{rs}| \\ &= g \end{aligned} \qquad (A.17)$$

The general form of the Laplacian, Eq. (A.8), can now be calculated. Let the function f of Eq. (A.8) be the eikonal Ψ. Examination of the expression $(\partial\Psi/\partial\underline{x}^r)$ yields

$$\frac{\partial \Psi}{\partial \underline{x}^r} = \left(\frac{\partial \Psi}{\partial x^i}\right)\left(\frac{\partial x^i}{\partial \underline{x}^r}\right) \qquad (A.18)$$

If both sides are multiplied by $\underline{g}^{rs}$, it is seen that

$$\begin{aligned} \underline{g}^{rs}\left(\frac{\partial \Psi}{\partial \underline{x}^r}\right) &= \sum_j \left(\frac{\partial \underline{x}^r}{\partial x^j}\right)\left(\frac{\partial \underline{x}^s}{\partial x^j}\right)\left(\frac{\partial \Psi}{\partial x^i}\right)\left(\frac{\partial x^i}{\partial \underline{x}^r}\right) \\ &= \sum_j \left(\frac{\partial \Psi}{\partial x^j}\right)\left(\frac{\partial \underline{x}^s}{\partial x^j}\right) \end{aligned} \qquad (A.19)$$

But from Eq. (3-D.4) it is known that

$$\frac{\partial \Psi}{\partial x^j} = \frac{1}{c_0}\left(\frac{\partial x^j}{\partial \underline{x}^s}\right)\Bigg|_{s=1} \quad . \tag{A.20}$$

It therefore follows that

$$\underline{g}^{rs}\left(\frac{\partial \Psi}{\partial \underline{x}^r}\right) = \frac{1}{c_0}\left(\frac{\partial \underline{x}^s}{\partial x^j}\right)\left(\frac{\partial x^j}{\partial \underline{x}^s}\right)\Bigg|_{s=1}$$

$$= c_0^{-1}[\,1\,,0\,,0\,] \quad . \tag{A.21}$$

If Eqs. (A.16) and (A.21) are substituted into Eq. (A.8), it is seen that

$$\nabla^2 \Psi = J^{-1}\,\partial(J/c_0)/\partial s \quad . \tag{A.22}$$

Use of Eq. (A.7) yields

$$\nabla^2 \Psi = A_0^{-1}\,\partial(A_0/c_0)/\partial s \quad , \tag{A.23}$$

which is Eq. (3-E.1). The Laplacian of the eikonal is proportional to the variation of the ratio of ray tube area to the small-signal sound speed.

APPENDIX B

THE PARAMETER OF NONLINEARITY FOR SEAWATER

In this appendix the analytic formulation of the parameter of nonlinearity B/A (see, for example, Beyer 1974, p. 99) is discussed. Some empirical relations developed by Morfey (1984c) for use in the numerical evaluation of the parameter for seawater are then presented. The parameter of nonlinearity accounts for the curvature of the pressure-density relationship of a fluid. It can be seen from Fig. B.1 that by moving a finite amount from the quiescent values of the density and pressure, ρ_0 and P_0, the slope of the pressure-density curve changes. By definition, the square of the sound speed is equal to the slope of the pressure-density curve,

$$c^2 \equiv \left\{\frac{\partial P}{\partial \rho}\right\}_{\xi,\chi} \quad . \tag{B.1}$$

An investigation of the definition of the sound speed yields an analytic expression for the parameter of nonlinearity. This expression may be evaluated numerically by use of empirical formulas.

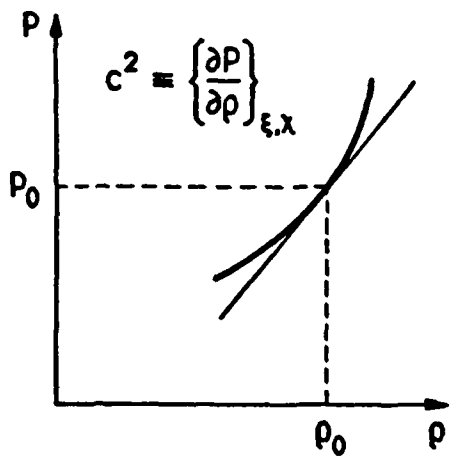

FIGURE B.1
THE NONLINEARITY OF THE PRESSURE DENSITY RELATIONSHIP

In order to develop an expression for c, we start with the equation of state for seawater:

$$P = P(\rho, \xi, \chi) \quad , \tag{B.2}$$

where ξ is the salinity, and χ is the entropy. Using a Taylor series expansion and retaining terms up to second order yields

$$P = P_0 + A\eta + \frac{B\eta^2}{2!} + (\xi - \xi_0)\left\{\frac{\partial P}{\partial \xi}\right\}_{\rho,\chi,\xi=\xi_0} + (\chi - \chi_0)\left\{\frac{\partial P}{\partial \chi}\right\}_{\rho,\xi,\chi=\chi_0} \quad , \tag{B.3}$$

where

$$A \equiv \rho_0\left\{\frac{\partial P}{\partial \rho}\right\}_{\chi,\xi,\rho=\rho_0}$$

$$= \rho_0 c_0^2 \quad , \tag{B.4}$$

$$B \equiv \rho_0^2\left\{\frac{\partial^2 P}{\partial \rho^2}\right\}_{\chi,\xi,\rho=\rho_0} \quad , \tag{B.5}$$

$$\eta \equiv (\rho - \rho_0)/\rho_0 \quad ; \tag{B.6}$$

η is called the condensation. In arriving at Eq. (B.3), we assumed that variations in the salinity and entropy are of second order in smallness. Equation (B.1) can be expanded by differentiating Eq. (B.3) with respect to ρ:

$$c^2 = \left\{\frac{\partial P}{\partial \eta}\frac{\partial \eta}{\partial \rho}\right\}_{\xi,\chi}$$

$$= (A + B\eta)/\rho_0 \quad , \tag{B.7}$$

or

$$= (A/\rho_0)(1 + \eta B/A) \quad . \tag{B.8}$$

Using a binomial expansion and retaining terms up to second order yields the following equation:

$$c = (A/\rho_0)^{1/2}(1 + \eta B/2A) \quad . \tag{B.9}$$

The next step is to determine the sound speed as a function of the particle velocity u. In the case of progressive plane waves traveling in the positive x direction it can be shown that

$$\eta = u/c_0 \quad . \tag{B.10}$$

The use of Eq. (B.10) in the case of outgoing waves in an inhomogeneous medium deserves some attention. In the derivation of nonlinear acoustic theory presented in Chapter 4, we used ray theory. There it is seen that an arbitrary sound wave may be regarded as being composed of many locally plane waves (Landau and Lifshitz 1959, p. 256). Since Eq. (B.10) is valid for plane waves and the wavefronts in the inhomogeneous medium are locally plane, it is assumed that, by envoking the substitution rule (Chapter 2, Section C), Eq. (B.10) may be used to eliminate η from Eq. (B.9). Use of Eq. (B.10) along with the definition of A, Eq. (B.4), yields the following equation:

$$c = c_0 + (B/2A)u \quad , \tag{B.11}$$

where u is the particle velocity in the direction of the ray path. In Eq. (B.11) it is seen that within the second-order approximation, the sound speed of a finite-amplitude disturbance is the sum of the small-signal sound speed c_0

and a perturbation term (B/2A)u.

We now recast B/2A in a way that lends itself to numerical evaluation. Use of the definitions of A and B, Eqs. (B.4) and (B.5), leads to the following:

$$\frac{B}{2A} = \frac{\rho_0^2 \left\{ \frac{\partial}{\partial \rho} \left(\frac{\partial P}{\partial \rho} \right) \right\}_{\xi, \chi, \rho = \rho_0}}{2\rho_0 \left\{ \frac{\partial P}{\partial \rho} \right\}_{\xi, \chi, \rho = \rho_0}} \quad . \tag{B.12}$$

Algebraic manipulation of terms held under the same constraints yields

$$\frac{B}{2A} = \rho_0 c_0 \left\{ \frac{\partial c_0}{\partial P} \right\}_{\xi, \chi, \rho = \rho_0} \quad . \tag{B.13}$$

Following the method of Beyer (1974, p. 100), we use the chain rule to express the partial derivative of c_0 in terms of temperature and pressure. The result is as follows:

$$\frac{B}{2A} = \rho_0 c_0 \left[\left\{ \frac{\partial c_0}{\partial P} \right\}_{\xi, T, \rho = \rho_0} + \left\{ \frac{\partial T}{\partial P} \right\}_{\chi} \left\{ \frac{\partial c_0}{\partial T} \right\}_{\xi, P, \rho = \rho_0} \right] \quad , \tag{B.14}$$

where

$$\left\{ \frac{\partial T}{\partial P} \right\}_{\chi} = \frac{\alpha_T (T + 273.15)}{\rho C_p} \quad , \tag{B.15}$$

α_T is the coefficient of thermal expansion, C_p is the specific heat at constant pressure, and T is the temperature in ^{0}C. Morfey (1984c) has

developed empirical relations for the density and the specific heat at constant pressure. These relations are given below. Chen and Millero (1976) have developed an expression for α_T which is valid to pressures of 100 μPa. Thus B/2A can be numerically evaluated over a wide range of salinities, temperatures, and pressures.

The following is Morfey's empirical relation for the density of both fresh and seawater, $\rho(P,T,\xi)$. The relative error is typically 10^{-04} for the temperature range $0^0 < T < 100^0$C and 0.5×10^{-04} for the range $10^0 < T < 40^0$C. The independent variables, their units, and the ranges over which they may vary are listed below:

P = pressure (Pa)	absolute	$0 < P < 10^7$,
T = temperature (^{0}C)	zero salinity	$0 < T < 100$,
	salt water	$0 < T < 40$,
ξ = salinity ($^0/_{00}$)		$30 < S < 40$.

The empirical equation is as follows:

$$\rho = 1000/\nu \quad , \tag{B.16}$$

where

$$\nu = V_0 + \lambda/F \quad , \tag{B.17}$$

where

$$\lambda = \Sigma_{i=0,3} A_i T^i + (A_{10} + A_{11}T)\xi \quad , \tag{B.18}$$

where

$$F = \Sigma_{i=0,3} B_i T^i + B_{10}\xi + P/(9.80665 \times 10^4) + G_1[P/(9.80665 \times 10^4)]^2 \quad . \tag{B.19}$$

The constants are defined in Table B.1.

TABLE B.1

CONSTANTS REQUIRED IN THE EMPIRICAL EQUATION FOR DENSITY

i	A_i	B_i	V_i	G_i
0	$0.25357 \times 10^{+04}$	$0.71540 \times 10^{+04}$	$0.64575 \times 10^{+00}$	-0.23430×10^{-04}
1	$0.14894 \times 10^{+02}$	$0.43124 \times 10^{+02}$		
2	-0.72023×10^{-01}	$-0.36324 \times 10^{+00}$		
3	-0.91030×10^{-04}	0.24620×10^{-03}		
10	$-0.35771 \times 10^{+01}$	$0.62851 \times 10^{+01}$		
11	-0.95138×10^{-02}			

Morfey's empirical relation for the specific heat at constant pressure $C_p(\underline{P},T,\xi)$ is given below. For seawater at pressures up to 100 μPa, we estimate C_p from

$$C_p = C_1(T,\xi) + C_0[\underline{P}/(9.80665 \times 10^4) + \underline{K}\xi, T] - C_0(1 + \underline{K}\xi, T) \quad , \tag{B.20}$$

where $\underline{K}$ = 12 (bar/ $^0/_{00}$) is an empirical constant which relates the increase of C_p with pressure for seawater to that for freshwater. The error in C_p is typically 10^{-04}. The function C_1 gives the specific heat of seawater at atmospheric pressure and is defined as follows:

$$C_1 = \Sigma_{i=1,4} \Sigma_{j=i,3} B_{ij} T^{i-1} \xi^{j-1} \quad . \tag{B.21}$$

The error in this equation is typically 10^{-04} over the temperature range 0 - 40° C and over the salinity range 0 - 40 $^0/_{00}$. The function C_0 gives specific heat of pure water and is defined as follows:

$$C_0 = \Sigma_{i=1,4} \Sigma_{j=1,3} A_{ij} T^{i-1} [\underline{P}^{j=1}/(9.80665 \times 10^4)] \quad . \tag{B.22}$$

This equation is valid for ξ = 0 (zero salinity) over the temperature and pressure ranges T = 0 - 90° C and $\underline{P}$ = 0 - 100 μPa. The relative error is typically 10^{-03}. The constants A_{ij} and B_{ij} are listed in Table B.2.

TABLE B.2
CONSTANTS REQUIRED IN THE EMPIRICAL EQUATION FOR SPECIFIC HEAT AT CONSTANT PRESSURE

i	j	A_{ij}	B_{ij}
1	1	$0.42160 \times 10^{+04}$	$0.42179 \times 10^{+04}$
2	1	$-0.24895 \times 10^{+01}$	$-0.34218 \times 10^{+01}$
3	1	0.46273×10^{-01}	0.97816×10^{-01}
4	1	-0.22446×10^{-03}	-0.91609×10^{-03}
1	2	$-0.46649 \times 10^{+00}$	$-0.72849 \times 10^{+01}$
2	2	0.12204×10^{-01}	$0.19149 \times 10^{+00}$
3	2	-0.19241×10^{-03}	-0.65990×10^{-02}
4	2	0.98686×10^{-06}	0.73197×10^{-04}
1	3	0.12458×10^{-03}	0.22227×10^{-01}
2	3	-0.25157×10^{-05}	-0.27630×10^{-02}
3	3	0.16518×10^{-07}	0.11588×10^{-03}
4	3	0.37555×10^{-10}	-0.13749×10^{-05}

APPENDIX C

ANALYTIC SOLUTIONS FOR FINITE AMPLITUDE WAVES VIA WEAK SHOCK THEORY

In this appendix the analytic solution for a weak shock with an exponentially decaying tail propagating through a homogeneous medium is developed. The solution is used to verify the accuracy of the propagation routine discussed in Chapter 5; the results of the numerical routine are compared with those of the analytic solution. The development proceeds as follows. The propagation of a finite amplitude wave through a homogeneous medium is considered. A general solution is obtained for the case in which the waveform contains weak shocks. This solution is not new; see, for example, Blackstock (1972). Since the propagation routine operates with nondimensional variables, the solution is nondimensionalized. The nondimensional solution is then applied to the particular problem of the propagation of a weak shock with an exponentially decaying tail. The solution for this waveform is not new either (Rogers 1977; also see Blackstock 1983).

Before discussing the propagation of weak shocks, we examine the propagation of a continuous (i.e., no shocks present) finite amplitude wave

through a homogeneous medium. The following equation is the exact plane wave equation for a gas:

$$u_t + c_0 u_x + \beta u u_x = 0 \quad . \tag{C.1}$$

The Earnshaw solution (see, for example, Blackstock 1962, Eq. 18) satisfies Eq. (C.1) exactly. However, Earnshaw's solution is a bit cumbersome, and particularly so for problems involving sources for which the boundary condition is given in the form

$$u = f(t) \quad \text{at} \quad x = 0 \quad . \tag{C.2}$$

It is convenient to use an approximate wave equation. Use of the first-order plane wave equation and the substitution rule of Chapter 2 converts Eq. (C.1) into

$$u_x + c_0^{-1} u_t - \beta c_0^{-2} u u_t = 0 \quad . \tag{C.3}$$

Use of the definition of retarded time for a plane wave, Eq. (3-C.1), transforms Eq. (C.3) into

$$u_x - \beta c_0^{-2} u u_{t'} = 0 \quad . \tag{C.4}$$

An equally valid expression in terms of the presssure P' is

$$P'_x - (\beta/\rho_0 c_0^3) P' P'_{t'} = 0 \quad . \tag{C.5}$$

Equation (C.5) is obtained from Eq. (C.4) by using the expression (see, for example, Blackstock 1962, Eq. 95)

$$u = P'/\rho_0 c_0 - \beta P'/2\rho_0^2 c_0^3 \quad . \tag{C.6}$$

The "Earnshaw solution" of Eq. (C.6) for the boundary condition

$$P' = g(t) = g(t') \quad \text{at} \quad x = 0 \tag{C.7}$$

is

$$P' = g(\phi) \tag{C.8}$$

where

$$\phi = t' + \beta g(\phi) x/\rho_0 c_0^3 \quad . \tag{C.9}$$

By using the transforms of the independent and dependent variables given in Table C.1, the solution presented in Eqs. (C.8) and (C.9) can be used for nonplanar geometries and inhomogeneous fluids (Blackstock 1966; Carlton and Blackstock 1974).

TABLE C.1
DISTORTION RANGE AND TRANSFORM PRESSURE VARIABLES

	Z	W
Plane	x	P'
Cylindrical	$2\sqrt{r_0}(\sqrt{r} - \sqrt{r_0})$	$P' (r/r_0)^{1/2}$
Spherical	$r_0 \ln (r/r_0)$	$P' (r/r_0)$
Inhomogeneous Fluid	$s_0 \ln (Gs/s_0)$	$P' (A\rho_0 c_0/A_0 \rho c)^{1/2}$

Here r is the range and r_0 is the reference range. If the boundary condition

is

$$W = g(t) \text{ at } Z = 0 \quad , \tag{C.10}$$

the general solution to a second approximation is as follows:

$$W = g(\phi) \quad , \tag{C.11}$$

where

$$\phi = t' + g(\phi)\beta Z/\rho_0 c_0^3 \quad . \tag{C.12}$$

This solution is referred to as the generalized approximate Earnshaw solution.

We now discuss weak shocks within the context of the Earnshaw solution. The approximate Earnshaw solution is valid on either side of a weak shock; knowledge of the shock strength allows one to tie the two Earnshaw solutions together. The relative arrival time of the shock is, however, unknown; we therefore seek an equation for the relative shock arrival time. It turns out, however, that we must first find an expression for the shock velocity.

Application of the equations of hydrodynamics to a propagating weak shock leads to an equation for the shock velocity. Consider a plane weak shock propagating through a homogeneous fluid. The fluid ahead of the shock is assumed to be undisturbed; its properties are denoted by the subscript a. The properties of the fluid behind the shock are denoted by the subscript b. If the continuity, momentum, and energy equations are applied to the control volume moving with the shock velocity V_{sh}, several relations, called the Rankine-Hugoniot shock relations, can be derived:

$$\rho_b(V_{sh} - u_b) = \rho_a V_{sh} \quad , \tag{C.13}$$

$$P_b = P_a + \rho_a u_b V_{sh} \quad , \tag{C.14}$$

$$V_{sh}^2 - \beta u_b V_{sh} - c_0^2 = 0 \quad . \tag{C.15}$$

Following Blackstock (1972), we solve Eq. (C.15) for an approximate expression for the shock velocity V_{sh}:

$$V_{sh} = c_0 + \beta u_b/2 \quad . \tag{C.16}$$

If the particle velocity in front of the wave had been the nonzero value u_a, the following equation would have obtained:

$$V_{sh} = c_0 + \beta(u_b + u_a)/2 \quad . \tag{C.17}$$

Since the particle velocity both ahead of and behind the shock are known from the two Earnshaw solutions, the shock velocity can be calculated.

Use of the expression for the shock velocity, Eq. (C.17), leads to an expression for the relative shock arrival time. Still following Blackstock, we assume that the shock first occurred at time $\underline{t}$ and position $\underline{x}$. The current position and time of the shock are denoted by x_{sh} and t_{sh}, respectively, where

$$t_{sh} = \underline{t} + \int_{\underline{x}} dx/V_{sh} \quad . \tag{C.18}$$

If a binomial expansion is used and terms up to second order are retained, Eq. (C.17) may be expressed as

$$1/V_{sh} = 1/c_0 - \beta(u_b + u_a)/2c_0^2 \quad . \qquad (C.19)$$

Substitution of Eq. (C.19) into Eq. (C.18) and simplification of the result using the definition of the retarded time variable, Eq. (3-C.1), as well as the progressive wave impedance relation, yields

$$t'_{sh} = \underline{t}' - (\beta/2\rho_0 c_0^3)\int_{\underline{x}} (P_b' + P'_a)\, dx \quad . \qquad (C.20)$$

The above equation can be expressed in the terms of the transformed independent and dependent variables, W and Z, since the Rankine-Hugoniot relations are invariant under the tranformations (Blackstock 1966, Appendix A). Restating Eq. (C.20) in terms of W and Z gives

$$t'_{sh} = \underline{t}' - (\beta/2\rho_0 c_0^3) \int_{\underline{Z}} (W_b + W_a)\, dZ \quad . \qquad (C.21)$$

The differential form of Eq. (C.21) is

$$dt'_{sh}/dZ = -\beta(W_b + W_a)/2\rho_0 c_0^3 \quad . \qquad (C.22)$$

Equations (C.21) and (C.22) give the relative shock arrival time. Other useful relations regarding the relative shock arrival time are obtained from the solution for the propagation of continuous waves, Eqs. (C.11) and (C.12). By noting that the value of W is different before and after the shock, we obtain the following:

$$t'_{sh} = \phi_b - (\beta Z/\rho_0 c_0^3)\, g(\phi_b) \quad , \qquad (C.23)$$

$$t'_{sh} = \phi_a - (\beta Z/\rho_0 c_0^3)\, g(\phi_a) \quad . \qquad (C.24)$$

As was mentioned earlier, we are developing this solution to compare with the results of the propagation routine. Since the computer algorithm operates on nondimensional variables, we nondimensionalize the solution. This is done using characteristic dimensions of the problem. The nondimensional variables are defined below:

$$V \equiv W/P'_0 \quad , \tag{C.25}$$

$$\tau \equiv t/t_c \quad , \tag{C.26}$$

$$\tau' \equiv t'/t_c \quad , \tag{C.27}$$

$$\sigma \equiv \beta W_0 Z/\rho_0 c_0^3 t_c \quad , \tag{C.28}$$

$$\Phi \equiv \phi/t_c \quad , \tag{C.29}$$

$$\epsilon \equiv P'/\rho_0 c_0^2 \quad , \tag{C.30}$$

$$G(\Phi) \equiv g(\phi)/P'_0 \quad , \tag{C.31}$$

where t_c is a characteristic time, and P'_0 is the reference pressure amplitude. In terms of the nondimensional variables, the nonlinear wave equation and its solution are expressed as follows:

Nonlinear wave equation $$V_\sigma - VV_{\tau'} = 0 \quad , \tag{C.32}$$

Boundary condition $$V = G(\tau) \text{ at } \sigma = 0 \quad , \tag{C.33}$$

Continuous wave solution $$V = G(\Phi) \quad , \tag{C.34}$$

where

$$\Phi = \tau' + \sigma G(\Phi) \quad , \tag{C.35}$$

Relative shock arrival time $$\tau'_{sh} = \tau' - 1/2 \int_{\Sigma} (V_a + V_b)\, d\sigma \quad , \tag{C.36}$$

$$d\tau'_{sh}/d\sigma = -1/2\,(V_a + V_b) \quad . \tag{C.37}$$

We now use the nondimensional solution to solve for the relative shock arrival time, the shock amplitude, and the 1/e decay time of a weak shock with an exponentially decaying tail. The boundary condition for the waveform is as follows:

$$P' = A \exp(-t/T_0)\, H(t) \quad \text{at} \quad r = r_0 \quad , \tag{C.38}$$

which converts to

$$W = A \exp(-t/T_0)\, H(t) \quad \text{at} \quad Z = 0 \quad , \tag{C.39}$$

where H(t) is the step function. Expressing the boundary condition in terms of the nondimensional variables yields

$$V = \exp(-\tau)\, H(t) \quad \text{at} \quad \sigma = 0 \quad , \tag{C.40}$$

where the characteristic values t_c and W_0 are defined to be T_0 and A, respectively. Use of Eqs. (C.34) and (C.35) leads to the solution to the continuous portion of wave:

$$V = \exp(-\Phi) \quad , \tag{C.41}$$

where

$$\Phi = \tau' + \sigma \exp(-\Phi) \quad . \tag{C.42}$$

We now solve for the shock amplitude. Considering only the shock, we may write Eqs. (C.41) and (C.42) as follows:

$$V_b = \exp(-\Phi_b) \quad , \tag{C.43}$$

$$\Phi_b = \tau'_{sh} + \sigma V_b \quad . \tag{C.44}$$

Taking the natural logarithm of Eq. (C.43), and then substituting the result into Eq. (C.44) and rearranging, we obtain the following:

$$\tau'_{sh} = -[\ell n(V_b) + \sigma V_b] \quad . \tag{C.45}$$

By taking the derivative of Eq. (C.45) with respect to σ and using Eq. (C.37) noting that V_a is equal to zero, we arrive at the following expression:

$$-1/2\ V_b + (1 + \sigma V_b)\, dV_b/d\sigma = 0 \quad . \tag{C.46}$$

If Eq. (C.46) is integrated with respect to σ, noting that the integration constant must be chosen to fit the boundary conditions, a quadratic equation with the following roots is obtained:

$$V_b = [-1 \pm \sqrt{(1 + 2\sigma)}]/\sigma \quad . \tag{C.47}$$

The positive root in Eq. (C.47) allows the boundary condition, $V_b = 1$ at $\sigma = 0$, to be recovered.

We now solve for the relative shock arrival time. We start by substituting the positive root of Eq. (C.47) into Eq. (C.36), again noting that V_a is zero. If the starting time of the shock is assumed to be 0, the result is as follows:

$$\tau'_{sh} = -[\ell n V_b + \sigma V_b] \quad . \tag{C.48}$$

The expression for the 1/e decay time is obtained using Eqs. (C.47)

and (C.48). The 1/e decay time is defined as the time required for the pulse to decay to 1/e of its current value, V_b/e. Substitution of V_b/e for V_b in Eq. (C.48) yields the relative time of the 1/e point of the waveform. The following expression for the 1/e decay time is obtained by subtracting the relative time of 1/e point from the relative shock arrival time,

$$\tau'_{1/e} = -[1 + \sigma V_b(1 - 1/e)] \quad , \tag{C.49}$$

where $\tau'_{1/e}$ is the 1/e decay time.

In summary we have found the solution for the shock amplitude, the relative shock arrival time, and the 1/e decay time of a weak shock with an exponentially decaying tail, Eqs. (C.47), (C.48), and (C.49), respectively. This information, coupled with the definitions of W and Z described in Table C.1, permits us to calculate the shock amplitude, relative shock arrival time, and the 1/e decay time independent of whether the wave is plane, cylindrical, spherical, or confined to a ray tube in an inhomogeneous medium.

APPENDIX D

COMPUTER PROGRAM

Computer program PLPROP is a FORTRAN 4 program which implements nonlinear geometrical acoustics. The program is described at length in Chapter 5. The heart of the program is the pair of subroutines WAVPROP and RESAMP which were written by Pestorius (1973). The fast Fourier Transform routine and plotting routines, which were written at Applied Research Laboratories, The University of Texas at Austin, Austin, Texas, are used extensively in the program.

The input files and other parameters required of the user are described in the program. The computer code has a running commentary on its function which should help the user understand operation of the program.

```
      PROGRAM PLPROP(INPUT,OUTPUT,WAVE,PLOT,PLTINF,
     &    RAYDAT=/500,TMPDAT,SALDAT,PHDAT,ATTEN,DEBUG,
     &    TAPE2=WAVE,TAPE3=PLTINF,TAPE4=RAYDAT,TAPE5=INPUT,
     &    TAPE6=OUTPUT,TAPE7=TMPDAT,TAPE8=SALDAT,TAPE9=PHDAT,
     &    TAPE18=ATTEN,TAPE19=DEBUG)
C
C    THIS PROGRAM WILL MODEL THE PROPAGATION OF A FINITE AMPLITUDE ACOUSTIC
C    WAVE FORM OF ARBITRARY SHAPE.  IT CAN PROPAGATE THIS WAVEFORM IN ONE OF
C    FOUR WAYS: AS A PLANE WAVE, AS A CYLINDRICAL WAVE, AS A SPHERICAL WAVE, OR
C    AS A WAVE MOVING THROUGH A INHOMOGENEOUS OCEAN.
C
C    THE PROGRAM ACCOUNTS FOR ATTENUATION DUE TO BOTH VISOCITY AND RELAXATION BY
C    USING THE FREQUENCY DOMAIN COEFFICIENTS EMPIRICALLY DERIVED BY FRANCOIS
C    AND GARRISON.   DISPERSION DUE TO RELAXATION IS ACCOUNTED FOR IN THE SAME
C    WAY.
C
C    IF BOTH FINITE AMPLITUDE EFFECTS AND ATTENUATION ARE BEING CONSIDERED THE
C    PROGRAM WILL APPLY RELAXATION AT ALL TIMES, WHEREAS VISCOSITY IS EXPLICTEDLY
C    ACCOUNTED FOR ONLY WHEN THERE IS NO SHOCK PRESENT.
C
C    THE OUTPUT ARE PLOTS OF THE TIME WAVEFORM AND THE CORRESPONDING ENERGY
C    SPECTRUM AT ANY POINT ON THE TRAVEL PATH.
C
C    THERE ARE A WIDE VARIETY OF OPTIONS:
C
C        1)  FINITE AMPLITUDE EFFECTS MAY BE TURNED OFF AT ANY RANGE
C        2)  ATTENUATION DUE TO VISCOSITY MAY BE TURNED ON OR OFF
C        3)  ATTENUATION AND DIPERSION DUE TO RELAXATION MAY BE TURNED ON OR OFF
C        4)  DISPERSION ALONE MAY BE  TURNED ON OR OFF
C
C
C      THERE ARE FOUR MAIN MODES OF OPERATION FOR THIS PROGRAM.   THEY ARE
C      REPRESENT BY THE VALUE OF THE VARIABLE WAVTYPE:
C
C         1) PROPAGATE WAVEFORM AS A PLANE WAVE
C         2) PROPAGATE WAVEFORM AS A CLYINDRICAL WAVE
C         3) PROPAGATE WAVEFORM AS A SPHERICAL WAVE
C         4) PROPAGATE WAVEFORM THROUGH A INHOMOGENEOUS MEDIUM
C
C      IF ANY OF THE MODES ARE CHOSEN THE USER MUST PROVIDE THE FOLLOWING FILE
C
C         WAVE   - THE INPUT WAVEFORM WITH INTEGER POWER OF 2 POINTS (SEE MAKWAV)
C
C      IF HOWEVER THE USER CHOOSES THE FOURTH MODE (INHOMOGENEOUS MEDIUM) HE
C      MUST ALSO PROVIDE THE FOLLOWING FILES:
```

```
C
C        RAYDAT - THE RAY PATH IMFORMATION WITH THE PARAMETER Q (SEE CALCQ AND
C                 MEDUSA'S RAYFAN)
C
C        TMPDAT - TEMPERATURE PROFILE WITH DEPTH IN KM (1 ENTRY PAIR PER LINE)
C
C        SALDAT - THE SALINITY PROFILE WITH THE DEPTH IN KM
C
C        PHDAT  - THE PH PROFILE WITH DEPTH IN KM
C
C     THE PROGRAM GENERATES A PAIR OF OUTPUT FILES:
C
C        PLOT   - THE PLOTS OF THE IME WAVEFORM AND THE FREQUENCY SPECTRUM
C
C        PLTINF - THE INFORMATION CORRESPONDING TO THE WAVEFORM AND ENVIRONMENT
C
C
C
C      VARIABLES RELATED TO THE PARTICLE VELOCITY WAVEFORM
C
C
C    V       - NONDIMENSIONAL PARTICLE VELOCITY WAVEFORM ARRAY
C
C    VF      - FOURIER TRANSFORM OF V, HENCE COMPLEX
C
C    UO      - NONDIMENSIONALIZING PARAMETER FOR THE PARTICLE VELOCITY
C              V = U/UO
C
C    EPSILN  - THE NONDIMENSIONAL MAGNITUDE OF THE PEAK PARTICLE VELOCITY
C              EPSILN = UO/COS
C
C    NPOINT  - THE NUMBER OF POINTS IN THE INPUT WAVEFORM
C
C    NP      - NUMBER OF POINTS IN THE WAVEFORM AT ANY TIME
C
C    NR      - NUMBER OF POINTS IN THE WAVEFORM AFTER RESAMPLING
C
C    DELTAU  - DEL TAU, NOT DELTA U... THE NONDIMENSIONAL TIME BETWEEN
C              POINTS ON THE WAVEFORM
C
C    TSUBC   - THE CHARACTERISTIC TIME USED TO NONDIMENSIONALIZE THE TIME
C              TAU = TIME/TSUBC
C
C    TAU     - THE NONDIMENSIONAL TIME ARRAY COORESPONDING TO THE V ARRAY
C
```

```
C
C           ENVIRONMENTAL INFORMATION
C
C
C    PHILAT - THE LATITUDE PHI OF THE SOURCE
C
C    DPTHOS - THE DEPTH OF THE SOURCE
C
C    TEMPOS - THE TEMPERATURE AT THE SOURCE DEPTH
C
C    SALNOS  - THE SALINITY AT THE SOURCE DEPTH
C
C    PHOS    - THE PH AT THE SOURCE DEPTH
C
C    BETAOS - THE PARAMETER OF NONLINEARITY AT THE SOURCE DEPTH
C
C    RHOOS   - THE DENSITY AT THE SOURCE DEPTH
C
C    COS     - THE SPEED OF SOUND AT THE SOURCE DEPTH
C
C    DPTHO   - THE DEPTH OF THE CURRENT LOCATION
C
C    TEMPO   - THE TEMPERATURE OF THE CURRENT LOCATION
C
C    SALNO   - THE SALINITY OF THE CURRENT LOCATION
C
C    PHO     - THE PH OF THE CURRENT LOCATION
C
C    BETAO   - THE PARAMETER OF NONLINEARITY OF THE CURRENT LOCATION
C
C    RHOO    - THE DENSITY OF THE CURRENT LOCATION
C
C    CO      - THE SPEED OF SOUND OF THE CURRENT LOCATION
C
C    ALPHOS - THE THERMODYNAMIC VARIABLE ALPHA AT THE SOURCE DEPTH
C
C
C           VARIABLES RELATED TO THE DISANCE PROPAGATED
C
C
C    SPATH  - THE DIMENSIONAL RANGE
C
C    SPATHO - THE REFERENCE RANGE
C
C    DISNDP - THE NONDIMENSIONALIZING PARAMETER FOR DISTANCE
```

```
C
C    SIG     - THE NONDIMENSIONAL DISTANCE, ((BETA*U0)/(TSUBC*COS**2))*Z
C
C    SIGCUR  - THE CURRENT VALUE OF SIGMA
C
C    DELSIG  - THE NONDIMENSIONAL DISTANCE THAT THE WAVE IS PROPAGATED
C              EACH TIME SUBROUTINE WAVPROP IS CALLED.
C
C    DDSIG   - THE INCREMENTAL STEPS THAT SUBROUTINE WAVPROP USES TO
C              PROPAGATE THE WAVE TO THE DISTANCE DELSIG
C
C    ETA     - A UNUSED VARIABLE FOR SUBROUTINE WAVPROP
C
C    DLSIG1  - THE INITIAL VALUE OF DELSIG
C
C    DDSIG1  - THE INITIAL VALUE OF DDSIG
C
C
C           VARIBLES RELATED TO THE PLOTTING OF OUTPUT
C
C
C    NPLOTS  - THE NUMBER OF PLOTS
C
C    SIGPLT  - AN ARRAY CONTAINING NONDIMENSIONAL DISTANCES AT WHICH
C              PLOTS ARE TO BE DRAWN
C
C    PLTRNG  - THE ACTUAL DISTANCE ALONG THE WAVE PATH TO THE LOCATION
C              WHERE THE PLOT IS DESIRED
C
C    NFRG    - NUMBER OF FREQUENCY CELLS
C
C    DELFRG  - THE FREQUENCY WIDTH OF EACH CELL
C
C    FRGS    -
C
C    YDB1    -
C
C    YDB2    -
C
C
C              FLAGS FOR THE OPTIONS
C
C
C    ZPAD    - ZERO PADDING FLAG, SET TRUE IF ZEROS ARE TO ADDED TO THE
C              TAIL OF THE WAVEFORM
```

```
C
C
C    FINSIG - THE NONDIMENSIONAL PATH LENGTH AFTER WHICH FINITE AMPLITUDE EFFECTS
C             ARE NEGLECTED
C
C    FINITE - A FLAG THAT INDICATES WHETHER OR NOT FINITE AMPLITUDE
C             EFFECTS ARE TO BE TAKEN INTO ACCOUNT.
C
C    RELAX  - A FLAG TO INDICATE WHETHER OR NOT ATTENUATION IS TO BE INCLUDED
C
C    DISPER - A FLAG THAT INDICATES WHETHER OR NOT DISPERSION (DUE TO
C             RELAXATION) IS TO BE INCLUDED.
C
C    VISCOS - A FLAG THAT INDICATES THAT ATTENUATION DUE VISCOUS EFFECTS
C             IS TO BE INCLUDED.
C
C    ATTEN  - A FLAG INDICATING THE IF ATTENUATION IN EXCESS OF THE
C             WEAK SHOCK LOSSES IS TO BE ACCOUNTED FOR.
C
C    LOCATT - A FLAG INDICATING IF THE ATTENUATION COEFFICIENTS ARE TO
C             RECALCULATED AS THE WAVE MOVES THROUGH THE INHOMOGENEOUS FLUID
C
C
C    EOFLAG - A FLAG INDICATING THE END OF THE RAY DATA FILE
C             OR OF THE END OF THE USER PLOT RANGE INPUTS
C
C
C             VARIABLES RELATED TO THE ATTENUATION
C
C
C    DELFRQ - DELTA FREQUENCY.  THE FREQUENCY DIFFERENCE BETWEEN TWO
C             FREQUENCY CELLS
C
C    NFRQ   - THE NUMBER OF FREQUENCY CELLS
C
C    ALFA   - THE ARRAY CONTAINING THE ATTENUATION COEFFICIENTS AS
C             A FUNCTION OF FREQUENCY FOR THERMOVISCOUS ATTENUATION
C             AND RELAXATION
C
C    ALFARX - THE ARRAY CONTAINING THE ATTENUATION COEFFICIENTS FOR
C             RELAXATION ONLY.
C
C    DPATH1 - THE ACTUAL DISTANCE PROPAGATED WITHOUT SHOCKS
C
C    DPATH2 - THE ACTUAL DISTANCE PROPAGATED WITH SHOCKS
```

```
C
C    DISNOSK- THE NONDIMSIONAL DISTANCE TRAVELED WITHOUT SHOCKS
C
C
C
C                    COMMON BLOCKS
C
C
C    /DEE/  - COMMON BLOCK WITH THE CURRENT STEP ENDPOINT DEPTH AND SLOPE
C
C    DO     - THE DEPTH AT THE BEGINNING OF THE CURRENT STEP
C
C    D1     - THE DEPTH AT THE END OF THE CURRENT STEP
C
C    DELD   - THE SLOPE (WRT TO Z) OVER THE CURRENT STEP
C
C
C    /ZEE/  - COMMON BLOCK WITH CURRENT STEP ENDPOINT RANGE AND SLOPE
C
C    ZO     - THE EQUIVALENT PLANE WAVE DISTACE AT THE BEGINNING OF THE STEP
C
C    Z1     - THE EQUIVALENT PLANE WAVE DISTANCE AT THE END OF THE STEP
C
C    DELZ   - A NON VARIABLE
C
C
C    /GEE/  - COMMON BLOCK WITH CURRENT STEP ENDPOINT G AND CORRESPONDING SLOPE
C
C    GO     - THE VALUE OF "G" AT THE BEGINNING OF THE CURRENT STEP
C
C    G1     - THE VALUE OF "G" AT THE END OF THE CURRENT STEP
C
C    DELG   - THE SLOPE OF "G" (WRT TO Z) OVER THE CURRENT STEP
C
C
C    /CMRAY/  COMMON BLOCK CONTAINING CURRENT RAY PATH DATA
C
C    /SOURCE/ COMMON BLOCK CONTAINING THE RAY PATH DATA AT THE SOURCE POSITION
C
C    R      - THE RADIAL RANGE TO THE SOURCE
C
C    S      - THE PATH LENGTH FROM THE SOURCE
C
C    ZETA   - THE PARTIAL DERIVATIVE OF Z WRT INITIAL LAUNCH ANGLE
```

```
C
C    ZETAP - THE PARTIAL DERIAVATIVE OF ZETA WRT RANGE, R
C
C    ZETAPP - THE PARTIAL DERIVATIVE OF ZETAP WRT RANGE, R
C
C    D      - THE DEPTH OF THE POINT IN QUESTION
C
C    DP     - THE PARTIAL DEIERIVATIVE OF THE DEPTH WRT RANGE, R
C
C    DPP    - THE SEDOUBLE PATRTAIL DERIVATIVE OF THE DEPTH D WRT R
C
C    SINTH  - THE SIN OF THE ANGLE OF THE POINT IN QUESTION
C
C    COSTH  - THE COSINE OF THE ANGLE OF THE POINT IN QUESTION
C
C
C              LOGICAL UNIT NUMBERS  AND THE FILES ASSOCIATED WITH THEM
C
C    LUNPLT - THE LOGICAL UNIT NUMBER OF THE TIME PLOT FILE
C
C    LUNPLF - THE LOGICAL UNIT NUMBER OF THE FREQUENCY PLOT FILE
C
C    LUNWAV - THE LOGICAL UNIT NUMBER OF THE INPUT WAVEFORM FILE
C
C    LUNSAL - THE LOGICAL UNIT NUMBER OF THE SALINITY PROFILE
C
C    LUNTMP - THE LOGICAL UNIT NUMBER OF THE TEMPERATURE PROFILE
C
C    LUNPH  - THE LOGIAL UNIT NUMBER OF THE PH PROFILE
C
C    LUNRAY - THE LOGICAL UNIT NUMBER OF THE RAY PATH DATA FILE
C
C
C
C    WAVTYP - A CODE NUMBER INDICATING THE TYPE OF WAVEFORM IS BEING
C             PROPAGATED.          1  PLANE WAVE
C                                  2  CYLINDERICAL WAVE
C                                  3  SPHERICAL WAVE
C                                  4  ARBITRARY WAVE  (INHOMOGENEOUS MEDIUM)
C
C
C
C    ..................................................................
C
```

```
C
      COMMON /CMRAY/ R,S,ZETA,ZETAP,D,DP,DPP,SINTH,COSTH,COC,Q
      COMMON /DEE/ DO,D1,DELD
      COMMON /ZEE/ ZO,Z1,DELZ
      COMMON /QEE/ QO,Q1,DELQ,QK
C
      DIMENSION V(4096),TAU(4096),WRKSP1(4096),WRKSP2(4096)
      DIMENSION FRQS(2048),DB(2048)
      COMPLEX VF(2048),ALFA(2048),ALFARX(2048),DABSEA
C
      LOGICAL ZPAD,FINITE,DISPER,VISCOS,RELAX,ATTEN,LOCATT,EOFLAQ
      EQUIVALENCE (V(1),VF(1))
C
      DATA LUNWAV/2/ , LUNRAY/4/ , LUNTMP/7/
      DATA LUNSAL/8/ , LUNPH /9/ , LUNPLT/4LPLOT/ , LUNPLF/4LPLOF/
      DATA LUNOUT/3/
      DATA EOFLAG/.FALSE./
      DATA DLSIQ1/0.1/ , DDSIQ1/0.01/
      DATA ETA /1.0/
C
C
C
C   READ IN THE REQUIRED PARAMETERS
C
      CALL INPUT1(UO,DELTAU,TSUBC,ZPAD,ATTEN,WAVTYP,
     &            FINSIQ,FINITE,VISCOS,RELAX,DISPER,LOCATT)
C
C   ALTERNATIVE WAVETYPE FOR COMPARATIVE TESTING
C
      IF (WAVTYP.NE.5.0) GOTO 25
         WRITE(6,*)" ENTER THE Q SLOPE , QK",
         READ (5,*) QK
   25 CONTINUE
C
C   READ IN THE NONDIMENSIONAL PARTICAL VELOCITY WAVEFORM
C
      CALL GETWAV(LUNWAV,V,NPOINT,M)
      NP = NPOINT
C
C   READ IN ENVIRONMENTAL DATA
C      IF HOMOGENEOUS MEDIUM, THEN PROMPT USER (INPUT2)
C
C      IF INHOMOGENEOUS MEDIUM (INPUT3) READ IN THE TEMPERATURE, SALINITY, AND PH
C         PROFILES, THEN CUBIC T SPLINE FIT THE DATA.  REQUIRES THE
C         FILES ASSOCIATED WITH THE LOGICAL UNIT NUMBERS LUNTMP,LUNSAL,AND LUNPH
```

```
C          ALSO READS IN THE THE SOURCE INFORMATION FROM THE FILE LUNRAY
C          INITIALIZE THE COMMON BLOCKS  CMSALIN, CMPH, AND CMTEMP WITH
C          THE CUBIC T SPLINE FIT DATA
C          ALSO INITAILIZE THE GEE, DEE, ZEE, AND SOURCE COMMON BLOCKS
C
      IF (WAVTYP.EQ.4.0) GOTO 30
         CALL INPUT2(PHILAT,DPTHOS,TEMPOS,SALNOS,PHOS,COS,
     &                RHOOS,BETAOS)
         GOTO 40
   30    CONTINUE
         CALL INPUT3(PHILAT,DPTHOS,TEMPOS,SALNOS,PHOS,COS,
     &                RHOOS,BETAOS,LUNTMP,LUNSAL,LUNPH,LUNRAY)
   40 CONTINUE
C
C   CALCULATE THE REFERENCE RANGES AND NONDIMENSIONAL PARAMETERS
C
      EPSILN = UO/COS
      SPATHO = COS*TSUBC/(BETAOS*EPSILN)
      IF (WAVTYP.EQ.1.0) SPATHO = 0.0
      DISNDP    = BETAOS*EPSILN/(TSUBC*COS)
C
C     OUTPUT THE INITIAL CONDITIONS
C
      CALL OUT1(LUNOUT,NPOINT,UO,DELTAU,TSUBC,
     & ATTEN,ZPAD,WAVTYP,PHILAT,DPTHOS,TEMPOS,SALNOS,PHOS,COS,
     & RHOOS,BETAOS,FINITE,FINSIG,VISCOS,RELAX,DISPER,LOCATT)
      CALL OUT2(LUNOUT,EPSILN,SPATHO,DISNDP)
C
C   CALCULATE THE FREQUENCY ARRAY FOR THE PLOTTING
C
      NFRQ = NPOINT/2
      DELFRQ = 1.0/(NPOINT*DELTAU*TSUBC)
      DO 90 I = 1,NFRQ
         FRQS(I) = (I-1)*DELFRQ
   90 CONTINUE
C
C   CALCUALTE THE FREQUENCY PLOT PLOTTING PARAMETERS
C
      IF (DELFRQ.LT.1.0) XF1 = 10.0**(INT(ALOG10(DELFRQ) - 1.0))
      IF (DELFRQ.GE.1.0) XF1 = 10.0**(INT(ALOG10(DELFRQ)))
      IF (FRQS(NFRQ).LT.1.0) XF2 = 10.0**(INT(ALOG10(FRQS(NFRQ))))
      IF (FRQS(NFRQ).LT.1.0) XF2 = 10.0**(INT(ALOG10(FRQS(NFRQ))))
      IF (FRQS(NFRQ).GE.1.0) XF2 = 10.0**(INT(ALOG10(FRQS(NFRQ))+1.0))
      YDB2 = -9999.0
      YDB1 = 0.0
```

```
C
C    CALCULATE THE ATTENUATION PARAMETERS
C
       CALL CALATT(NFRQ, DELFRQ, TEMPOS, SALNOS, DPTHOS,
     &                  PHOS, VISCOS, RELAX, DISPER, ALFA, ALFARX)
C
C    CALCULATE THE DISTANCE CORRESPONDING TO A 1 DB DROP DUE TO ATTENUATION
C
       CALL RNG1DB(NFRQ, ALFA, ATNRNG)
C
C    CREATE THE TAU (NONDIMENSIONAL TIME) ARRAY
C
       DO 110 I = 1, NPOINT
          TAU(I) = (I-1)*DELTAU
  110 CONTINUE
C
C    INITIALIZE SIG AND THE STEP COUNTER
C
C    GETENV UPDATES COMMON BLOCKS ZEE, DEE, QEE, AND CMRAY
C
       IF(WAVTYP.EQ.4.0)CALL GETENV(LUNRAY, SPATHO, DISNDP, SIGENV, EOFLAG)
       SIG    = 0.0
       SIGCUR = 0.0
       DISNOSK = 0.0
       ISTEP = 1
C
C    CALCULATE AND OUTPUT INITIAL SHOCK DATA
C    PLOT THE INITIAL WAVEFORM AND ENERGY SPECTRUM
C
       CALL SHKDAT(LUNOUT, V, TAU, NP, WAVTYP, DISNDP, SPATHO,
     &            UO, COS, RHOOS, BETAOS, PHILAT, SIG, DELTAU, WRKSP1)
       CALL TIMPLT(V, TAU, WRKSP1, WRKSP2, NP, LUNPLT, SIG)
       CALL ENERGY(M, V, DELFRQ, UO, RHOOS, COS, WRKSP1, DB)
       CALL FRQPLT(FRQS, DB, NFRQ, XF1, XF2, YDB1, YDB2, WRKSP1,
     &                    WRKSP2, LUNPLF, SIG)
C
C    ENTER THE WAVE PROPAGATION LOOP_____________________________________
C
  200 CONTINUE
C
C    GET THE NONDIMENSIONAL RANGE OF THE NEXT PLOT
C
       CALL GETRNG(SIGPLT, EOFLAG)
       WRITE(19,*)" SIGPLT = ", SIGPLT
C
```

```
C    IF END OF DATA,  EXIT PROGRAM
C
       IF (EOFLAG) GOTO 500
          WRITE(6,*) "PROPAGATION STEP ",ISTEP
          IF(SIGPLT.LT.SIGCUR) STOP " PLPROP CANNOT GO BACKWARDS"
C
C    LET SIGNXT BE THE SMALLER OF SIGENV AND SIGPLT
C
 225   CONTINUE
       SIGNXT = SIGPLT
       IF (WAVTYP.NE.4.0) GOTO 260
          IF (SIGNXT.LT.SIGENV) GOTO 250
             SIGNXT = SIGENV
             CALL GETENV(LUNRAY,SPATHO,DISNDP,SIGENV,EOFLAG)
 250      CONTINUE
 260   CONTINUE
C
C         PROPAGATE TO THE RANGE SIGNXT IN STEPS OF DELSIG
C
  300    CONTINUE
C
C    CALCULATE THE NONDIMENSIONAL DISTANCE TO BE PROPAGATED
C
          CALL CALSIG(DLSIG1,DDSIG1,SIGNXT,ATNRNG,DISNDP,SPATHO,
     &                WAVTYP,SIG,DELSIG,DDSIG)
C
C    UPDATE NONDIMENSIONAL DISTANCE VARIABLES
C
             SIGCUR = SIG
             SIG    = SIG + DELSIG
       WRITE(19,*)" SIG SIGENV SIGPLT DELSIG",SIG,SIGENV,SIGPLT,DELSIG
C
C    ENTERING FINITE AMPLITUDE PROPAGTION STAGE .........................
C
C    DO NOT ENTER LOOP IF FINITE AMPLITUDE EFFECTS ARE NOT REQUIRED AT THIS RANGE
C
             IF (.NOT.FINITE) GOTO 425
             IF (SIGCUR.GT.FINSIG) GOTO 425
C
C    PROPAGATE THE WAVE A DISTANCE DELSIG IN STEPS OF DDSIG
C
                CALL WAVPROP(V,TAU,DELSIG,DDSIG,NP,ETA,DISNOSK)
                NR = NP-4
C
C    RESAMPLE THE WAVE,  THEN ZERO THE POINTS NO LONGER REQUIRED
```

```
C
                CALL RESAMP(V, TAU, WRKSP1, NR, NP, DELTAU, IERR)
                IF (IERR.NE.0) STOP "TROUBLE IN RESAMP"
                NR = NR - 1
                NP = NPOINT
                DO 400 J = NR, NP
                   V(J) = 0.0
                   TAU(J) = TAU(J-1) + DELTAU
  400           CONTINUE
  425       CONTINUE
C
C   IF ATTENUATION IS TO BE APPLIED.....
C
            IF (.NOT.ATTEN) GOTO 490
      WRITE(19,*)" SIGCUR,SIG",SIGCUR,SIG
C
C   FIND THE ACTUAL DISTANCES PROPAGATED WITH AND WITHOUT SHOCKS
C
                CALL DELRNG(WAVTYP, DISNDP, SPATHO, SIGCUR, DISNOSK,
     &                           DELSIG, DPATH1, DPATH2)
       WRITE(19,*)"DELSIG, DISNOSK, DPATH1, DPATH2",
     &              DELSIG, DISNOSK, DPATH1, DPATH2
C
C   IF THE MEDIUM IS INHOMOGENEOUS RECALCULATE THE ATTENUATION COEFFICIENTS
C   ENVOUR REQUIRES THE COMMON BLOCKS DEE AND ZEE
C
                IF (.NOT.LOCATT) GOTO 450
                   CALL ENVOUR(TEMPO, SALNO, DPTHO, PHO, SIGCUR, DELSIG,
     &                         DISNDP)
                   CALL CALATT(NFRQ, DELFRQ, TEMPO, SALNO, DPTHO,
     &                PHO, VISCOS, RELAX, DISPER, ALFA, ALFARX)
  450           CONTINUE
C
C   FFT THE WAVE, APPLY THE ATTENUATION, AND REFFT BACK TO THE TIME DOMAIN
C
                CALL FFTDF(V, M)
                CALL APPATT(NFRQ, DPATH1, DPATH2, ALFA, ALFARX,
     &                      V, VF)
                CALL FFTDB(V, M)
C
C   ZERO THE ENDS OF THE WAVEFORM TO GET RID OF SPURIOUS DATA
C
                DO 460 I = 1,25
                   V(I) = 0.0
                   V(NP - I + 1) = 0.0
```

```
  460          CONTINUE
  490       CONTINUE
C
C
            IF (ABS(SIG-SIGNXT).GT.1.0E-10) GOTO 300
C
C  IF THE DISTANCE SIGNXT WAS NOT REACHED  TAKE ANOTHER DELSIG STEP
C
            IF (ABS(SIG-SIGPLT).GT.1.0E-10) GOTO 225
C
C   IF THE REQUIRED DISTANCE FOR PLOTTING HAS BEEN MET,  THEN
C   PLOT THE TIME WAVEFORM AND ITS CORRESPONDING FREQUENCY SPECTRUM
C
        CALL SHKDAT(LUNOUT,V,TAU,NP,WAVTYP,DISNDP,SPATHO,
     &          UO,COS,RHOOS,BETAOS,PHILAT,SIGPLT,DELTAU,WRKSP1)
        CALL TIMPLT(V,TAU,WRKSP1,WRKSP2,NP,LUNPLT,SIG)
        CALL ENERGY(M,V,DELFRQ,UO,RHOOS,COS,WRKSP1,DB)
        CALL FRQPLT(FRQS,DB,NFRQ,XF1,XF2,YDB1,YDB2,WRKSP1,
     &                  WRKSP2,LUNPLF,SIG)
        ISTEP = ISTEP + 1
        GOTO 200
  500 CONTINUE
      STOP " THE END OF FINITE AMPLITUDE PLANE WAVE PROPAGATION"
      END
C
C
C  ..............................................................
C
C
      SUBROUTINE GETWAV(LUNWAV,V,NPOINT,M)
C
C   THIS SUBROUTINE READS IN THE NONDIMENSIONAL TIME WAVEFORM
C   AND COUNTS THE NUMBER OF POINTS IN THE WAVEFORM
C
      DIMENSION V(1)
C
      NPOINT = 1
   10 CONTINUE
         READ (LUNWAV,*) V(NPOINT)
         IF (EOF(LUNWAV).NE.0) GOTO 20
         NPOINT = NPOINT + 1
         GOTO 10
   20 CONTINUE
      NPOINT = NPOINT - 1
C
```

```
C    TEST THE NUMBER OF POINTS
C
       IF (NPOINT.EQ.0) STOP "NO INPUT WAVEFORM"
       TEMP1 = ALOG10(FLOAT(NPOINT))/ALOG10(2.0)
       M = IFIX(TEMP1 + 0.5)
       TEMP2 = 2.0**M
       IF (IFIX(TEMP2).NE.NPOINT) STOP "NUMBER OF POINTS NOT POWER OF 2"
C
       RETURN
       END
C
C
C     ..................................................................
C
C
       SUBROUTINE INPUT1(UO,DELTAU,TSUBC,ZPAD,ATTEN,WAVTYP,
      &            FINSIG,FINITE,VISCOS,RELAX,DISPER,LOCATT)
C
C    THIS ROUTINE PROMPTS THE USER ON THE MANY WONDERFUL OPTIONS
C    OF THIS PROGRAM
C
       LOGICAL VISCOS,RELAX,DISPER,FINITE,LOCATT
       LOGICAL ZPAD,ATTEN
C
C
       WRITE(6,*) " INPUT THE INITIAL PEAK PARTICLE VELOCITY",
       READ (5,*)    UO
C
       WRITE(6,*) " TIME BETWEEN WAVEFORM POINTS",
       READ (5,*)   TRASH
C
       WRITE(6,*) " INPUT THE CHARACTERISTIC TIME ",
       READ (5,*)    TSUBC
       DELTAU = TRASH/TSUBC
C
       WRITE(6,*) " ZERO PADDING DURING THE PROPAGATION [Y/N = 1/0]",
       READ (5,*)   IFLAG
       ZPAD = .FALSE.
       IF (IFLAG.EQ.1) ZPAD = .TRUE.
C
       WRITE(6,*) " FINITE AMPLITUDE EFFECTS TO BE INCLUDED [Y/N = 1/0]",
       READ (5,*)   IFLAG
       FINITE = .FALSE.
       IF (IFLAG.EQ.1) FINITE = .TRUE.
C
```

```
      WRITE(6,*) " FINITE AMPLITUDE EFFECTS TO WHAT VALUE OF SIGMA",
      READ (5,*)  FINSIG
C
      WRITE(6,*) " INCLUDE ATTENUATION DUE TO VISCOSITY (Y/N = 1/0)",
      READ (5,*)   IFLAG
      VISCOS = .FALSE.
      IF (IFLAG.EQ.1) VISCOS = .TRUE.
C
      WRITE(6,*) " INCLUDE ATTENUATION DUE TO RELAXATION (Y/N = 1/0)",
      READ (5,*)   IFLAG
      RELAX = .FALSE.
      IF (IFLAG.EQ.1) RELAX = .TRUE.
C
      WRITE(6,*) " INCLUDE DISPERSION DUE TO RELAXATION (Y/N = 1/0)",
      READ (5,*)   IFLAG
      DISPER = .FALSE.
      IF (IFLAG.EQ.1) DISPER = .TRUE.
C
      ATTEN = .FALSE.
      IF (DISPER.OR.VISCOS.OR.RELAX) ATTEN = .TRUE.
C
      WRITE(6,*) " ATTENUATION BASED ON LOCAL ENVIRONMENT (Y/N = 1/0)",
      READ (5,*)   IFLAG
      LOCATT = .FALSE.
      IF (IFLAG.EQ.1) LOCATT = .TRUE.
C
      WRITE(6,*) " ENTER THE WAVE TYPE CODE NUMBER "
      WRITE(6,*) "            PLANE WAVE                          = 1"
      WRITE(6,*) "            CYLINDERICAL WAVE                   = 2"
      WRITE(6,*) "            SPHERICAL WAVE                      = 3"
      WRITE(6,*) "            ARBITRARY WAVE (STRATIFIED MEDIUM) = 4",
      READ (5,*) WAVTYP
C
      RETURN
      END
C
C
C  ....................................................................
C
C
      SUBROUTINE INPUT2(PHILAT,DPTHOS,TEMPOS,SALNOS,PHOS,COS,
     &    RHOOS,BETAOS)
C
C   THIS SUBROUTINE READS IN THE MEDIUM DATA FOR THE HOMOGENEOUS PROBLEM
C
```

```
      WRITE(6,*) " ENTER THE LATITUDE OF THE SOURCE ",
      READ (5,*) PHILAT
C
      WRITE(6,*) " ENTER TEMPERATURE, SALINITY, PH, DEPTH",
      READ (5,*) TEMPOS, SALNOS, PHOS, DPTHOS
C
      WRITE(6,*) " ENTER 0.0 FOR VALUES TO BE CALCULATED"
      WRITE(6,*) " ENTER SOUND SPEED, DENSITY, BETA",
      READ (5,*) COS, RHOOS, BETAOS
C
      APRES  = ABSPRES(PHILAT, DPTHOS)
      IF (COS.EQ.0.0) COS = CALCC(SALNOS, TEMPOS, APRES)
      IF (RHOOS.EQ.0.0) RHOOS = DENSITY(SALNOS, TEMPOS, APRES)
      IF (BETAOS.EQ.0.0) BETAOS = EVALBTA(SALNOS, TEMPOS, APRES)
C
      RETURN
      END
C
C
C   ..................................................................
C
C
      SUBROUTINE INPUT3(PHILAT, DPTHOS, TEMPOS, SALNOS, PHOS, COS,
     &     RHOOS, BETAOS, LUNTMP, LUNSAL, LUNPH, LUNRAY)
C
C   THIS SUBROUTINE READS IN THE PROPERTIES FOR THE INHOMOGENEOUS MEDIUM
C   IT READS THE TEMPERATURE, SALINITY AND PH PROFILES, THEN GET THE
C   CUBIC T SPLINE FIT TO THE CURVES.  USING THE CUBIC T SPLINE, IT
C   EVALUATES THE REQUIRED DATA USING EMPERICAL RELATIONS.
C
      COMMON /SOURCE/ ZETAS, COSTHS, TEMPS, SALINS, PHS, CS, RHOS, BETAS
      COMMON /CMRAY/ R, S, ZETA, ZETAP, D, DP, DPP, SINTH, COSTH, COC, Q
      COMMON /DEE/ D0, D1, DELD
      COMMON /ZEE/ Z0, Z1, DELZ
      COMMON /QEE/ Q0, Q1, DELQ, QK
C
      WRITE(6,*) " ENTER THE LATITUDE OF THE SOURCE ",
      READ (5,*) PHILAT
C
      READ (LUNRAY, 1000)RS, SS, ZETAS, ZETAPS, DS, DPS, DPPS, SINTHS, COSTHS,
     &    COCS, QS
 1000 FORMAT(11(1X,F17.4))
      READ (LUNRAY, 1100)RS, SS, ZETAS, ZETAPS, DS, DPS, DPPS, SINTHS, COSTHS,
     &    NOS, N2S, QS
 1100 FORMAT(12(1X,020))
```

```
      COCS = N2S/NOS
C
C     SET THE VALUES OF THE /CMRAY/ COMMON BLOCK
C
      R = RS
      S = SS
      ZETA = ZETAS
      ZETAP = ZETAPS
      D = DS
      DP = DPS
      DPP = DPPS
      SINTH = SINTHS
      COSTH = COSTHS
      COC = COCS
      Q = QS
C
      DPTHOS = DS
C
      DO = DPTHOS
      D1 = DPTHOS
      QO = 1.0
      Q1 = 1.0
      ZO = 0.0
      Z1 = 0.0
C
      CALL GETTEM (LUNTMP)
      CALL GETSAL  (LUNSAL)
      CALL GETPH   (LUNPH)
C
      TEMPOS = TEMP (DPTHOS)
      SALNOS = SALIN (DPTHOS)
      PHOS   = PH    (DPTHOS)
C
      APRES  = ABSPRES(PHILAT, DPTHOS)
      COS    = CALCC(SALNOS, TEMPOS, APRES)
      RHOOS  = DENSITY(SALNOS, TEMPOS, APRES)
      BETAOS = EVALBTA(SALNOS, TEMPOS, APRES)
C
      TEMPS = TEMPOS
      SALINS = SALNOS
      PHS    = PHOS
      CS     = COS
      RHOS   = RHOOS
      BETAS  = BETAOS
      RETURN
```

```
      END
C
C
C     ..................................................................
C
C
      SUBROUTINE OUT1(LUNOUT,NPOINT,UO,DELTAU,TSUBC,
     & ATTEN,ZPAD,WAVTYP,PHILAT,DPTHOS,TEMPOS,SALNOS,PHOS,COS,
     & RHOOS,BETAOS,FINITE,FINSIG,VISCOS,RELAX,DISPER,LOCATT)
C
      LOGICAL VISCOS,RELAX,DISPER,FINITE,LOCATT
      LOGICAL ZPAD,ATTEN
C
C
C     JUST FOR THE RECORD.....
C
      WRITE(LUNOUT,*) " "
      WRITE(LUNOUT,*) " THE PROGRAM PLPROP WAS INPUT THE FOLLOWING"
      WRITE(LUNOUT,*) " NUMBER OF POINTS IN THE WAVEFORM IS ",NPOINT
      WRITE(LUNOUT,*) " PEAK PARTICLE VELOCITY ",UO
      WRITE(LUNOUT,*) " NONDIMENSIONAL TIME INCREMENT ", DELTAU
      WRITE(LUNOUT,*) " CHARACTERISTIC TIME ", TSUBC
      WRITE(LUNOUT,*) " ZERO PADDING DURING PROPAGATION ", ZPAD
      WRITE(LUNOUT,*) " FINITE AMPLITUDE EFFECTS INCLUDED", FINITE
      WRITE(LUNOUT,*) " EFFECTS TO NONDIMENSIONAL RANGE", FINSIG
      WRITE(LUNOUT,*) " VISCOUS ATTENUATION INCLUDED ", VISCOS
      WRITE(LUNOUT,*) " RELAXATION ATTENUATION INCLUDED ",RELAX
      WRITE(LUNOUT,*) " DISPERSION DUE TO REALXATION INCLUDED ",DISPER
      WRITE(LUNOUT,*) " LOCAL ATTENUATION AND DISPERSION ", LOCATT
      WRITE(LUNOUT,*) " THE WAVE TYPE CODE IS ",WAVTYP
      WRITE(LUNOUT,*) " THE LATITUDE OF THE SOURCE ",PHILAT
      WRITE(LUNOUT,*) " THE SOURCE DEPTH ", DPTHOS
      WRITE(LUNOUT,*) " THE SOURCE TEMPERATURE ",TEMPOS
      WRITE(LUNOUT,*) " THE SOURCE SALINITY ", SALNOS
      WRITE(LUNOUT,*) " THE SOURCE PH        ",PHOS
      WRITE(LUNOUT,*) " THE SOURCE SOUND SPEED ", COS
      WRITE(LUNOUT,*) " THE SOURCE DENSITY ",RHOOS
      WRITE(LUNOUT,*) " THE PARAMATER BETA ",BETAOS
      RETURN
      END
C
C
C     ..................................................................
C
C
```

```
      SUBROUTINE OUT2(LUNOUT,EPSILN,SPATHO,DISNDP)
C
      WRITE(LUNOUT,*) " EPSILON IS ",EPSILN
      WRITE(LUNOUT,*) " THE REFERENCE RANGE IS ", SPATHO
      WRITE(LUNOUT,*) " THE DISTANCE NONDIMENSIONALIZING PARAMETER ",
     & DISNDP
      RETURN
      END
C
C
C     ..................................................................
C
C
      SUBROUTINE GETENV(LUNRAY,SPATHO,DISNDP,SIGENV,EOFLAG)
C
C     THIS SUBROUTINE READS IN THE ENVIRONMENTAL INFORMATION AND CALCULATES THE
C     EQUIVALENT PLANE WAVE DISTANCE TO THE NEXT RANGE.
C
      COMMON /CMRAY/ R,S,ZETA,ZETAP,D,DP,DPP,SINTH,COSTH,COC,Q
      COMMON /DEE/ DO,D1,DELD
      COMMON /ZEE/ ZO,Z1,DELZ
      COMMON /QEE/ QO,Q1,DELQ,QK
C
      LOGICAL EOFLAG
C
      READ (LUNRAY,1000)R,S,ZETA,ZETAP,D,DP,DPP,SINTH,COSTH,COC,Q
 1000 FORMAT(11(1X,F17.4))
      IF (EOF(LUNRAY).NE.0) GOTO 200
      READ (LUNRAY,1100)R,S,ZETA,ZETAP,D,DP,DPP,SINTH,COSTH,NO,N2,Q
 1100 FORMAT(12(1X,O20))
      COC = N2/NO
      QO = Q1
      Q1 = Q
      DO = D1
      D1 = D
      SPATH = S
      Z = (SPATHO*ALOG((SPATH/SPATHO)*Q))
      ZO = Z1
      Z1 = Z
      DELQ = (Q1 - QO)/(Z1 - ZO)
      DELD = (D1 - DO)/(Z1 - ZO)
      SIGENV = Z * DISNDP
      RETURN
C
C
```

```
C      IF (WAVTYP.NE.1.0) GOTO 130
C         Z = SPATH
C  130 CONTINUE
C
C      IF (WAVTYP.NE.2.0) GOTO 140
C         Z = (2.0*SQRT(SPATHO)*(SQRT(SPATH)-SQRT(SPATHO)))
C  140 CONTINUE
C
C      IF (WAVTYP.NE.3.0) GOTO 150
C         Z = (SPATHO*ALOG(SPATH/SPATHO))
C  150 CONTINUE
C
C      IF (WAVTYP.NE.5.0) GOTO 170
C         Z = SPATHO*ALOG(SPATH*(GK*SPATH + 1.0)/SPATHO)
C  170 CONTINUE
C
C      RETURN
C
   200 CONTINUE
       EOFLAG = .TRUE.
       RETURN
       END
C
C
C   ....................................................................
C
C
       SUBROUTINE GETRNG(SIGPLT,EOFLAG)
C
C   THIS SUBROUTINE READS IN THE NONDIMENSIONAL EQUIVALENT PLANE
C   WAVE DISTANCE TO THE NEXT PLOT.
C
       LOGICAL EOFLAG
C
       WRITE(6,*) " ENTER A NEGATIVE RANGE TO EXIT"
       WRITE(6,*) " ENTER THE NONDIMENSIONAL RANGE FOR THE NEXT PLOT",
       READ (5,*) SIGPLT
       IF (SIGPLT.LT.0.0) GOTO 200
       RETURN
C
   200 CONTINUE
       EOFLAG = .TRUE.
       RETURN
       END
C
```

```
C
C     ..................................................................
C
C
      SUBROUTINE DELRNG(WAVTYP,DISNDP,SPATHO,SIGCUR,DISNOSK,
     &                  DELSIG,DPATH1,DPATH2)
C
C     THIS SUBROUTINE CALCULATES THE ACTUAL DISTANCES THAT THE
C     WAVEFORM TRAVELED WITH AND WITHOUT A SHOCK.  IN THE CASE OF
C     THE INHOMOGENEOUS MEDIUM, THIS REQUIRED THE USE OF A LINEAR
C     APPROXIMATION.  IT WAS ASSUMED THAT THE VALUE "G" VARIED
C     LINEARLY (WRT Z) OVER THE STEP.  THIS IS NOT TOO GROSS AN
C     ASSUMPTION SINCE MEDUSA HAS A VARIABLE STEP SIZE THAT IS
C     DETERMINED BY MINIMIZING THE ERROR IN THE RAY IN THE
C     RAY PATH TRAJECTORY.  THE TRAJECTORY IS DICTATED BY THE
C     VARIATION IN THE SOUND SPEED PROFILE; HENCE RAPID CHANGES IN
C     THE SOUND SPEED PROFILE LEAD TO SMALL STEP SIZES
C
      COMMON /GEE/ G0,G1,DELG,GK
      COMMON /DEE/ D0,D1,DELD
      COMMON /ZEE/ Z0,Z1,DELZ

      ZCUR = SIGCUR/DISNDP
      DZ1 = DISNOSK/DISNDP
      DZ2 = DELSIG/DISNDP
      DZ3 = ZCUR + DZ1
      DZ4 = ZCUR + DZ2
C
      IF (WAVTYP.NE.1.0) GOTO 100
         SPATH  = ZCUR
         DPATH1 = DZ3 - SPATH
         DPATH2 = DZ4 - (SPATH + DPATH1)
  100 CONTINUE
C
      IF (WAVTYP.NE.2.0) GOTO 110
         SPATH = (SPATHO + ZCUR + (ZCUR **2.0)/(4.0*SPATHO))
         DPATH1 = (SPATHO + DZ3 + (DZ3**2.0)/(4.0*SPATHO)) - SPATH
         DPATH2 = (SPATHO + DZ4 + (DZ4**2.0)/(4.0*SPATHO))
         DPATH2 = DPATH2 - (SPATH + DPATH1)
  110 CONTINUE
C
      IF (WAVTYP.NE.3.0) GOTO 120
         SPATH  = SPATHO*EXP(ZCUR /SPATHO)
         DPATH1 = SPATHO*EXP(DZ3/SPATHO) - SPATH
         DPATH2 = SPATHO*EXP(DZ4/SPATHO)
```

```
         DPATH2 = DPATH2 - (SPATH + DPATH1)
  120 CONTINUE
C
      IF (WAVTYP.NE.4.0) GOTO 130
         GCUR = DELG*(ZCUR-ZO)   + GO
         G3   = DELG*((ZCUR-ZO) + DZ1/2.0) + GO
         G4   = DELG*((ZCUR-ZO) + DZ1 +((DZ2 - DZ1)/2.0)) + GO
         SPATH  = (SPATHO/GCUR) * EXP(ZCUR  /SPATHO)
         DPATH1 = (SPATHO/G3  ) * EXP(DZ3/SPATHO) - SPATH
         DPATH2 = (SPATHO/G4  ) * EXP(DZ4/SPATHO)
         DPATH2 = DPATH2 - (SPATH + DPATH1)
  130 CONTINUE
C
      IF (WAVTYP.NE.5.0) GOTO 140
         SPATH=(-1.0+SQRT(1.0+4.0*GK*SPATHO*EXP(ZCUR/SPATHO)))/(2.0*GK)
         DPATH1=(-1.0+SQRT(1.0+4.0*GK*SPATHO*EXP(DZ3/SPATHO)))/(2.0*GK)
         DPATH1 = DPATH1 - SPATH
         DPATH2=(-1.0+SQRT(1.0+4.0*GK*SPATHO*EXP(DZ4/SPATHO)))/(2.0*GK)
         DPATH2 = DPATH2 - (SPATH + DPATH1)
  140 CONTINUE

C
      RETURN
      END
C
C
C  ..................................................................
C
C
      SUBROUTINE ENVOUR(TEMPO,SALNO,DPTHO,PHO,SIGCUR,DELSIG,DISNDP)
C
      COMMON /DEE/ DO,D1,DELD
      COMMON /ZEE/ ZO,Z1,DELZ
C
      ZCUR = (SIGCUR + DELSIG)/DISNDP
      ZFORM = SIGCUR/DISNDP
      DCUR = DELD*(ZCUR - ZO) + DO
      DFORM= DELD*(ZFORM - ZO) + DO
      TEMP1 = TEMP  (DFORM)
      TEMP2 = TEMP  (DCUR)
      TEMPO = (TEMP1 + TEMP2)/2.0
      SAL1  = SALIN (DFORM)
      SAL2  = SALIN (DCUR)
      SALNO = (SAL1 + SAL2)/2.0
      PH1    = PH     (DFORM)
```

```
      PH2     = PH      (DCUR)
      PHO     = (PH1 + PH2)/2.0
      DPTHO = (DFORM + DCUR)/2.0
      WRITE(19,*) ' DEPTH, TEMPERATURE,  SALINITY,  PH ARE ',
     &              DPTHO, TEMPO,        SALNO,     PHO
      RETURN
      END
C
C
C  ....................................................................
C
C
      SUBROUTINE CALATT(NFRQ, DELFRQ, TEMPO, SALNO, DPTHO,
     &                  PHO, VISCOS, RELAX, DISPER, ALFA, ALFARX)
C
      COMPLEX ALFA(NFRQ), ALFARX(NFRQ), DABSEA
      LOGICAL VISCOS, RELAX, DISPER
C
C     TESTING CODE FOR TEMPORARY USE ONLY
C
C     DO 10 I = 1, NFRQ
C        ALFA(I) = (0.0, 0.0)
C        ALFARX(I) = ALFA(I)
C10   CONTINUE
C     RETURN
C
         DO 100 I = 1, NFRQ
            FREQ = DELFRQ*I
            ALFA(I) = - DABSEA(FREQ, TEMPO, SALNO, DPTHO, PHO, CO2)
            ALFARX(I) = ALFA(I) + DABSEA(FREQ, TEMPO, 0.0, DPTHO, PHO, CO2)
            IF (DISPER) GOTO 60
               TEMP = REAL(ALFA(I))
               ALFA(I) = CMPLX(TEMP, 0.0)
               TEMP = REAL(ALFARX(I))
               ALFARX(I) = CMPLX(TEMP, 0.0)
   60       CONTINUE
            IF (RELAX) GOTO 70
               ALFA (I)  = ALFA(I) - ALFARX(I)
               ALFARX(I) = CMPLX(0.0, 0.0)
   70       CONTINUE
            IF (VISCOS) GOTO 80
               ALFA(I) = ALFARX(I)
   80       CONTINUE
  100 CONTINUE
      WRITE(18, 1000)(ALFA(I), ALFA(I), I=1, NFRQ)
```

```
 1000 FORMAT(2020,2012.5)
      RETURN
      END
C
C
C.....................................................................
C
C
      SUBROUTINE RNG1DB(NFRG,ALFA,ATNRNG)
C
C    FIND THE MIDBAND FREQUENCY AND THEN THE ATTENUATION (DB/M) ASSOCIATED WITH T
C
      COMPLEX ALFA(NFRG)
C
      MIDBND = NFRG/2
      TRASH = REAL(ALFA(MIDBND))
      IF(TRASH.NE.0.0) ATNRNG = ABS(1.0/TRASH)
      IF(TRASH.EQ.0.0) ATNRNG = 1.0E+10
      WRITE(19,*) "ATNRNG = ",ATNRNG
      RETURN
      END
C
C
C    ..................................................................
C
C
      SUBROUTINE CALSIG(DLSIG1,DDSIG1,SIGPLT,ATNRNG,DISNDP,SPATHO,
     &                  WAVTYP,SIG,DELSIG,DDSIG)
C
C    THIS ROUTINE CALCULATES THE DISTANCE DELSIG BY FIRST CHOSING THE
C    CHOSING THE LARGER BETWEEN THE 0.1 SIGMA RANGE AND THE 1 DB RANGE.
C
C    IT THEN CHECKS THAT DELSIG DOES NOT EXTEND BEYOND THE SIGPLT, AND ENSURES
C    DELSIG IS AN INTEGER MULTIPLE OF DDSIG.
C
      TRASH = SIG + DLSIG1
      CALL SIGRNG(SIG,DISNDP,SPATHO,WAVTYP,RNGCUR)
      CALL SIGRNG(TRASH,DISNDP,SPATHO,WAVTYP,RNGFUT)
      RNG01 = RNGFUT - RNGCUR
C
      IF (ATNRNG.GT.RNG01) GOTO 100
         DELSIG = DLSIG1
         GOTO 110
  100    CONTINUE
         RNGFUT = RNGCUR + ATNRNG
```

```
         CALL RNGSIG(RNGFUT,DISNDP,SPATHO,WAVTYP,SIGFUT)
         DELSIG = SIGFUT - SIG
 110  CONTINUE
C
      GARB = (SIG + DELSIG) - SIGPLT
      IF (GARB .GT. 0.0) DELSIG = SIGPLT - SIG
      IF (DELSIG.GT.DDSIG1) GOTO 310
         DDSIG = DELSIG
         GOTO 320
 310     CONTINUE
         DDSIG = DELSIG/(AINT((DELSIG/DDSIG1)+0.5))
 320  CONTINUE
C
      RETURN
      END
C
C
C   ....................................................................
C
C
      SUBROUTINE RNGSIG(RNG,DISNDP,SPATHO,WAVTYP,SIG)
C
C  THIS ROUTINE CONVERTS FROM RANGE TO SIGMA
C  IT IS APPROXIMATE IN THE CASE OF WAVTYP = 4
C
      COMMON /CMRAY/ R,S,ZETA,ZETAP,D,DP,DPP,SINTH,COSTH,COC,G
C
      IF (WAVTYP.NE.4.0) GOTO 120
         Z = (SPATHO*ALOG((RNG/SPATHO)*G))
 120  CONTINUE

      IF (WAVTYP.NE.1.0) GOTO 130
         Z = RNG
 130  CONTINUE

      IF (WAVTYP.NE.2.0) GOTO 140
         Z = (2.0*SQRT(SPATHO)*(SQRT(RNG)-SQRT(SPATHO)))
 140  CONTINUE

      IF (WAVTYP.NE.3.0) GOTO 150
         Z = (SPATHO*ALOG(RNG/SPATHO))
 150  CONTINUE
C
      SIG = Z * DISNDP
C
```

```
      RETURN
      END
C
C
C  ..................................................................
C
C
      SUBROUTINE SIGRNG(SIG,DISNDP,SPATHO,WAVTYP,RNG)
C
C  THIS ROUTINE CONVERTS FROM SIGMA TO RANGE
C  IT IS APPROXIMATE IN THE CASE OF WAVTYP = 4
C
      COMMON /CMRAY/ R,S,ZETA,ZETAP,D,DP,DPP,SINTH,COSTH,COC,Q
C
      Z = SIG/DISNDP
C
      IF ((WAVTYP.NE.1.0).AND.(WAVTYP.NE.5.0)) GOTO 10
         RNG = Z
   10 CONTINUE
C
      IF (WAVTYP.NE.2.0) GOTO 20
         RNG = (SPATHO + Z + (Z**2.0)/(4.0*SPATHO))
   20 CONTINUE
C
      IF (WAVTYP.NE.3.0) GOTO 30
         RNG = SPATHO*EXP(Z/SPATHO)
   30 CONTINUE
C
      IF (WAVTYP.NE.4.0) GOTO 40
         RNG = (SPATHO/Q)*EXP(Z/SPATHO)
   40 CONTINUE
C
      RETURN
      END
C
C
C  ..................................................................
C
C
      SUBROUTINE APPATT(NFRQ,DPATH1,DPATH2,ALFA,ALFARX,
     &                  V,VF)
C
      COMPLEX ALFA(NFRQ),ALFARX(NFRQ),VF(NFRQ),CARQ
C
      DIMENSION V(1)
```

```
C
      ARG = REAL(ALFA(NFRG)*DPATH1/20.0)
     &               + REAL(ALFARX(NFRG))*DPATH2/20.0
      I = 2
      IF (ARG.GT.-200.0) V(I) = V(I) * 10.0**ARG
      IF (ARG.LE.-200.0) V(I) = 0.0
C
      DO 100 I = 2,NFRG
         CARG = ALFA(I-1)*DPATH1/20.0 + ALFARX(I-1)*DPATH2/20.0
         IF (REAL(CARG).GT.-200.0) VF(I) = VF(I) * 10.0**CARG
         IF (REAL(CARG).LT.-200.0) VF(I) = (0.0,0.0)
  100 CONTINUE
      RETURN
      END
C
C
C   ....................................................................
C
C
      SUBROUTINE GETTEM (LUNTMP)
      INTEGER NZ, MZ, LEXTBL
      REAL Z(40), TEMP(40), ASCOEF(120,3), ZS(120), TEMPS(120)
      COMMON /CMTEMP/ NZ, MZ, Z, TEMP, ASCOEF, NZS, MZS, ZS, TEMPS
      DATA MZ /40/, MZS /120/
C
C     READ IN TEMP PROFILE
C
      IF (LEXTBL (LUNTMP, NZ, MZ, 2, TEMP, "FP",Z, "FP") .LE. 0)
     &  CALL ERROR ("PROBLEM IN READING TEMP PROFILE")
C
C     CONVERT THE DEPTH FROM (KM) TO (M)
C
      DO 10 I= 1,NZ
         Z(I) = Z(I)*1000.0
   10 CONTINUE
C
C     FIT TLF SPLINE
C
      CALL ICSTLF (Z, TEMP, NZ, 5.0, 0.3, 2.5, ZS, TEMPS,
     &  ASCOEF(1,1), ASCOEF(1,2), ASCOEF(1,3), NZS, MZS)
      RETURN
      END
C
C
C   ..... ..............................................................
```

```
C
C
      REAL FUNCTION TEMPP (Z)
C
      INTEGER NZ, MZ, NZS, MZS, BINX
      REAL Z, DZ, ZP(40), TEMP(40), ASCOEF(120,3), ZS(120),
     &  TEMPS(120)
      COMMON /CMTEMP/ NZ, MZ, ZP, TEMP, ASCOEF, NZS, MZS, ZS,
     &  TEMPS
      DATA I /1/
C
      I = BINX (Z, ZS, 1, NZS, I)
      DZ = Z - ZS(I)
      TEMPP = ((3. * ASCOEF(I,3) * DZ + 2. * ASCOEF(I,2)) *
     &         DZ + ASCOEF(I,1))
      RETURN
      END
C
C
C     ..................................................................
C
C
      REAL FUNCTION TEMP (Z)
      INTEGER NZ, MZ, NZS, MZS, I, BINX
      REAL Z, DZ, ZP(40), TEMPX(40), ASCOEF(120,3), ZS(120), TEMPS(120)
      COMMON /CMTEMP/ NZ, MZ, ZP, TEMPX, ASCOEF, NZS, MZS, ZS, TEMPS
      DATA I /1/
C
      I = BINX (Z, ZS, 1, NZS, I)
      DZ = Z - ZS(I)
      TEMP = (((ASCOEF(I,3) * DZ + ASCOEF(I,2)) * DZ +
     &         ASCOEF(I,1)) * DZ + TEMPS(I))
      RETURN
      END
C
C
C     ..................................................................
C
C
      SUBROUTINE GETPH (LUNPH)
      INTEGER NZ, MZ, LEXTBL
      REAL Z(40), PH(40), ASCOEF(120,3), ZS(120), PHS(120)
      COMMON /CMPH/ NZ, MZ, Z, PH, ASCOEF, NZS, MZS, ZS, PHS
      DATA MZ /40/, MZS /120/
C
```

```
C      READ IN PH PROFILE
C
       IF (LEXTBL (LUNPH, NZ, MZ, 2,PH, "FP",Z, "FP") .LE. 0)
      &  CALL ERROR ("PROBLEM IN READING PH PROFILE")
C
C      CONVERT THE DEPTH FROM (KM) TO (M)
C
       DO 10 I= 1,NZ
          Z(I) = Z(I)*1000.0
 10    CONTINUE
C
C      FIT TLF SPLINE
C
       CALL ICSTLF (Z, PH, NZ, 5.0, 0.3, 2.5, ZS, PHS,
      &  ASCOEF(1,1), ASCOEF(1,2), ASCOEF(1,3), NZS, MZS)
       RETURN
       END
C
C
C  ....................................................................
C
C
       REAL FUNCTION PHP (Z)
C
       INTEGER NZ, MZ, NZS, MZS, BINX
       REAL Z, DZ, ZP(40), PH(40), ASCOEF(120,3), ZS(120),
      &  PHS(120)
       COMMON /CMPH/ NZ, MZ, ZP, PH, ASCOEF, NZS, MZS, ZS,
      &  PHS
       DATA I /1/
C
       I = BINX (Z, ZS, 1, NZS, I)
       DZ = Z - ZS(I)
       PHP = ((3. * ASCOEF(I,3) * DZ + 2. * ASCOEF(I,2)) *
      &          DZ + ASCOEF(I,1))
       RETURN
       END
C
C
C  ....................................................................
C
C
       REAL FUNCTION PH (Z)
       INTEGER NZ, MZ, NZS, MZS, I, BINX
       REAL Z, DZ, ZP(40), PHX(40), ASCOEF(120,3), ZS(120), PHS(120)
```

```
      COMMON /CMPH/ NZ, MZ, ZP, PHX, ASCOEF, NZS, MZS, ZS, PHS
      DATA I /1/
C
      I = BINX (Z, ZS, .1, NZS, I)
      DZ = Z - ZS(I)
      PH = (((ASCOEF(I,3) * DZ + ASCOEF(I,2)) * DZ +
     &         ASCOEF(I,1)) * DZ + PHS(I))
      RETURN
      END
C
C
C     ..................................................................
C
C
      SUBROUTINE GETSAL (LUNSAL)
      INTEGER NZ, MZ, LEXTBL
      REAL Z(40),SALIN(40),ASCOEF(120,3),ZS(120),SALINS(120)
      COMMON /CMSALIN/ NZ, MZ, Z, SALIN, ASCOEF, NZS, MZS, ZS, SALINS
      DATA MZ /40/, MZS /120/
C
C     READ IN SALIN PROFILE
C
      IF (LEXTBL (LUNSAL, NZ, MZ, 2,SALIN, "FP",Z, "FP") .LE. 0)
     &  CALL ERROR ("PROBLEM IN READING SALIN PROFILE")
C
C     CONVERT THE DEPTH FROM (KM) TO (M)
C
      DO 10 I= 1,NZ
         Z(I) = Z(I)*1000.0
 10   CONTINUE
C
C     FIT TLF SPLINE
C
      CALL ICSTLF (Z, SALIN, NZ, 5.0, 0.3, 2.5, ZS, SALINS,
     &  ASCOEF(1,1), ASCOEF(1,2), ASCOEF(1,3), NZS, MZS)
      RETURN
      END
C
C
C     ..................................................................
C
C
      REAL FUNCTION SALINP (Z)
C
      INTEGER NZ, MZ, NZS, MZS, BINX
```

```
      REAL Z, DZ, ZP(40), SALIN(40), ASCOEF(120,3), ZS(120),
     &  SALINS(120)
      COMMON /CMSALIN/ NZ, MZ, ZP, SALIN, ASCOEF, NZS, MZS, ZS,
     &  SALINS
      DATA I /1/
C
      I = BINX (Z, ZS, 1, NZS, I)
      DZ = Z - ZS(I)
      SALINP = ((3. * ASCOEF(I,3) * DZ + 2. * ASCOEF(I,2)) *
     &          DZ + ASCOEF(I,1))
      RETURN
      END
C
C
C     ..................................................................
C
C
      REAL FUNCTION SALIN (Z)
      INTEGER NZ, MZ, NZS, MZS, I, BINX
      REAL Z,DZ,ZP(40),SALINX(40),ASCOEF(120,3),ZS(120),SALINS(120)
      COMMON /CMSALIN/ NZ, MZ, ZP, SALINX, ASCOEF, NZS, MZS, ZS, SALINS
      DATA I /1/
C
      I = BINX (Z, ZS, 1, NZS, I)
      DZ = Z - ZS(I)
      SALIN = (((ASCOEF(I,3) * DZ + ASCOEF(I,2)) * DZ +
     &          ASCOEF(I,1)) * DZ + SALINS(I))
      RETURN
      END
C
C
C     ******************************************************************
C
C
      COMPLEX FUNCTION DABSEA(FREQ,TEMP,SALIN,DEPTH,PH,C)
C
C*****************************************************************************
C     FUNCTION COMPUTES THE TOTAL SOUND ABSORPTION COEFFICIENT
C     (COMPLEX) OF SEAWATER FOR THE GIVEN INPUT PARAMETERS, BASED
C     ON THE FRANCOIS-GARRISON EQUATIONS (JASA 72(6), DEC 1982).
C
C       INPUT PARAMETERS@D
C     FREQ    - FREQUENCY IN HERTZ
C     TEMP    - TEMPERATURE IN DEGREES CELSIUS
```

```
C     SALIN  - SALINITY IN PARTS PER THOUSAND
C     DEPTH  - DEPTH IN METERS
C     PH     - PH OF THE SEAWATER
C
C       OUTPUT PARAMETERS@D
C     C      - SPEED OF SOUND (M/S) AT THE INPUT TEMP, SALIN AND DEPTH
C
C*****************************************************************************
C
      F=FREQ/1000.
      FSQ=F*F
      THETA=TEMP+273.
      C=1412.+3.21*TEMP+1.19*SALIN+.0167*DEPTH
C
C**** BORIC ACID (H3BO3) CONTRIBUTION; RELAXATION FREQ, F1, IN KHZ.
C
      A1=8.86/C* 10.**(.78*PH-5.)
      P1=1.
      F1=2.8* ((SALIN/35.)**.5)* 10.**(4.-1245./THETA)
      ALH3BO3=A1*P1*F1*FSQ/(FSQ+F1*F1)
C
C**** MAGNESIUM SULFATE (MGSO4) CONTRIBUTION; RELAX FREQ, F2, IN KHZ.
C
      A2=21.44*SALIN/C* (1.+.025*TEMP)
      P2=1.-1.37E-4*DEPTH+6.2E-9*DEPTH*DEPTH
      F2=8.17* 10.**(8.-1990/THETA)/ (1.+.0018*(SALIN-35.))
      ALMGSO4=A2*P2*F2*FSQ/(FSQ+F2*F2)
C
C**** PURE WATER CONTRIBUTION.
C
      TSQ=TEMP*TEMP
      TCUBE=TEMP*TSQ
      IF (TEMP.LE.20.)
     1   A3=4.937E-4-2.59E-5*TEMP+9.11E-7*TSQ-1.5E-8*TCUBE
      IF (TEMP.GT.20.)
     1   A3=3.964E-4-1.146E-5*TEMP+1.45E-7*TSQ-6.5E-10*TCUBE
      P3=1.-3.83E-5*DEPTH+4.9E-10*DEPTH*DEPTH
      ALH2O=A3*P3*FSQ
C
C**** TOTAL ABSORPTION COEFFICIENT (CONVERT FROM DB/KM TO DB/M).
C
      ALR=ALH3BO3+ALMGSO4+ALH2O
      ALI=0.
      IF (F1.GT.0) ALI=F/F1*ALH3BO3
      ALI=ALI+ F/F2*ALMGSO4
```

```
      TLOW=T(1)-1.0
CCCCCCCCCCCCCCCCCCCCCCCCCCCCCCCCCCCCCCCCCCCCCCCCCCCCCCCCCCCCCCCCCCCCCCCCCCCCCCC
C
C  THIS LOOP TESTS FOR SHOCK OVERTAKING AND SHIFTS OUT POINTS
C  IN THE INTERSHOCK REGION
C
CCCCCCCCCCCCCCCCCCCCCCCCCCCCCCCCCCCCCCCCCCCCCCCCCCCCCCCCCCCCCCCCCCCCCCCCCCCCCCC
      DO 30 INDEX=1,NPOINTS
      NPOINT=INDEX-NSHIFT
      T(NPOINT)=T(INDEX)-U(INDEX)*DISFACT
      U(NPOINT)=U(INDEX)
      IF (T(NPOINT) .GT. TLOW) GO TO 30
C
C  CODE MODIFIED F.D. COTARAS JUNE 10 1985
C  CALCULATED THE DISTANCE PROPAGATED BEFORE THE FIRST SHOCK FORMATION
C
      IF (.NOT. FIRST) GOTO 5
         FIRST = .FALSE.
         DISNOSK = (NDISTOR-1)*DISINC
 5    CONTINUE
C
C  END MODIFICATION
C
      TAVG=(T(NPOINT)+T(NPOINT-1))/2.0
      IF (NS.LE.0) I=1
      IF (NS.LE.0) GOTO 15
      DO 10 IND=1,NS
      I=IND
      IF(TAVG .LE. TS(I)) GO TO 20
   10 CONTINUE
      I=I+1
   15 CONTINUE
      NS=NS+1
      TS(NS)=TAVG
      LOCS(NS)=NPOINT
      GO TO 30
   20 NSHIFT=NSHIFT+NPOINT-LOCS(I)
      LOC=LOCS(I)-1
      T(LOC+1)=T(NPOINT)
      U(LOC+1)=U(NPOINT)
      TS(I)=(T(NPOINT)+T(LOC))/2.0
      NS=I
   30 TLOW=T(NPOINT)
      NPOINTS=NPOINTS-NSHIFT
      TLEFT=AMNIF(T(1),T(NPOINTS))
```

```
      DABSEA=CMPLX(ALR,-ALI)/1000.
C
      RETURN
      END
C
C
      SUBROUTINE WAVPROP(U,T,DISTANC,DISINC,NPOINTS,ETA,DISNOSK)
         DIMENSION TS(2052),LOCS(2052),T(1),U(1)
         LOGICAL FIRST
C
C     SPHERICAL SPREADING, VARIABLE SPEED OF SOUND VERSION
C     ****************************************************************
C        WAVEPROP IS THE WEAK-SHOCK PROPAGATION ALGORITHM
C        CALL PARAMETERS.....
C     U   U IS A REAL ONE DIMENSIONAL ARRAY DESCRIBING THE PARTICLE
C         VELOCITY OF A POINT ON THE WAVE FORM IN EITHER ENGLISH OR
C         METRIC UNITS.  IF METRIC UNITS ARE USED, CO, THE SMALL
C         SIGNAL SPEED OF SOUND, MUST BE SUPPLIED IN METRIC UNITS.
C
C     T   T IS A REAL ONE DIMENSIONAL ARRAY DESCRIBING THE TIME
C         (SECONDS) COORDINATE FOR A PARTICULAR POINT ON THE WAVEFORM.
C         THE PAIR (U(I),T(I)) THEN DESCRIBES A WAVEFORM POINT IN
C         THE PARTICLE VELOCITY-TIME PLANE.
C
C     DISTANC---A REAL VARIABLE, IT IS THE DISTANCE OVER WHICH THE WAVE
C         IS TO BE PROPAGATED.
C
C     DISINC----A REAL VARIABLE.  IT IS THE INCREMENTAL STEP SIZE USED
C         TO COVER THE DISTANCE, DISTANCE.
C
C     NPOINTS--AN INTEGER VARIABLE, IT IS THE NUMBER OF POINTS USED TO
C         DESCRIBE THE WAVE FORM TO BE PROPAGATED.
C
C*****************************************************************************
C
      FIRST = .TRUE.
      NIN=NPOINTS
      DISNOSK=0.
      PERIOD=T(NPOINTS)
      DISFACT=ETA*DISINC
      NDISTS=DISTANC/DISINC+0.5
      DO 140 NDISTOR=1,NDISTS
C
      NS=0
      NSHIFT=0
```

```
      IF(TLEFT.LT.0.0) 40,50
   40 PRINT 150,DISTANC,NDISTOR
      STOP
   50 TBIG=AMX1F(T(1),T(NPOINTS))
      IF(TBIG.GT.PERIOD) 60,70
   60 PRINT 160,DISTANC,NDISTOR
      STOP
   70 CONTINUE
      IFLAG=0
      NSHIFT=0
      TLOW=T(1)-1.0
CCCCCCCCCCCCCCCCCCCCCCCCCCCCCCCCCCCCCCCCCCCCCCCCCCCCCCCCCCCCCCCCCCCCCCCCCCCCCCC
C
C  THIS LOOP ADJUSTS VELOCITIES AT THE SHOCKS AND SHIFTS OUT POINTS
C  IN THE OVERLAP REGION
C
CCCCCCCCCCCCCCCCCCCCCCCCCCCCCCCCCCCCCCCCCCCCCCCCCCCCCCCCCCCCCCCCCCCCCCCCCCCCCCC
      DO 130 INDEX=1,NPOINTS
      NPOINT=INDEX-NSHIFT
      T(NPOINT)=T(INDEX)
      U(NPOINT)=U(INDEX)
      IF(IFLAG .EQ. 1) GO TO 100
      IF(T(NPOINT) .GT. TLOW) GO TO 120
      TAVG=(T(NPOINT)+T(NPOINT-1))/2.0
      IFLAG=1
      I=NPOINT-2
      GO TO 90
   80 I=I-1
      NSHIFT=NSHIFT+1
      T(I+2)=T(NPOINT)
      U(I+2)=U(NPOINT)
   90 IF (TAVG LT T(I)) GO TO 80
      U(I+1)=U(I)+(U(I+1)-U(I))*(TAVG-T(I))/(T(I+1)-T(I))
      T(I+1)=TAVG
      GO TO 130
  100 IF (T(NPOINT)  LT  TAVG) GO TO 110
      U(NPOINT-1)=U(NPOINT-1)+(U(NPOINT)-U(NPOINT-1))*(TAVG-T(NPOINT-1))
     */(T(NPOINT)-T(NPOINT-1))
      T(NPOINT-1)=TAVG
      IFLAG=0
      GO TO 120
  110 NSHIFT=NSHIFT+1
      GO TO 130
  120 TLOW=T(NPOINT)
  130 CONTINUE
```

```
C
C      IF (NPOINTS.EQ.NIN) DISNOSK=NDISTOR*DISINC
C
C  ESTES'S DISNOSK CALCUALTION REMOVED JUNE 10 1985
C
  140 NPOINTS =NPOINTS-NSHIFT
      RETURN
  150 FORMAT(1H1,*EXCEEDED TIME BASE TO THE LEFT*,//,10X,*DIST=*
     1   ,E15.5,10X,I5,3X,*ITERATIONS*)
  160 FORMAT(1H1,*EXCEEDED TIME BASE TO THE RIGHT*,//,10X,*DIST=*
     1   ,E15.5,10X,I5,3X,*ITERATIONS*)
      END
C
C
      SUBROUTINE RESAMP(U,T,FT,N,NPOINTS,DT,IERR)
      DIMENSION U(1),T(1),FT(1)
C
C ***************************************************************************
C
C     ARRAYS AND VARIABLES
C
C  ***************************************************************************
C
C     U        -- REAL ONE-DIMENSIONAL PARTICLE VELOCITY (OR PRESSURE)
C                 INPUT-OUTPUT ARRAY.
C     T        -- REAL ONE-DIMENSIONAL TIME INPUT-OUTPUT ARRAY.
C     N        -- THE NUMBER OF OUTPUT DATA POINTS DESIRED.
C     NPOINTS  -- THE NUMBER OF INPUT DATA POINTS.
C     DT       -- THE SAMPLING INTERVAL OF THE OUTPUT DATA POINTS.
C     FT       -- A SCRATCH ARRAY OF DIMENSION N.
C     IERR     -- ERROR FLAG, RETURNS 1 ON ERROR AND 0 ON NO ERROR.
C  ***************************************************************************
C
C     THE U AND T ARRAYS ENTER THE SUBROUTINE WITH NPOINTS AND ARE
C     RETURNED WITH N POINTS
C     IF NN IS GREATER THAN NPOINTS INTERPOLATION HAS PROCEEDED
C     BEYOND THE END OF THE USEFULL DATA IN THE U ARRAY (USEFULL
C     INFORMATION CAN BE INTERPOLATED ONLY WHEN  T(N).GE.N*DT
C     OTHERWISE AN ERROR CONDITION IS SET,  IERR=1)
      NN = 2
      DO 30 I=1,N
 10      TLIM = T(NN)
         TT = (I-1)*DT
         IF ((TT-TLIM).LE.1.0E-12) GOTO 20
         NN = NN+1
```

```
         IF (NN.GT.NPOINTS) GOTO 50
         GOTO 10
 20      FT(I) = (TT-T(NN-1))*(U(NN)-U(NN-1))/(T(NN)-T(NN-1))+U(NN-1)
 30    CONTINUE
C
       DO 40 I=1,N
         T(I) = (I-1)*DT
         U(I) = FT(I)
 40    CONTINUE
       IERR=0
       GO TO 60
C
 50    IERR=1
 60    RETURN
       END
```

REFERENCES

Arons, A.B. (1954). "Underwater Explosion Shock Wave Parameters at Large Distances from the Charge," J. Acoust. Soc. Am. **26**, 343-346.

Barton, Edwin H. (1901). "On the Refraction of Sound by Wind," Philos. Mag. Ser. 6 **1**,159-165.

Bergmann, Peter G. (1946). "The Wave Equation in a Medium with a Variable Index of Refraction," J. Acoust. Soc. Am. **17**, 329-333.

Beyer, Robert T. (1974). *Nonlinear Acoustics* (U.S. Department of the Navy, Washington, D.C.).

Blackstock, David T. (1962). "Propagation of Plane Sound Waves of Finite Amplitude in Nondissipative Fluids," J. Acoust. Soc. Am. **34**, 9-30.

_____ (1964). "On Plane, Spherical, and Cylindrical Sound Waves of Finite Amplitude in Lossless Fluids," J. Acoust. Soc. Am. **36**, 217-219(L).

_____ (1966). "Connection Between the Fay and Fubini Solutions for Plane Sound Waves of Finite Amplitude," J. Acoust Soc Am. **39**, 1019 1026

_____ (1969). "History of Nonlinear Acoustics and a Survey of Burgers' and Related Equations," in "Nonlinear Acoustics", edited by T G Muir Proceedings of the Conference on Nonlinear Acoustics, November 1969 (Applied Research Laboratories, The University of Texas at Austin, Austin, Texas), pp 3-27

_____ (1972). "Nonlinear Acoustics (Theoretical)," in *American Institute of Physics Handbook*, 3rd ed., edited by Dwight E. Gray (McGraw-Hill Book Co., Inc., New York), pp. 3-183 to 3-205.

_____ (1983). "Propagation of a Weak Shock Followed by a Tail of Arbitrary Waveform," in Proceedings of the 11th International Congress on Acoustics, Paris, France, 1983 (Imprimerie de l'Indre, Argenton-Sur-Creuse, France), Vol. 1, pp. 305-308.

_____ (1985). "Generalized Burgers Equation for Plane Waves," J. Acoust. Soc. Am. **77**, 2050-2053.

Blokhintzev, D. (1946a). "The Propagation of Sound in an Inhomogeneous and Moving Medium I," J. Acoust. Soc. Am. **18**, 322-328.

_____ (1946b). "The Propagation of Sound in an Inhomogeneous and Moving Medium II," J. Acoust. Soc. Am. **18**, 329-334.

Born, Max, and Emil Wolf (1980). *Principles of Optics*, 6th ed. (Pergamon Press, Oxford).

Brekhovskikh, L.M., and Yu. Lysanov (1982). *Fundamentals of Ocean Acoustics* (Springer-Verlag, Berlin).

Bruns, Heinrich (1895). "Das Eikonal," Abhandlungen d.k.s. Ges. d. Wiss. Math. Phys. Cl. **21**, 327-436.

Carlton, Thomas W., and David T. Blackstock (1974). "Propagation of Plane Waves of Finite Amplitude in Inhomogeneous Media with Applications to Vertical Propagation in the Ocean," ARL Technical Report No. 74-31 (ARL-TR-74-31), Applied Research Laboratories, The University of Texas at Austin (ADA 004 648).

Chen, Chen-Tung, and Frank J. Millero (1976). "The Specific Volume of Seawater at High Pressures," Deep-Sea Research **23**, 595-612.

Conway, A.W., and J.L. Synge, editors (1931). *The Mathematical Papers of Sir William Rowan Hamilton, Vol. I, Geometrical Optics* (Cambridge University Press, Cambridge, England).

Cotaras, F.D., C.L. Morfey, and D.T. Blackstock (1984). "Nonlinear Effects in Long Range Underwater Propagation," J. Acoust. Soc. Am. **76**, S39(A).

Eby, Edward S. (1967). "Frenet Formulation of Three-Dimensional Ray Tracing," J. Acoust. Soc. Am. **42**,1287-1297.

_____ (1970). "Geometric Theory of Ray Tracing," J. Acoust. Soc. Am. **47**, 273-275.

Foreman, Terry L. (1983). "Ray Modeling Methods for Range Dependent Ocean Environments," ARL Technical Report No. 83-41 (ARL-TR-83-41), Applied Research Laboratories, The University of Texas at Austin (ADA 137 202).

François, R. E., and G. R. Garrision (1982). "Sound Absorption Based on Ocean Measurements. Part II: Boric Acid Contribution and Equation for Total Absorption," J. Acoust. Soc. Am. **72**, 1879-1890.

Frank, P.G., P.G. Bergmann, and A. Yaspan (1969). "Ray Acoustics," in *The Physics of Sound in the Sea*, Summary Technical Report of Division 6, NDRC, Vol. 8, Part I, edited by P.G. Bergmann and A. Yaspan (originally published in 1946 and reissued in 1969) (U.S. Department of the Navy, Washington, D.C.).

Fujiwhara, S. (1912). "On the Abnormal Propagation of Sound Waves in the Atmosphere," Bull. Cent. Meteorol. Obs. Jap. **1**, No. 2.

_____ (1916). "On the Abnormal Propagation of Sound Waves in the Atmosphere," Bull. Cent. Meteorol. Obs. Jap. **4**, No. 2.

Goldstein, Herbert (1950). *Classical Mechanics* (Addison-Wesley Press, Inc., Cambridge, Massachusetts).

Gradshteyn, I.S., and I.M. Ryzhik (1980). *Table of Integrals, Series, and Products.* Corrected and enlarged edition, edited by Alan Jeffrey (Academic Press, New York).

Gubkin, K.E. (1958). "Propagation of Discontinuities in Sound Waves," Prikl. Matem. Mekham. **22**, 561-564 (English Translation, 787-793).

Guy, William T. (1985). Personal Communication.

Haselgrove, J. (1954). "Ray Theory and a New Method for Ray Tracing," in Report of the Conference on the Physics of the Ionosphere (London Phys. Soc., London), pp. 355-364.

Hayes, Wallace D., Rudolph C. Haefeli, and H.E. Kulsrud (1969). "Sonic Boom Propagation in a Stratified Atmosphere, with Computer Program," NASA Contractor Report 1299, National Aeronautics and Space Administration, Washington, D.C.

Heller, G.S. (1953). "Propagation of Acoustic Discontinuities in an Inhomogeneous Moving Liquid Medium," J. Acoust. Soc. Am. **25**, 950-951.

Hunt, Frederick V. (1955). "Notes on the Exact Equations Governing the Propagation of Sound in Fluids," J. Acoust. Soc. Am. **27**, 1019-1039.

Jeffery, A., and T. Taniuti (1964). *Nonlinear Wave Propagation* (Academic Press, New York).

Keller, Joseph B. (1954). "Geometrical Acoustics. I. The Theory of Weak Shock Waves", J. Appl. Phys. **25**, 938-947.

Kornhauser, E.T. (1953). "Ray Theory for Moving Fluids," J. Acoust. Soc. Am. **25**, 945-949.

Landau, L.D., and E.M. Lifshitz (1959). *Fluid Mechanics* (Pergamon, Oxford).

Lighthill, M.J. (1956) "Viscosity Effects in Sound Waves of Finite Amplitude," in *Surveys in Mechanics*, edited by G.K. Batchelor and R.M. Davies (Cambridge University Press, Cambridge, England).

_____ (1965). "Group Velocity," J. Inst. Maths Applics. **1**, 1-28.

Lovett, J. R. (1978). "Merged Seawater Sound-Speed Equations," J. Acoust. Soc. Am. **63**,1713-1718.

Mal'tsev, N.E. (1983). "Ray Equations in Barycentric Coordinates," Sov. Phys.-Acoust. **29**, 390-392.

McDonald, B.E., and W.A. Kuperman (1984). "Time Domain Solution of Nonlinear Pulse Propagation," in *Hybrid Formulation of Wave Propagation and Scattering*, edited by L. B. Felsen, Symposium Proceedings, NATO Advanced Research Workshop, IAFE Castel Gandolfo, Italy.

Milne, E.A. (1921). "Sound Waves in the Atmosphere," Philos. Mag. **42**, 96-114.

Morfey, Christopher L. (1984a). "Nonlinear Propagation in a Depth-Dependent Ocean," ARL Technical Report No. 84-11 (ARL-TR-84-11), Applied Research Laboratories, The University of Texas at Austin (ADA 145 079).

_____ (1984b). "Aperiodic Signal Propagation at Finite Amplitudes: Some Practical Applications," in *Proceedings of the 10th International Congress on Nonlinear Acoustics*, Kobe, Japan, edited by A. Nakamura (Teikohsha Press, Kadoma).

_____ (1984c). Personal Communication.

_____ (1985). Personal Communication.

Officer, C.B. (1958). *Introduction to the Theory of Sound Transmission, with Application to the Ocean* (McGraw-Hill Book Co., Inc., New York).

Oppenheim, Alan V., and Ronald W. Schafer (1975). *Digital Signal Processing* (Prentice-Hall, Inc., Englewood Cliffs).

Ostrovsky, L.A. (1963). "On the Theory of Waves in Nonstationary Compressible Media," Prikl. Matem. Mekham. **27**, 924-929 (English Translation, 1412-1421).

_____ (1976). "Short-Wave Asymptotics for Weak Shock Waves and Solutions in Mechanics," Int. J. Non-Linear Mech. **11**, 401-416.

Ostrovsky, L.A., E.N. Pelinovsky, and V.E. Fridman (1975). "Propagation of Finite-Amplitude Acoustic Waves in the Stratified Ocean," Sixth International Symposium on Nonlinear Acoustics, Moscow, USSR, Book of Abstracts, pp. 254-257.

_____ (1976). "Propagation of Finite-Amplitude Sound Waves in an Inhomogeneous Medium with Caustics," Sov. Phys.-Acoust. **22**, 516-520.

Panton, Ronald L. (1984). *Incompressible Flow* (John Wiley & Sons, Inc., New York).

Pelinovsky, E.N., Yu. V. Petukhov, and V.E. Fridman (1979). "Approximate Equations for the Propagation of Strong Acoustic Signals in the Ocean," Izv., Acad. Sci. USSR, Atmos. Oceanic Phys. **15**, 299-304.

Pelinovsky, E.N., and V.E. Fridman (1983). "Equations of Nonlinear Geometrical Acoustics," in *Nonlinear Deformation Waves*, edited by Uno Nigel and Jüri Engelbrecht, Symposium Proceedings, Tallinn, Estonian SSR, USSR, August, 1982 (Springer-Verlag, Berlin) pp.143-148.

Pestorius, F.M. (1973). "Propagation of Plane Acoustic Noise of Finite Amplitude," ARL Technical Report No. 73-23 (ARL-TR-73-23), Applied Research Laboratories, The University of Texas at Austin (ADA 778 868).

Pestorius, F.M., and Solon B. Williams (1974). "Upper Limit on the Use of Weak-Shock Theory," J. Acoust. Soc. Am. **55**, 1334-1335(L).

Pierce, Allan D. (1981). *Acoustics* (McGraw-Hill Book Company Inc., New York).

Pitre, Richard (1984). "On the Application of Horizontal Ray Theory to the Acoustic Propagation in the Ocean Waveguide," ARL Technical Report No. 84-1 (ARL-TR-84-1), Applied Research Laboratories, The University of Texas at Austin (ADA 143 944).

Rayleigh, Lord (John William Strutt) (1896). *The Theory of Sound*, 2d and revised ed. (Dover Publications, Inc., New York, 1945).

Rogers, Peter H. (1977). "Weak-Shock Solution for the Underwater Explosive Shock Waves," J. Acoust. Soc. Am. **62**,1412-1419.

Rothwell, P. (1947). "Calculation of Sound Rays in the Atmosphere," J. Acoust. Soc. Am. **19**, 205-220.

Seebass, R. (1969). "Sonic Boom Theory," Journal of Aircraft Noise **6**, 177-184.

Warshaw, Stephen I. (1980). "On a Finite Amplitude Extension of Geometric Acoustics in a Moving, Inhomogeneous Atmosphere," UCRL-53055, University of California, Lawrence Livermore Laboratory, Berkeley, California.

Whitham, G.B. (1956). "On the Propagation of Weak Shock Waves," J. Fluid Mech. **1**, 290-318.

_____ (1974). *Linear and Nonlinear Waves* (John Wiley & Sons, Inc., New York).

DISTRIBUTION LIST FOR
ARL-TR-85-32
under Contract N00014-84-K-0574

Copy No.	
	Office of Naval Research 800 North Quincy Street Arlington, VA 22217
1	Attn: R. M. Fitzgerald, Code 425U
2	L. E. Hargrove, Code 412
3 - 14	Defense Technical Information Center Cameron Station, Building 5 5010 Duke Street Alexandria, VA 22314
	Naval Research Laboratory Department of the Navy Washington, DC 20375
15 - 20	Attn: Director
21	W. A. Kuperman
22	B. E. McDonald
	Naval Ocean Research and Development Activity NSTL Station, MS 39529
23	Attn: R. A. Wagstaff
	New London Laboratory Naval Underwater Systems Center New London, CT 06320
24	Attn: Technical Center
25	R. H. Mellen
26	M. B. Moffett
	NASA Langley Research Center Mail Stop 460A Hampton, VA 23665
27	Attn: H. Lester

Distribution List for ARL-TR-85-32 under Contract N00014-84-K-0574 (cont'd)

Copy No.

	Naval Ocean Systems Center San Diego, CA 92152
28	Attn: F. M. Pestorius
	Naval Postgraduate School Monterey, CA 93940
29	Attn: Technical Library
30	S. B. Baker
31	A. B. Coppens
32	S. L. Garrett
33	H. Medwin
34	S. Y. Wang
	Naval Research Laboratory P. O. Box 8337 Orlando, FL 32856
35	Attn: A. L. Van Buren
	Naval Coastal Systems Center Panama City, FL 32407
36	Attn: D. H. Trivett
	Brown University Department of Physics Providence, RI 02912
37	Attn: R. T. Beyer
38	P. J. Westervelt
	University of California Lawrence Livermore Laboratory Theoretical Physics, L-71 P. O. Box 808 Livermore, CA 94550
39	Attn: C. E. Rosenkilde
40	S. I. Warshaw (Theoretical Phys., L-71)
	University of California at Los Angeles Physics Department Los Angeles, CA 90024
41	Attn: I. Rudnick

Distribution List for ARL-TR-85-32 under Contract N00014-84-K-0574 (cont'd)

Copy No.	
	Georgetown University Physics Department Washington, DC 20057
42	Attn: W. G. Mayer
	Georgia Institute of Technology School of Mechanical Engineering Atlanta, GA 30332
43	Attn: Y. H. Berthelot
44	J. H. Ginsberg
45	A. D. Pierce
46	P. H. Rogers
	Johns Hopkins University Department of Mechanical Engineering Baltimore, MD 21218
47	Attn: A. Prosperetti
	Kalamazoo College Department of Physics Kalamazoo, MI 49007
48	Attn: W. M. Wright
	University of Mississippi Physics Department University, MS 38677
49	Attn: H. E. Bass
50	L. A. Crum
51	K. Gilbert
	The Pennsylvania State University Applied Research Laboratory University Park, PA 16802
52	Attn: S. McDaniel
	University of Tennessee Department of Physics Knoxville, TN 37916
53	Attn: M. A. Breazeale
	Virginia Polytechnic and State University Engineering Science and Mechanics Blacksburg, VA 24061
54	Attn: M. S. Cramer
55	A. Nayfeh

Distribution List for ARL-TR-85-32 under Contract N00014-84-K-0574 (cont'd)

Copy No.

Yale University
Department of Engineering
Mason Laboratory
9 Mill House Avenue
New Haven, CT 06520
56 Attn: R. E. Apfel

University of Miami / RSMAS
4600 Rickenbacker Causeway
Miami, FL 33149
57 Attn: F. D. Tappert

Jet Propulsion Laboratory
4800 Oak Grove
Pasadena, CA 91103
58 Attn: T. G. Wang

Raytheon Co.
P. O. Box 360
Portsmouth, RI 02871
59 Attn: R. D. Pridham

Acoustics Systems
P. O. Box 3610
Austin, TX 78764
60 Attn: D. A. Nelson

National Research Council
Division of Physics
Montreal Road
Ottawa, ONT
CANADA K1A OS1
61 Attn: G. A. Daigle
62 T. F. W. Embleton

Carleton University
Mechanical & Aeronautical Engineering
Colonel By Drive
Ottawa, ONT
CANADA K1S 5B6
63 Attn: W. G. Richarz

Copy No.

Chief
Defence Research Establishment Atlantic
P. O. Box 1012
Dartmouth, Nova Scotia
CANADA B2Y 327

64 Attn: Technical Library
65 D. M. F. Chapman
66 I. A. Fraser
67 H. M. Merklinger

Chief
Defence Research Establishment Pacific
Forces Mail Office
Victoria, British Columbia
CANADA V0S 1B0

68 Attn: Technical Library

University of Toronto
Institute for Aerospace Studies
4925 Dufferin St.
Downsview, ONT
CANADA M3H 5TC

69 Attn: I. I. Glass

Technical University of Nova Scotia
P. O. Box 1000
Halifax, NS
CANADA B3J-2X4

70 Attn: H. S. Heaps

Technical University of Denmark
Industrial Acoustics Laboratory
Building 352
DK-2800 Lyngby
DENMARK

71 Attn: L. Bjørnø

Osaka University
The Institute of Scientific and Industrial Research
8-1, Mihogaoka, Ibaraki
Osaka 567
JAPAN

72 Attn: A. Nakamura

Distribution List for ARL-TR-85-32 under Contract N00014-84-K-0574 (cont'd)

Copy No.

The University of Electro-Communications
1-5-1, Chofugaoka
Chofu-shi
Tokyo, JAPAN
73 Attn: T. Kamakura

Chinhae City
P. O. Box 18
Kyeong Nam
REPUBLIC OF KOREA
74 Attn: S. H. Kim

Universitet I Bergen
Matematisk Institutt
Allegaten 53-55
5000 Bergen
NORWAY
75 Attn: Sigve Tjøtta
76 Jacqueline Naze Tjøtta

Instituto de Acustica
Laboratorio de Ultrasonidos
Consejo Superior de Investigaciones Cientificas
Serrano, 144
Madrid-6
SPAIN
77 Attn: J. A. Gallego-Juarez

Admiralty Underwater Weapons Establishment
Portland
Dorset DT5 2
UNITED KINGDOM
78 Attn: D. E. Weston

Institute of Sound and Vibration Research
The University
Southampton S09 5NH
UNITED KINGDOM
79 Attn: R. Buckley
80 C. L. Morfey

Distribution List for ARL-TR-85-32 under Contract N00014-84-K-0574 (cont'd)

Copy No.

	University of Bath School of Physics Claverton Down Bath BA2 7AY UNITED KINGDOM
81	Attn: H. O. Berktay
	University of Leeds Applied Math. Studies Leeds, Yorkshire LS2 9JT UNITED KINGDOM
82	Attn: D. G. Crighton
83	Anthony M. Bedford, ASE&EM: UT
84	Francis X. Bostick, Jr., ECE: UT
85	Mark F. Hamilton, ME:UT
86	Elmer L. Hixson, ECE:UT
87	David T. Blackstock, ARL:UT
88	Ilene J. Busch-Vishniac, ARL:UT
89	C. Robert Culbertson, ARL:UT
90	Glen E. Ellis, ARL:UT
91	James M. Estes, ARL:UT
92	Terry L. Foreman, ARL:UT
93	James A. Hawkins, Jr., ARL:UT
94	John M. Huckabay, ARL:UT
95	David P. Knobles, ARL:UT
96	T. G. Muir, ARL:UT
97	James A. TenCate, ARL:UT
98	Arnold J. Tucker, ARL:UT

Distribution List for ARL-TR-85-32 under Contract N00014-84-K-0574 (cont'd)

Copy No.

99	Library, ARL:UT
100-119	Reserve, ARL:UT